A FLOW REACTOR STUDY OF GAS PHASE HYDROCARBON OXIDATION

A thesis submitted in partial fulfilment of the requirements of the Council for National Academic Awards for the degree of Doctor of Philosophy

by

PETER JOHN STANFORD

City of London Polytechnic

September 1982

ABSTRACT

A stirred flow reactor was adapted to study the rate of formation of hydrocarbons in the low pressure, 10mmHg, Oxidation of propanal, n-butanal and iso-butanal over the temperature range 710-783K. The technique simplified to some extent the analysis of this kinetically complex system but although less than 1% of the substrate was reacted in these experiments, the possibility of some degenerate branching via H_2O_2 cannot be excluded. Much of the kinetic data for propanal conformed to a rate law,

$$\frac{d}{dt}[C_2H_4 + C_2H_6] = k[O_2]^{1.0}[C_2H_5CHO]^{0.8-1.2}$$

and an overall activation energy of 115± KJ which compares favourably with 125KJ[1] obtained in a static reactor system. The precision of rate measurements, in particular the relative rates of hydrocarbon products were studied. Hydrocarbon products of the reaction of propanal are ethene and ethane. Ethene has been attributed to the reaction (3) and ethane to reaction (6).

$$C_2H_5^{\cdot} + O_2 \longrightarrow C_2H_4 + HO_2^{\cdot} \quad (1) \qquad (3)$$

$$C_2H_5^{\cdot} + C_2H_5CHO \longrightarrow C_2H_6 + C_2H_5CO^{\cdot} \qquad (6)$$

On this basis values of k_3 were calculated from the relative yields of these products. The results support a mechanism involving the intramolecular decomposition of a peroxyradical intermediate $C_2H_5OO^{\cdot}$ with Arrhenious parameters E = 116± 25KJ and A = 1.00×10^{13} sec^{-1}. rather than the one stage bimolecular reaction (3). Other interpretations of the relative yields of ethene and ethane are discussed together with the yields of analagous products from the higher aldehydes.

TABLE OF CONTENTS

INTRODUCTION

The object of this work is to study the high temperature oxidation of propanal and higher aldehydes using a stirred flow reactor. Throughout investigations of hydrocarbon oxidation difficulties arise from the complexities of the reaction mechanism, the fact that the nature of the radicals involved varies as the reaction proceeds and the reaction intermediates are more reactive than the parent hydrocarbon. The study of the hydrocarbon oxidation soon becomes a study of the reactions of its intermediates. In studying the oxidation of propanal, it was wished to obtain kinetic parameters for major and minor products formed; these include: C_2H_4, CO, H_2O_2, C_2H_6 and CH_3CHO, then to account quantitatively for the characteristics of the overall reaction and to obtain information on the reactivity of radical intermediates. This task is complicated by the nature of the general degenerate branching mechanism. This makes it impossible to approach a steady state system. A stirred flow reactor was employed to reduce the complexity inherrent in the mechanism if possible by looking at the initial stages of reaction this would exploit the potential of flow methods to 'freeze' the reaction at an early stage of development by artificially introducing a quasi-steadystate. One of the first objectives is an investigation of the suggested mechanism for the formation of olefins from the aldehydes, in particular the formation ethene from propanal. It has been suggested that the production of ethene arises from a single bimolecular step, although some evidence supports the existance of an intermediate peroxy radical.

The following review chapters elaborate on hydrocarbon oxidation in general and aldehydes in particular. The section on flow reactors include their major gas phase applications and makes comparisons with other types of reactors.

THE GAS PHASE OXIDATION OF HYDROCARBONS

The kinetic mechanism of hydrocarbon oxidation can be described as a chain reaction with degenerate branching. A mixture of a hydrocarbon and oxygen shows regions of slow reaction, explosive reaction and cool flames.

Common features of these types of reaction include an induction period. The slow oxidation usually displays the phenomenon of a region of a negative temperature coefficient between about 300°C and 400°C where the rate of reaction actually decreases with increasing temperature. Baker and Yorke[2] present in a review on the slow, gas phase oxidation of hydrocarbons, two theories on the mechanism of the reaction: The alkene theory of Knox and the alkylperoxy - radical - isomerization theory attributed mainly to Fish.

The Alkylperoxy - radical - isomerization theory

This suggests that many of the products are formed through the rearrangement of an alkyl · peroxy - radical in the course of hydrocarbon oxidation.

$$R\,H + O_2 \rightarrow R^{\bullet} + H\,O_2 \quad \text{(Initiation)}$$

$$R^{\bullet} + O_2 \rightarrow R\,O\,O^{\bullet} \quad \text{(Propagation)}$$

isomerization

$$R\,O\,O^{\bullet} \rightarrow \text{Product} + \text{Radical}$$

$$R\,H + \text{Radical} \rightarrow R^{\bullet} + (\text{Radical H})$$

The overall scheme also includes degenerate branching and termination reactions. The theory has been extended by Fish to explain the formation of the products of hydrocarbon oxidation in terms of the rearrangements of the alkylperoxy radical and the different routes of decomposition of the hydroperoxy radical so formed. The basic modes of rearrangement and decomposition are:

1. Intramolecular hydrogen abstraction giving the rearranged radical.

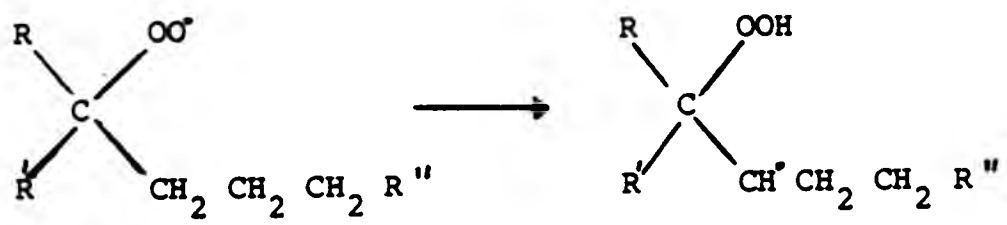

2. Decomposition of the rearranged radical.

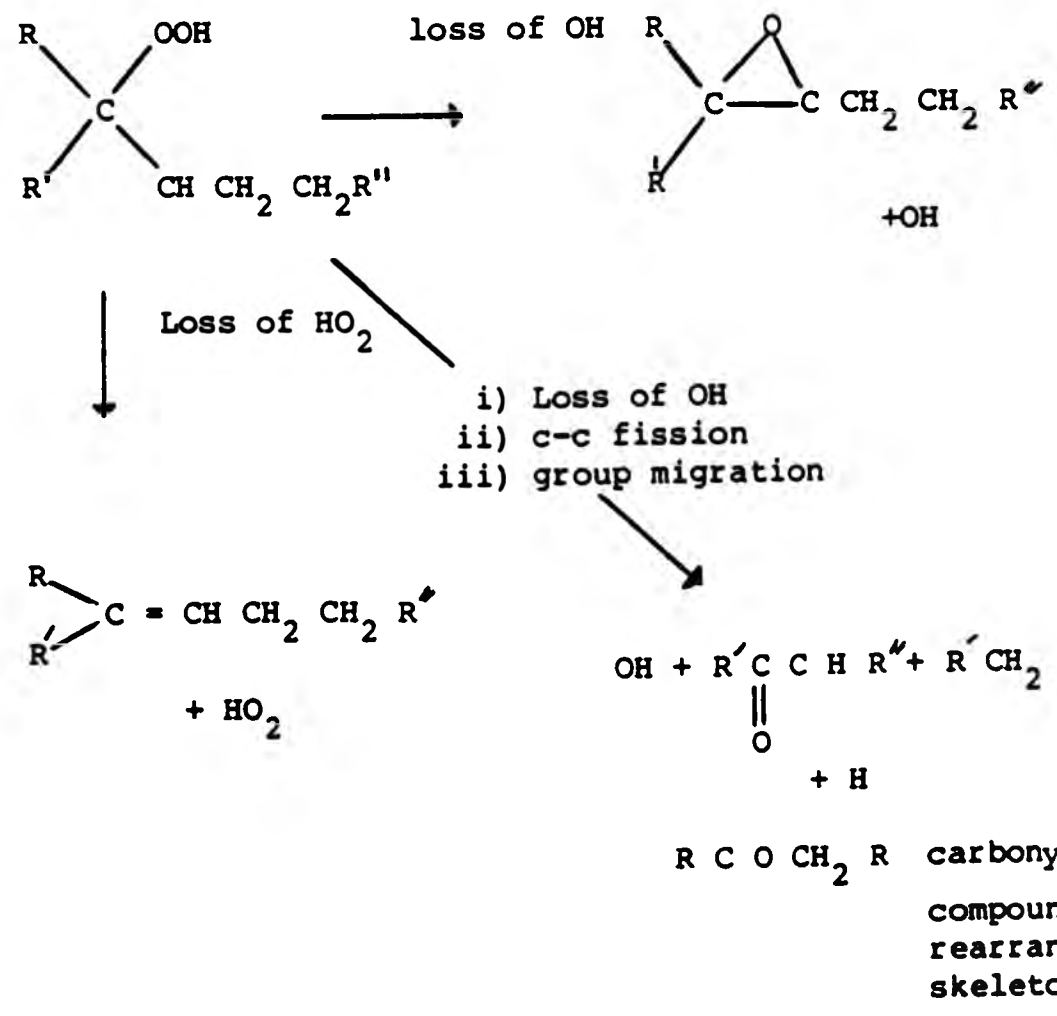

3. Isomerization by group transfer followed by decomposition of the rearranged radical.

$$R\,\acute{R}\,\acute{\acute{R}}C\,O\,O\cdot \rightarrow R\,\acute{R}C\,O\,O\,\acute{\acute{R}} \xrightarrow{O\text{–}O\ \text{fission}} R\,\acute{R}C\,O \quad \text{carbonyl compounds}$$

$$+\ \acute{\acute{R}}O\cdot \quad \text{alkoxy radicals}$$

Process 1. can also occur with internal hydrogen abstraction from the β or γ carbon atoms leading to oxetans, oxolans and carbonyl compounds

Fish has used the theory to account for the formation of over forty different products from the oxidation of 2 - methyl pentane, also to account satisfactorily for the existance of the negative temperature coefficient during the slow combustion of hydrocarbons.

In the low temperature region where the oxidation is quite selective it is suggested that degenerate branching results from the alkylmonohydroperoxide produced by a linear chain involving intermolecular hydrogen abstraction by the alklyperoxy radical.

$$R\,O_2^{\bullet} \xrightarrow{RH} ROOH \longrightarrow RO^{\bullet} + OH \quad \text{(branching)}$$

$$\uparrow\!\!\_\_\_\_\_ +\ O_2 \quad + \quad R^{\bullet}$$

As the temperature is increased, intramolecular hydrogen abstraction (which is assumed to be unimolecular, with a high activation energy) becomes increasingly important and competes with the formation of the alkylmonohydroperoxide.

3. Isomerization by group transfer followed by decomposition of the rearranged radical.

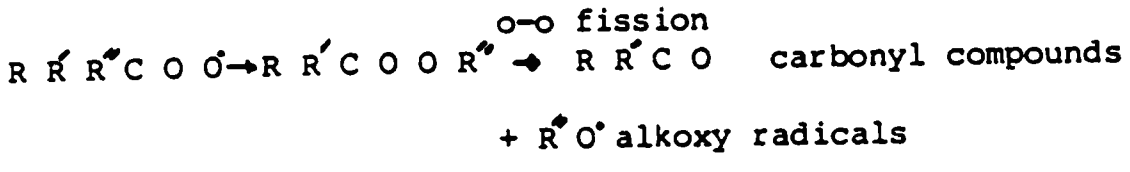

Process 1. can also occur with internal hydrogen abstraction from the β or γ carbon atoms leading to oxetans, oxolans and carbonyl compounds

Fish has used the theory to account for the formation of over forty different products from the oxidation of 2 - methyl pentane, also to account satisfactorily for the existance of the negative temperature coefficient during the slow combustion of hydrocarbons.

In the low temperature region where the oxidation is quite selective it is suggested that degenerate branching results from the alkylmonohydroperoxide produced by a linear chain involving intermolecular hydrogen abstraction by the alklyperoxy radical.

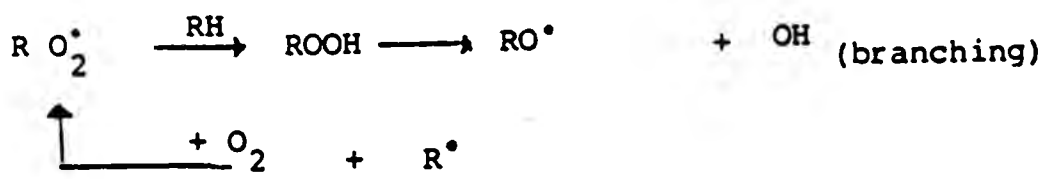

As the temperature is increased, intramolecular hydrogen abstraction (which is assumed to be unimolecular, with a high activation energy) becomes increasingly important and competes with the formation of the alkylmonohydroperoxide.

As decomposition of the rearranged peroxy radical is not a branching process unlike the decomposition of the monohydroperoxide, an increase in the temperature will therefore result in a reduction of the rate of branching. Thus the rate of the overall oxidation will fall as the temperature is increased.

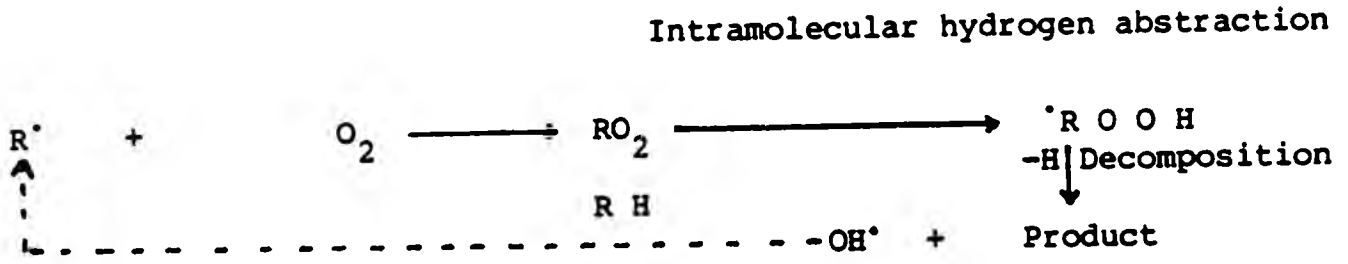

In the high temperature region, the oxidation rate is increasing with temperature, because branching is re-established by the decomposition of dihydroperoxides which are formed by the further addition of oxygen.

The Alkene theory

The Alkene theory develops from the observation that during the oxidation of the lower alkenes between 300°C and 500°C at least 70% of the alkene lost during the initial appears whenever possible as the conjugate alkene. Knox suggested that the alkene (AB) was formed in reaction (5')

$$R + O_2 = AB + HO_2 \quad (5')$$

$$R + O_2 = \text{Oxygenated product} \quad (6')$$

It contrasts with the Fish mechanism where the alkene is only favoured at higher temperatures (because of the competition of reaction 5'). Knox believed that any scheme for alkane oxidation, even as low as 300°C must not only involve the formation of the alkene as the major product but also involve the reactions of the alkene under the conditions of the oxidation. Aldehydes Ketones and to a lesser extent oxirans are major products of alkene oxidation and this probably explains the large yields of these products after a significant reaction time.

Knox's results have been interpreted to show that minor products of hydrocarbon oxidation were formed heterogeneously from alkylperoxy radicals. The system is represented by the reactions.

R	+	O_2	80% =	AB	+	$H O_2$	(5')
R	+	O_2	20% =	ROO•			(6')
	ROO•		Wall =	minor products			(8')

It is supposed that the main propagating chain in such a system are reactions (5') and (8')

$$RH + HO_2 = R^{\bullet} + H_2O_2 \qquad (9')$$

The selectivity of $HO_2^{\bullet}$ radicals is high, removing the alkane alone initially. There is a marked decrease in selectivity between the earliest stages of alkane oxidation and the intermediate stages. He attributes this to a more reactive and unselective radical OH which becomes important later on in the reaction.

Knox postulated the following scheme which illustrates the fate of the alkene produced and the conversion of the HO_2 radical into an OH radical.

AB	+	HO_2	=	ABOOH	(9')
ABOOH	+	O_2	=	OOABOOH	(10')
OOABOOH	+	HO_2	=	HOOABOOH	(11')
HOOABOOH			=	2OH + AO + BO	(12')

The overall reaction $2HO_2$ + AB = 2OH + AO + BO

AB is the conjugate alkene of the parent alkane RH, and AO and BO are carbonyl compounds or oxirans.

Degenerate branching can occur by oxidation of the carbonyl compounds AO and BO giving radicals.

RCHO + $\cdot O_2$ = RCO + HO_2

or from the decomposition into radicals of alkylhydroperoxides. Below about 400°C termination is effected by disproportion of HO_2 radicals.

HO_2 + HO_2 = H_2O_2 + O_2

Knox explains the existance of a negative temperature coefficient by the disappearance of OH radicals and so the relative proportion of alkene abstraction by OH radicals will decrease. Thus the overall reaction rate also decreases because abstraction of hydrogen from alkane by HO_2 is much slower than that by OH radicals. Above the temperature where there is absolutely no conversion of HO_2 to OH the overall rate will

gradually increase due to the normal increase in the velocity for HO_2 abstraction with temperature. The increase in overall rate with temperature will become more marked about 456°C when homogeneous decomposition of H_2O_2 into OH radicals occurs and abstraction by OH radicals is established once again.

Both theories explain the formation of products and account for kinetic features. The Alkyl peroxy-radical-somerization theory relies on the formation of oxygenated products via isomerization. Knox believes that the activation energies are high and their occurance below about 500°C will be negligible relative to other reactions of RO_2 radicals.

Between 300°C and 400°C Carthidge and Tipper[3] have shown that the predominant reaction of the rearranged peroxy radical is the further addition of O_2 and not decomposition.

The alkene theory breaks down for alkanes higher than C_4H_{10}, the conjugate is in fact less reactive than the parent alkane which would suggest it plays no further part in the mechanism of alkane oxidation.

Fish has combined the two theories into a single comprehensive mechanism reproduced below, this combination is shown to hold if $k_A > k_B$ and $k_C > k_D$ (RH) It is suggested this scheme is a good approximation to the mechanism of many alkane oxidation systems.

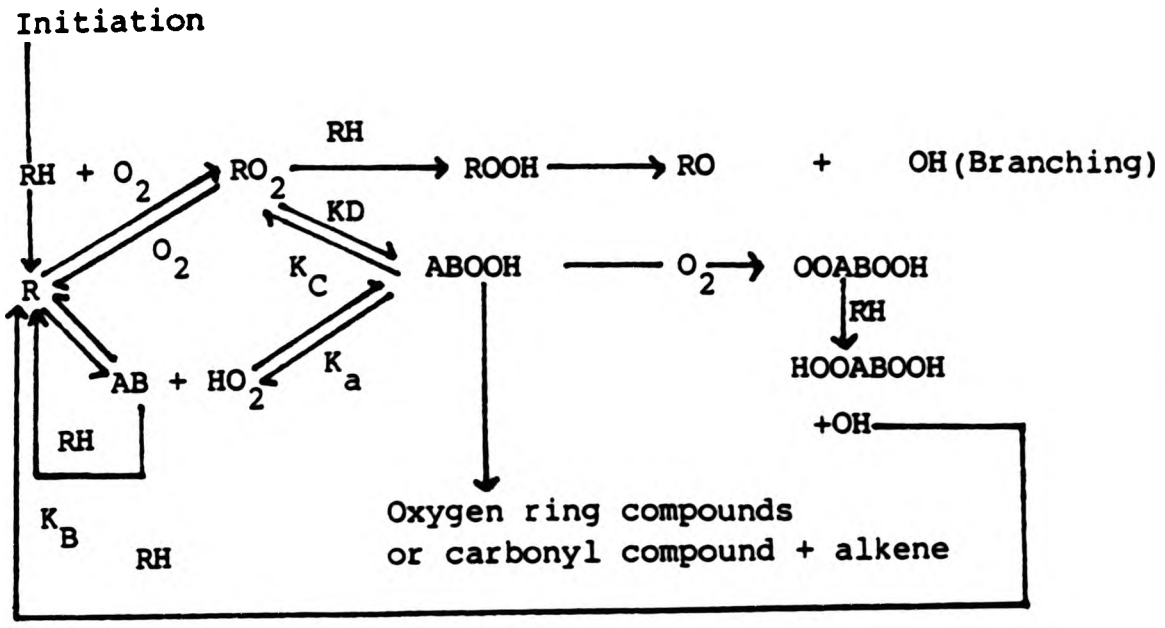

A more basic mechanism for hydrocarbon oxidation is given by Walker[4] in a review of rate constants for gas phase hyrdocarbon oxidation.

RH	+	O_2	⟶	R	$+HO_2$	(1')
X	+	RH	⟶	XH	+R	(2')
R	(+M)		⟶	R′	+AB(+M)	(3')
R	(+M)		⟶	H·	+AB(+M)	(4')
R	+	O_2	⟶	AB	$+HO_2$	(5')
R	+	O_2	⟶	ABO	+OH	(5b')
R	+	O_2	⟶	OR	+OH	(5c')
R	+	O_2	⟶	AB,ABO,OR		(6a',b,c,)
R	+	O_2(+M)	⟶	RO_2 (+M)		(7')
RO_2			⟶	AB,ABO,OR		(8'a,b,c,)
RO_2	+	RH	⟶	RO_2H	+R	(8'd)
RO_2			⟶	QOOH		(9')
QOOH	+	O_2	⟶	O_2QOOH		(10'e)
QOOH			⟶	AB,ABO,OR		(10'a,b,c,)

RO_2 + RO_2 ⟶ chain termination (11')

ROOH ⟶ RO + OH (12')

H_2O_2 + M ⟶ 2OH + M (13')

HO_2 + HO_2 ⟶ H_2O_2 + O_2 (14')

AB = Olefin

ABO = Carbonyl compound

R', AB' contain a smaller number of carbon atoms than R. Broken arrows in reactions indicate an overall process.

Aldehyde Oxidation

Aldehydes feature strongly in hydrocarbon oxidation and are frequently intermediates and products of the combustion of other compounds, their ease of oxidation and their susceptibility to radical attack and chain decomposition means that they may strongly influence the behaviour of systems in which they occur, because they are early products in hydrocarbon oxidation and as they are invariably more reactive than the parent compound an understanding of their oxidation characteristics is essential to the understanding of hydrocarbon oxidation.

Low temperature gas phase oxidation of Aldehydes

The gas phase oxidation at lower temperatures, between 70°C and 150°C for ethanal, propanal and the butanals have all been investigated.

The main elementary steps in the chain mechanism and their kinetic parameters at these temperatures appear to be well established and are reported in a review by J R Griffiths and G Skirrow.[5] Experimental features such as surface, inert gas effects and additives that inhibit have been discussed. Rate constants for each elementary reaction and the overall mechanisms have been reported.

Recently the gas phase oxidation of ethanal, propanal and the butanals in unpacked and packed vessels between 45°C and 120°C have been published by Dixon, Skirrow and Tipper[6]. Apparently between 70°C and 80°C earlier reports by Combe, Niclause and Letort[7] with very high aldehyde/oxygen ratio, had suggested deviations from the overall stoichometry.

$$RCHO + O_2 \longrightarrow RCO_3H$$

The variation of pressure with time agreed with that deduced from the usual accepted autocatlytic chain mechanism[7].

$RCHO$	+	O_2	$\xrightarrow{R_1}$	RCO + HO_2		(1)
RCO	+	O_2	$\xrightarrow{R_2}$	RCO_3		(2)
RCO_3	+	$RCHO$	$\xrightarrow{R_3}$	RCO_2H + RCO		(3)
	$2RCO_3$		$\xrightarrow{R_{4a}}$	Products		(4a)
RCO_3	+	RCO	$\longrightarrow$	inert		(4b)
		$2RCO$	$\longrightarrow$	"		(4c)
RCO_3H	+	$RCHO$	$\xrightarrow{R_5}$	radicals (RCO)		(5)
RCO	+	(M)	$\longrightarrow$	R	+CO	(6)

The rate coefficients of reactions (1 - 6) indicate that until the oxygen pressure in the reacting mixtures becomes less than a few torr the only steps occuring should be (1) (2) (3) (4a) and (5), the concentration of RCO radicals being very much less than that of RCO_3 radicals.

The rate determining step in the initiation is reported as first order with respect to both aldehyde and Oxygen, the branching process is first order with respect to both peracid and aldehyde and the addition of oxygen to acetyl radicals is second order overall. The variation of the second order rate coefficients with temperature and surface/volume ratio indicated that both initiation and branching are heterogeneous. However, the addition process is homogeneous, the rate coefficient being about 1.2×10^7 dm^3 mol^{-1} sec^{-1} between 62.5 and 83.5°C.

Several groups of workers (5',6,7,) have determined the overall activation energies for the oxidations of ethanal and propanal, almost invariably these values are based on pressure-time measurements. The overall activation energies for the oxidations of both ethanal and propanal in the oxygen independant regions is reported to be about 61- 90 KJ mol^{-1}

Mid temperature gas phase oxidation of aldehydes

The mechanism of the oxidation of Propanal is shown to be relatively simple below 150°C where peroxypropionic acid is produced stoichometrically. An increase in the temperature and change in the fuel oxygen ratio affects the overall oxidation, especially at two critical points

in the mechanism and the reaction becomes more complex. Finally at higher temperatures above 427^{o}C the mechanism again changes.

Cairns and Waddington[8] have recently investigated the changes of mechanism between the low and high temperature regions.

Peroxypropionic acid is the main product at 179^{o}C, the mechanism of its formation is well established as in reactions 1,2, and 3 of the last mechanism. The rate of formation of carbon monoxide is very low at this temperature. It is likely to be formed by a reaction leading to the production of acetaldeyde and by a radical decomposition reaction showing second order kinetics under the prevailing experimental conditions.

$C_2 H_5 CO + (M) \longrightarrow C_2 H_5 + CO (+M)$ II

Peroxypropionic acid is still the main primary product of Oxygen rich mixtures at 225^{o}C however carbon monoxide becomes the principle product in oxygen lean mixtures, where competitive hydrogen abstraction is reduced, contrasting with the results at 179^{o}C, with a 5:1, propanal: oxygen mixture where the peroxyacid was the major product.

At the first critical stage of the reaction, the mechanism is determined by the relative rates of the reactions I and II

$C_2 H_5 CO + O_2 \longrightarrow C_2 H_5 CO_3$ I

Increases in temperature not only promotes the rate of reaction II but the equilibrium position of reaction I favours the propionyl radicals.

Similarly the same effect is caused by an increase in aldehyde: oxygen ratio.

The increase in the rate of formation of ethyl radicals leads to the formation of ethyl peroxy radicals.

$$C_2H_5 + O_2 \rightleftharpoons C_2H_5COO \qquad \text{III}$$

At about 225°C in the early stages of reaction, large quantities of ethyl hydroperoxide, ethanol, formaldehyde, and methanol are produced. Reaction III is sensitive to change in temperature or or aldehyde: oxygen ratio. As the temperature rises equilibrium increasingly favours the ethyl radicals (reported also by Benson)[9]. Above 427°C reaction III predominates and the principle reactions are those of ethyl and alkylperoxy radicals.

Two sets of papers by R R Baldwin, R W Walker and co-workers (1,10,11,12) are considered to be directly relevant to the work on this thesis.

The maximum rate of oxidation of propanal in aged Boric-acid vessels at 440°C was found to have orders of 1.5 and 0.2 with respect to aldehyde and oxygen respectively. The rate was found to be independent of vessel diameter and was accelerated by the addition of an inert gas. The use of an aged-boric acid vessel

stems from earlier work [13] investigating the slow reaction between H_2 and O_2 the reproducibility of the reaction was attributed to the inertness of the surface in destroying H, HO_2 and H_2O_2.

HO_2 and H_2O_2 should occur in aldehyde oxidation in the temperature range 400-500°c and similar reproducibility was expected. The simple mechanism proposed for reactions at about 400°c was:

$$C_2H_5CHO + O_2 = C_2H_5CO + HO_2 \quad (1)$$

$$C_2H_5CO = C_2H_5 + CO \quad (2)$$

$$C_2H_5 + O_2 = C_2H_4 + HO_2 \quad (3)$$

$$HO_2 + C_2H_5CHO = C_2H_5CO + H_2O_2 \quad (4)$$

$$HO_2 + HO_2 = H_2O_2 + O_2 \quad (5)$$

The rate of reaction was followed by measurement of the pressure increase. The main primary products were C_2H_4 and CH_3CHO at about 10-20% relative yield of the former. Stoichiometric equations for their formation were written.

$$C_2H_5CHO + O_2 = C_2H_4 + CO + H_2O_2$$

$$C_2H_5CHO + O_2 = CH_3CHO + CO + H_2O$$

It was noted that severe reduction of the O_2 mole fraction could change the stoichometry so that the main reaction of C_2H_5 radicals became

$$C_2H_5 + C_2H_5CHO = C_2H_6 + C_2H_5CO \quad (6)$$

The ΔP - time curves were of an autocatalytic nature, this feature of the reaction was attributed to reaction (7)

$$H_2O_2 + M = 2OH + M \quad (7)$$

Autocatalysis will only occur if the OH produced in (7) continues the chain, the reaction proposed being (8):

$$OH + C_2H_5CHO = H_2O + C_2H_5CO \quad (8)$$

The OH radical being less selective than HO_2 might also be expected to produce abstraction from the alkyl group as well.

The maximum rate usually occured after about 20-40% reaction. A region of negative temperature coefficient was observed between 340^oC and 400^oC indicative of a change of mechanism. A temperature of 440^oC was chosen for a detailed study as a compromise between a lower temperature, where the contribution from the low temperature mechanism would be significant and a higher temperature where the rapid decomposition rate of H_2O_2 would give rates too high for measurement.

The variation of maximum rate with aldehyde pressure, while maintaining oxygen constant at 30mm Hg, was used to measure the order of reaction. The order in aldehyde, A, varied from 1.5 at low aldehyde to 2.5 at aldehyde greater than 10mms Hg. Over the range 4.0 -56 mms Hg the dependance on O_2 was much smaller, orders of 0.11 and 0.35 being obtained for the maximum and minimum rates. Study of the variation of vessel diameter showed the absence of any significant diameter effects, which supports the view that surface plays little part in the mechanism of oxidation when aged-boric-acid vessels are used.

If H_2O_2 is considered a stable product and if relatively long chains are assumed a mechanism involving reactions (1-5) gives the rate of reaction using stationary state treatment as:

$$-\frac{dA}{dt} = \frac{dP}{dt} = k_4 k_1^{\frac{1}{2}} [A]^{3/2} [O_2]^{\frac{1}{2}} / k_5^{\frac{1}{2}}$$

This analysis of the kinetics was no longer valid once reaction (7) was included in the mechanism. It was now necessary to write differential equations for both aldehyde loss and for H_2O_2 formation and these equations were solved by numerical integration using computer methods.

$$-\frac{d\,AH}{dt} = k_1[AH][O_2] + \frac{k_4}{k_5}^{\frac{1}{2}} G\,[AH] + 2k_7\,[H_2O_2]\,(M)$$

$$\frac{d\,H_2O_2}{dt} = k_1\,[AH]\,[O_2] + \frac{k_4}{k_5}^{\frac{1}{2}} G\,[AH]$$

where $G = k_5^{\frac{1}{2}}\,[HO_2]$

and is given by $G^2 = k_1\,[AH]\,[O_2] + k_7\,[H_2O_2]\,(M)$

k_7 being accurately known, the only unknown parameters were k_1 and $k_4/k_5^{\frac{1}{2}}$. Stepwise integrations were carried out using a time interval of two seconds. Basically the method was to fit as closely as possible the computer P time plots with the experimental points. The approximate value of k_1 was found in this way. A value of 10^{-4} mm Hg^{-1} s^{-1} gave a maximum rate initially and the rate fell off sharply as the reaction proceeded, with $k_1 = 10^{-8}$ mm Hg^{-1} s^{-1} the S shaped nature of the curve was excessive and a value of about 10^{-6}

mm Hg^{-1} s^{-1} gave a close fit between observed and calculated P time curves. For values of k_1 in this range the primary initiation process (1) is negligible compared to the dissociation of H_2O_2 at maximum rate, so that the parameter $k_4/k_5^{\frac{1}{2}}$ can be obtained from the maximum rate for the standard mixture. The value of k_1 could then be calculated in two ways:

a) as the value (1.4×10^{-6} (mm Hg sec^{-1}) that gave the experimentally determined rate of initial rate/maximum rate.

b) as the value (2.0×10^{-6} (mm Hg Sec)$^{-1}$) which was shown to give the best fit to the observed P time curve.

The difference between the two values was attributed to an accumulation of small effects such as difficulties in measuring the initial rate and the differences between (AH) and ΔP resulting from further reactions of the products, especially CH_3 CHO. A mean value $1.7 \pm 0.3 \times 10^{-6}$ (mms Hg sec)$^{-1}$ or 0.076 l mol^{-1} sec^{-1} at 440°c was adopted.

Other adjustments were made in the computer programming to take into account the inert gas effects and the effect of minor reactions especially those propagating radicals.

Activation energies could not directly be determined from the simple value of k_1 at 440°c. Use of pre-exponential factors of 10^9 10^{10} and 10^{11} gave values of E_1 equal to 138, 150 and 167 K J mol^{-1}, respectively which was compared with Kerr[14] who previously estimated an endothermicity of 167-171 K J mol^{-1}.

The lowest value of E_1 (138 KJ mol^{-1}) would decrease R_1 to 6×10^{-10} l mol^{-1} sec^{-1} at 123°C for comparison with values of 3.75×10^{-3} and 1.00×10^{-3} l mol^{-1} sec^{-1} reported by Farmer and McDowell and Combe, Niclause and Letort. These values are considered to be too high for a homogeneous initiation by (1) and therefore represent either a heterogeneous initiation of some secondary initiation process.

A study of the analytical results showed products other than those predicted by the proposed mechanism ie C_2H_4, CO and H_2O_2. There were smaller and significant amounts of C_2H_4O, CH_4, C_2H_6 and H_2.

CH_3 CHO was formed as a reaction product in quantities of up to 10% from a standard mixture. Reaction (9) is not considered to be responsible for the formation of ethanal.

$$C_2H_5 \cdot + O_2 \longrightarrow CH_3CHO + OH \quad (9)$$

on grounds of earlier experimental work.[15]

The reaction suggested as the source of CH_3CHO is the radical attack on C_2H_5CHO at the secondary position in the C_2H_5 group.

$$HO_2 + CH_3CH_2CHO \longrightarrow CH_3CH\ CHO + H_2O$$

$$CH_3CH\ CHO + O_2 \longrightarrow CH_3 - \underset{\underset{O-O}{|}}{CH} - CHO \longrightarrow CH_3CHO + CO + OH$$

Formation of C_2H_4O as a minor primary product possibly through a peroxy radical or more likely through a radical formed by attack at the terminal CH_3 group in C_2H_5 CHO, CH_4, HCHO and CH_3 OH are secondary products involving hydrogen abstraction and oxidation

of methyl radicals. The formation of hydrogen is markedly autocatalytic, the H_2 presumably being formed in H abstraction. CO_2 is a primary product and not derived from the oxidation of CO, C_2H_4 and C_2H_6 are both primary products resulting from chain reactions of the ethyl radical.

C_2H_5	+	O_2	=	C_2H_4	+	HO_2 (3)
C_2H_5	+	C_2H_5CHO	=	C_2H_6	+	C_2H_5CO (6)
C_2H_5	+	HO_2	=	C_2H_6	+	O_2 (10)

Ethane could be formed by reaction (10) as well as (6) but it was shown that reaction (10) is at most a minor source of C_2H_6.

Trotman-Dickenson AF[16] gives $\log k_6 = 8.1 - 5900/2.3\ RT$

whence $k_6 = 2 \times 10^6$ l mol^{-1} sec^{-1} at 440^oC.

Discounting reaction (10) the ratio of the products C_2H_4/C_2H_6 is given by:

$$r\ C_2H_4 / r\ C_2H_6 = k_3\ (O_2) / k_6\ (C_2H_5\ CHO)$$

A plot of C_2H_4 / C_2H_6 v O_2/C_2H_5 CHO at

P = 0.2 mms Hg for a series of mixtures with varying O_2 pressures and a constant pressure of 4mm Hg of C_2H_5CHO produced a straight line giving $k_3/k_6 = 41 \pm 5$.

R_3 was calculated at 440°C to be 8.2×10^7 l mol^{-1} sec^{-1}, this value was compared with 1.0×10^8 at 623°C obtained by Sampson[17]. The authors conclude that as the A factor for reaction 3 would be expected to be between 10^8 and 10^9, both figures imply a very small activation energy and little variation with temperature would be expected.

The rate of oxidation of Proponal in vessels freshly coated with KCl is higher than found in boric acid coated vessels and was highly erratic. The rate decreased considerably as the vessel was aged by repeated runs and reasonable reproducibility was obtained. In boric-acid- coated vessels the pressure change was always consistently less than the consumption of C_2H_5CHO. This was eventually attributed to the formation in the sampling bulb of an involatile complex between C_2H_5CHO and H_2O_2. In KCl vessels where the concentration of H_2O_2 was much smaller, the effect of the complex was expected to be smaller and correlation between pressure change and C_2H_5CHO was expected. In contrast to the boric-acid-coated vessels the reaction was not auto-catalytic consistent with a low H_2O_2 concentration, which indicated that H_2O_2 was destroyed at the surface with considerable efficiency. The lower initial rate in KCl vessels indicated that HO_2 was also destroyed at the surface.

Over the range 400°C - 500°C the (Log(rate) v $^1/_T$) plot was approximately linear corresponding to an activation energy of 58 ± 8 KJ mol^{-1}.

The effect of varying Propanal pressure was examined at a constant O_2 pressure of 30 torr and a constant total pressure of 60 torr,

between 10-56 torr the order with respect to propanal was 0.5 $\pm$ 0.2. At lower pressures 2 and 10 torr. The effect of varying oxygen pressure was examined with constant propanal pressure, between 2 and 10 torr, little variation of rate with oxygen was observed. The order rose sharply for pressures between 0.5 and 2 torr and decreased as the oxygen pressure was reduced to 0.1 torr. The results of the lower oxygen pressure were said to indicate a change of mechanism and possibly a change of surface characteristics.

CO and C_2H_4 were again major reaction products. Ethanal was also an important product in KCl vessels accounting for approximately 30% of propanal consumed, but its concentration passed through a maximum indicating that it was easily oxidised under the experimental conditions. The yields of CH_3 CHO were smaller in the experiments with boric-acid-coated vessels and are attributed to a heterogeneous reaction forming both CH_3CHO and C_2H_4 in almost equal proportions and which even in aged kcl vessels contributes about 45% to the rate.

C_2H_6 was formed as a primary product, because of the competition between reactions (3) and (6) in boric acid coated vessels, the ratio R_3/R_6 was measured at 46. This was corrected to 62 as reaction (3) was seen as contributing only 55% of the C_2H_4 formed.

The oxidation of isobutanal in aged boric acid coated vessels [18,19] has been published by Baldwin et al. Because of the thermal stability of the i - C_3H_7 radical it was thought that the oxidation of i-butanal would follow a similar mechanism to propanal.

i. C_3H_7 CHO + O_2 $\longrightarrow$ i-C_3H_7 CO + HO_2 (1i)

i-C_3H_7 CO (+M) $\longrightarrow$ i-C_3H_7 + CO (+M) (2i)

i-C_3H_7 + O_2 $\longrightarrow$ C_3H_6 + HO_2 (3i)

HO_2	+	$i\text{-}C_3H_7CHO$	$H_2O_2 + iC_3H_7\ CO$	(4i)
HO_2	+	HO_2	$H_2O_2 + O_2$	(5i)
H_2O_2	+	M	2OH + M	(6i)
OH	+	$i\text{-}C_3H_7CHO$	H_2O + $i\text{-}C_3H_7CO$	(7i)

Reactions (1i)- (7i) predict CO, H_2O_2 and C_3H_6 as the main products but do not account for the formation of acetone, propane oxide and CO_2. For three mixtures of widely different composition the ΔP against ($i\text{-}C_3H_7$ CHO) plots were closely linear up to at least 30% reaction unlike the discrepancy found in the oxidation of C_2H_5 CHO.

With $i\text{-}C_3H_7$ CHo there was shown to be a slight negative temperature coefficient, previously overlooked, between 385°C and 395°C. The effect of varying aldehyde pressure between 1-15 torr gave an order of 1.5^{+}_{-} 0.1. With aldehyde pressure 4 torr, and a total pressure of 60 torr, the maximum rate increased only slightly as the pressure of O_2 was increased from 1-56 torr and a mean order of 0.1^{+}_{-} 0.2 was obtained. Over the composition ranges studied, but excluding the results at high oxygen pressure, a simple experimental law was written for the maximum rate.

$$r_{max} = [i\text{-}C_3H_7CHO]^{1.5}\ [O_2]^{1.0}\ [N_2]^{0.3}$$

Acetone formation from $i\text{-}C_3H_7CHO$ was explained by radical attacks on the t-H bond, this may be compared with the formation of ethanal in the oxidation of propanal.

HO_2	+	$(CH_3)_2CHCHO$	=	H_2O_2	+ $(CH_3)_2$ C CHO	(4i)
OH	+	$(CH_3)_2CHCHO$	=	H_2O	+ $(CH_3)_2$ C CHO	(7i)

$(CH_3)_2$ C CHO + O_2 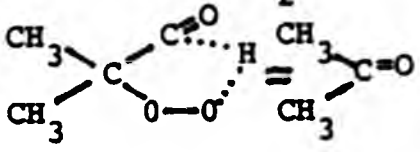 + CO + OH (8i)

The yield of C_3H_6 was independant of mixture composition, however acetone was significantly dependant on O_2 concentration, this was explained by the introduction of a decomposition reaction of the $(CH_3)_2$- C C CHO radical.

$$(CH_3)_2 - C - CHO + M \longrightarrow CH_3CH{=}CH_2 + HCO + M \quad (9i)$$

HCO radicals react readily with O_2 to form HO_2 and CO.

$$HCO + O_2 \longrightarrow HO_2 + CO \quad (10i)$$

Reaction (9i) competes with the reaction of the radical to give $(CH_3)_2$ CO by the peroxyradical isomerization and decomposition mechanism. The yield of propene oxide is higher than would be expected if it were formed solely from i-C_3H_7 radicals by reaction(3a),

$$i\text{-}C_3H_7 + O_2 \longrightarrow C_3H_6O + OH \quad (3a)$$

and its formation from the (CH_3) (CH_2) CH CHO radical is predicted both occuring by a peroxyradical isomerization and decomposition mechanism.

The analysis of a pressure v time profiles, determined as for propanal, gave rate constants k_1 = 0.12$\pm$ 0.01 dm^3 mol^{-1} sec^{-1} and k_4 = (1.83$\pm$ 0.10) x 10^6 dm^3 mol^{-1} sec^{-1}.

The oxidation of n-butanal was reported along with other aldehydes by R R Baldwin, R W Walker and other workers[12]. A similar mechanism to that for C_2H_5CHO was expected, but no initiation rate constant k_1 was reported as the initial rate was fast, and a significant proportion of reaction had occured by the time the rate was measured.

As initiation by secondary products might have taken place, the value k_1 was not considered reliable.

The propyl radical might undergo an oxidation reaction (3p) or a pyrolysis reaction (14p)

$$C_3H_7 + M \longrightarrow CH_3 + C_2H_4 + M \quad (14p)$$

$$C_3H_7 + O_2 \longrightarrow C_3H_6 + HO_2 \quad (3p)$$

The relative extent of pyrolysis was followed by measuring the relative yields of C_2H_4 and C_3H_6.

$$\frac{r\,C_2H_4}{rC_3H_6} = \frac{k_{14p}[M]}{k_{3p}[O_2]}$$

The graph was extrapolated to zero reaction to determine its initial value, because of subsequent oxidation of both alkenes. A graph of $r\,C_2H_4 / r\,C_3H_6$ against [M] at constant $[O_2]$, was non linear (14p) would be first order if independant of M and second order if a linear plot were obtained passing through the origin. The result showed the reaction to be in transition from first to second order. Using a simple Hinshelwood Lindemann treatment a plot of ([M]/ $(C_2H_4)/(C_3H_6)$) against M gave a straight line over the pressure ranges and the low-pressure and high pressure values of the ration k_{14p}/k_{3p} were obtained. Using the expression $k_{14p} = 3.47 \times 10^{12} \exp 131\ KJ/RT)\ sec^{-1}$ of Laidler and Lin in the literature this gave

k_{3p} at $450^oC = 5.8 \times 10^7\ 1\ mol^{-1}\ sec^{-1}$

Baldwin and co-workers investigated the high temperature oxidation of ethanal[21], after their work on propanal in aged boric-acid- coated vessels. The oxidation would produce CH_3 radicals whose reactions could be examined. Knowing the oxidation of CH_3 radicals give HCHO and OH radicals the probable mechanism they thought should include the following reactions:

CH_3CHO	+	O_2	=	CH_3CO	+	HO_2		(1)a
CH_3CO	+	M	=	CH_3	+	CO	+ M	(2)a
CH_3	+	O_2	=	HCHO	+	OH		(3)a
HO_2	+	CH_3CHO	=	H_2O_2	+	CH_3CO		(4)a
OH	+	CH_3CHO	=	H_2O	+	CH_3CO		(8)a

The reaction was studied over the temperature range 320°C - 540°C and showed there is a region of negative temperature coefficient between 440° and 500°C. At 540°C CH_4 was found to be a major product with significant yields of C_2H_6, H_2 and CH_3OH whereas at 440°C CH_4 and C_2H_6 were minor products. They conclude that reaction $(3)_a$ is not the main reaction by which CH_3 radicals oxidize at 540°C because of the process going through a negative temperature coefficient corresponding to an activation energy of -20 to-25 K cal mol^{-1}. The increasing yields of CH_4 relative to oxidation products as the temperature increases were explained by assuming that the oxidation process proceeds through CH_3O_2 radicals.

$$CH_3 + O_2 + M \rightleftharpoons CH_3O_2 + M \qquad (12)_a$$

$$CH_3O_2 \longrightarrow \text{Oxidation products.}$$

The predominant reaction of CH_3O_2 radicals is to dissociate back to $CH_3 + O_2$. The slow rate of the oxidation process for CH_3 radicals

at 540°C means that the stationary CH_3 concentration is sufficiently high for recombination of CH_3 radicals to become important.

$$CH_3 + CH_3CHO = CH_4 + CH_3CO \text{ (or } CH_2CHO) \quad (9)a$$

$$CH_3 + CH_3 = C_2H_6 \quad (10)a$$

From the relative yields of CH_4 and C_2H_6 the ratio $k_9/k_{10}^{\frac{1}{2}}$ was evaluated and by combining this value with independent estimates at lower temperatures the Arrehenius parameters $A_9 = 1.6 \times 10^9 dm^{+3}$ $Mols^{-1} sec^{-1}$ and $E_9 = 8.2$ K cal mol^{-1} were obtained. k_{10} was taken from a mean value in the literature at 165°C from the work of Shepp, Kistiakowsky and Roberts[22]. The approximation for a value at 813 k is based upon transition state theory $A_{10} \propto T^{-2}$ and no activation energy.

$$k_{10} = 0.84 \times 10^{10} \text{ l mol}^{-1} \text{ sec}^{-1}$$

$$\text{giving } k_9 = 9.7 \times 10^6 \text{ l mol}^{-1} \text{ sec}^{-1}$$

The authors assumed that if no branching occured the initiation could be equated to the rate of termination by the relation.

$$k_1 [CH_3CHO] [O_2] = k_{10} [CH_3]^2 = rC_2H_6$$

The resulting values of k_1 were reasonably constant in view of the wide range of mixture composition and the 300-fold change in r C_2H_6. The increase at higher CH_3CHO concentrations might indicate an occurance of branching.

The lower values of rC_2H_6 gave $k_1 = 4.00$ l mol^{-1} sec^{-1} at 500°C. r_1 propanal = 0.076 l mol^{-1} sec^{-1} 440°C, if E_1 propanal is estimated at 171 K J mol^{-1}, a calculated k_1 propanal = 2.7 l mol^{-1} sec^{-1} at 540°C. The agreement of the two figures at 540°C was considered striking.

Thermal decomposition of the aldehydes

The mechanism of pyrolysis is relevant to the present investigation because the majority of the experiments performed in this work were with low levels of oxygen. A number of experiments were executed with no oxygen and the carrier gas comprising wholly of nitrogen.

Ho[24] found in this work on the thermal decomposition of ethanal, propanal, n-butanal and iso-butanal, the reactions were homogeneous and inhibited by propene, iso-butane and small amounts of nitric acid. The kinetic order of the uninhibited experiments exhibited little regularity. However, the kinetic and analytical results could be approximately described by a Rice-Herzfeld type mechanisms, with the kinetics in each case largely determined by the stability of radicals and their reactions in chain propagation and termination.

Since Rice and Herzfeld in 1934 proposed their mechanism for the thermal decomposition of ethanal, a lot of work has been published.

Laidler and Liu[25] list the features of the reaction consistent with the original mechanism.

(1) The main reaction products are methane and carbon dioxide. These are produced in the chain propagating steps.

(2) The order of the reaction is three-halves, but they found many experimental results, inconsistent as well.

The minor products were expected only to be hydrogen and ethane, where as acetone, propanal and ethene were reported. A lot of studies had been carried out on the effect of inert gas and the effects on the reaction rate. The authors undertook to explain the various anomalies and to explain their own results suggested the following mechanism which is a modified Rice Herzfeld mechanism.

1.	CH_3CHO	⟶	CH_3	+	CHO
2.	CHO	⟶	CO	+	H
3.	$H + CH_3CHO$	⟶	H_2	+	CH_3CO
4.	$CH_3 + CH_3CHO$	⟶	CH_4	+	CH_3CO
5.	CH_3CO	⟶	CH_3	+	CO
6.	$CH_3 + CH_3CHO$	⟶	CH_4	+	CH_2CHO
7.	CH_2CHO	⟶	CH_2	+	H
8.	$CH_3 + CH_3CHO$	⟶	$CH_3CO\ CH_3$	+ H	
9.	$CH_3 + CH_3$	⟶	C_2H_6		
10.	$CH_3 + CH_2CHO$	⟶	CH_3CH_2CHO		

x Rice Herzfeld

The overall order of the reaction was confirmed as 3/2. If the minor termination step (10) is ignored the rate of disappearance of ethanal is approximately equal to the rate of formation of carbon monoxide and methane.

$$r(CH_3CHO) = rCO = rCH_4 = r_4 (k_1/k_9)^{\frac{1}{2}} (CH_3CHO)^{3/2}$$

The overall rate constant was 0.91 $ml^{\frac{1}{2}}\ mol^{-\frac{1}{2}}\ sec^{-1}$

k_1 was also calculated as $2.5 \times 10^{-7}\ s^{-1}$. 450°C

Laidler with Eusuc[26] also investigated the kinetic and mechanisms of the thermal decomposition of propanal. Carbon monoxide and ethane were shown to be the major products, whilst C_2H_4 and H_2 were minor products and a trace amount of n-butane. The initial rate order was between 1.25 and 1.30, although disagreeing with earlier workers it agreed with H. Addition of CO and C_2H_6 had no effect on the rate.

In the decomposition of propanal, C_2H_5 is the most abundant radical and the combination of C_2H_5 is the predominant chain terminating step. Since this step is pressure independant and inert gas has no effect on the rate of decomposition chain initiation must be the first order process (1) .

The ratio C_2H_4/C_2H_6 was found to decrease with a decrease in pressure but increased with a decrease in temperature, the two reactions were judged to be in competition with each other. These experimental factors lead to the following mechanism being proposed:

(1) $C_2H_5\ CHO \longrightarrow C_2H_5 + CHO$.

(2) $X + CHO \longrightarrow CO + H + X$

(3) $C_2H_5 + C_2H_5\ CHO \longrightarrow C_2H_6 + C_2H_5CO$

(4) $C_2H_5CO \longrightarrow C_2H_5 + CO$

(5) $H + C_2H_5CHO \longrightarrow H_2 + C_2H_5CO$

(6) $C_2H_5 \longrightarrow C_2H_4 + H$

(7) $C_2H_5 + C_2H_5 \longrightarrow C_4H_{10}$ or $C_2H_6 + C_2H_4$

with the assumption of large chain lengths, the rate of disappearance of $C_2H_5\ CHO$ is given by:

$$r = k_3 \left(\frac{k_1}{k_7}\right)^{\frac{1}{2}} (C_2H_5CHO)^{3/2} + k_6 \left(\frac{k_1}{k_7}\right)^{\frac{1}{2}} (C_2H_5CHO)^{\frac{1}{2}}$$

An estimation of a possible contribution to the formation of ethene by a molecular process.

$$C_2H_5\ CHO \longrightarrow C_2H_6 + CO$$

was found to be less than 10%.

Because the overall reaction was expressed as the sum of two terms calculation of the activation energies was treated in the same way.

$$E_{\frac{1}{2}} = E_6 + \frac{1}{2}(E_1 - E_7)$$

$$E_{3/2} = E_3 + \frac{1}{2}(E_1 - E_7)$$

Using values from the literature $E_{\frac{1}{2}}$ = 80.9 k cal mol^{-1} $E_{3/2}$ = 49.0 K cal mol^{-1}. The experimental values were found to be 70.8 and 57.1 k cal mol^{-1} respectively. The authors admitted the agreement was not good and thought the mechanism was oversimplified.

Because the overall reaction was expressed as the sum of two terms calculation of the activation energies was treated in the same way.

$$E_{\frac{1}{2}} = E_6 + \frac{1}{2}(E_1 - E_7)$$

$$E_{3/2} = E_3 + \frac{1}{2}(E_1 - E_7)$$

Using values from the literature $E_{\frac{1}{2}} = 80.9$ k cal mol^{-1} $E_{3/2} =$ 49.0 K cal mol^{-1}. The experimental values were found to be 70.8 and 57.1 k cal mol^{-1} respectively. The authors admitted the agreement was not good and thought the mechanism was oversimplified.

STIRRED FLOW REACTORS

Introduction

In flow reactors a physical process; the rate of flow is opposed to a chemical process, the rate of reaction. This opposition leads to a steady-state concentration of products and reactants in the reactor, and a determination of these concentrations combined with a knowledge of the volume of the reactor and the flowrates allows one to determine the rate of the chemical process. Since the physical process, the flowrate can be varied over a wide rante, flowrmethods are applicable to a very large dynamic range of reaction rates. Reactions with half lifes as samll as two milliseconds and as large as ten thousnad seconds have been investigated in such systems.

Two types of flow reactors exist, tube flow and stirred flow reactors. In a tubular flow reactor, concentrations change from entrance to exit. The concentrations of products and reactants at any point being invarient with time under steady-state conditions.

Stirred flow reactors are fundamentally different from tubular flow reactors because the concentrations of products and reactants are assumed to be uniform throughout the reactor volume.

Applications in gas phase kinetic studies

The early developments and derivation of kinetic parameters in gas phase stirred flow reactors and references to experimental work can be found in the review by Herndon[28], and Mulcahy's book on gas kinetics.[29] The reactor design used in our laboratory can be attributed to Mulcahy who first used the gas phase stirred flow reactor to study the pyrolysis of di-t-butyl peroxide[29].

The reactor was developed from a design by Longwell and Weiss[30] who studied the high temperature combustion of hydrocarbon fuels, where as rapid mixing as possible of the hydrocarbon with oxygen was required. The authors acknowledge the use of types of stirred flow reactor for kinetic investigations in the liquid phase and indicate that little attempt had been made to develop a stirred flow reactor technique for the study of gaseous reactions.

The object was to study the first order decomposition of di-t-butyl peroxide to ethane and ethanone.

$$((CH_3)_3 CO)_2 - 2 (CH_3)_2CO + C_2H_6$$

The relationship between the rate constant of a first order reaction k and the rate of influx of reagent n_o (moles sec^{-1}), efflux of products n_p and flow of the carrier gas n_c is given as;

$$k = \frac{n_p RT \left(x(n_o + n_c) + (x-1)\, n_p \right)}{x\, PV \left(x\, (n_o - n_p) \right)}$$

x = the number of products molecules formed by the reaction of one reagent molecule.

N N_p and N_c are respectively the number of moles of reagent, products and carrier gas in the reactor at the steady rate.

n = (moles sec^{-1}) is the rate of flow of reagent out of the reactor.

p = The total pressure in the reactor.

v = The volume of the reactor.

T = The absolute temperature.

k = The first order rate constant.

The above equation (1) stems from the steady state opposition of flow and reaction.

In the steady state we have

$$\frac{dN}{dc} = n_o - kN - n = o \qquad 2.$$

and $n_p = x\,kN$ 3.

whence $n = (xn_o - n_p)/ x$ 4.

Applying the gas equation we have:

$$P\,V = (N + N_p + N_c)\,R\,T \qquad 5.$$

from the assumption of complete mixing,

$$\frac{n}{n_c} = \frac{N}{N_c} \quad \text{and} \quad \frac{n}{n_p} = \frac{N}{N_p} \qquad 6 \text{ \& } 7$$

equations 4,5,6, and 7 give,

$$N = \frac{P\,V}{RT}\left(\frac{x(n_o - n_p)}{x\,(n_o + n_c) + (x-1)n_p}\right) \qquad 8.$$

Equation 3. yields ,

$$k = \frac{n_p}{xN} \qquad 9.$$

Combining these latter two equations together gives equation 1. The rate of reaction was determined by measuring the rate of generation of ethane (n_e mols sec^{-1}). Since $N_e = 1/3\ n_p$ and $x = 3$ in equation 1. the appropriate form of the equation becomes:

$$k = \frac{n_e\ R\,T\ (n_o + 2E + n_e)}{P\,V\ (n_o - n_e)} \qquad (A)$$

The design of the vessel was shown to be satisfactory by checking the consistency and accuracy of the rate constant calculated by substituting the appropriate measurements in equation (A).

The decomposition of di-t-butyl peroxide was chosen for the test on the reaction as the stoichometry had been previously well established.

The effect of side reactions and heterogeneous decompositions were small, and several investigators had obtained values for the rate constant that agreed over a range of temperatures by the static method.

They conclude their summary thus:

" The rate constant of the decomposition of di-t-butyl peroxide was determined over the temperature range 430K-530K. The values derived on the assumption of complete mixing in the reactor were independent of the degree of conversion and in excellent agreement with those obtained by previous authors using the static method".

A detailed study of a compound was reported by K J Hole and M F R Mulcahy[31] in the pyrolysis of biacetyl and the third body effect on the recombination of methyl radicals.

The study was carried out to examine the behaviour of methyl and acetyl radicals, to test the suitability of biacetyl as a pyrolytic source of methyl radicals for studies at higher temperatures than were suitable for less stable sources such as di-t-butyl peroxide and azomethane. They also reported a kinetic analysis of the overall reaction which had not been carried out previously.

The decomposition to carbon monoxide, methane, ketene, acetone, ethane and 2,3 pentanedione was shown to be a chain reaction initiated by reactiona, propagated by reactions b and c and terminated by reaction d which was strongly pressure dependant.

$$(CHCO)_2 \quad - \quad 2CH_3CO \qquad \text{a.}$$

$$CH_3 + (CHCO)_2 \quad - \quad CH_4 + CH_2COCOCH_3 \qquad \text{b.}$$

$$CH_3 + CH_3 \ (+M) \quad - \quad C_2H_6 \ (+M) \qquad \text{c.}$$

$$CH_3 + (CH_3CO)_2 \quad - \quad (CH_3)_2CO + CH_3CO \qquad \text{d.}$$

Pressures of biacetyl at which the second order rate constant for reaction 6. is half its limiting high pressure value, increased from 14 torr at 677K to 30 torr at 776K and were in satisfactory agreement with values calculated by previous authors on the basis of the R.R.K.M. theory assuming a "loose" activated complex and strong deactivating collisions. The experiment was performed in both packed and unpacked reactors, the surface exerted little effect on the overall kinetics.

Thermal decompositions at higher temperatures can proceed via radical chain reactions, which can give rise to complications in the interpretations of the results.

Szwarc[32] was able to use experimental conditions under which the chains were suppressed by using toluene as a carrier gas, in his flow system, thus he initiated the toluene carrier technique. The compound is pyrolysed in an excess of toluene which will then act as a radical scavenger.

The dissociation energy of a bond in a compound to be studied, must be lower than that of the $PhCH_2$- H, by an amount sufficient to make the extent of toluene decomposition negligible under the conditions used for the technique to be successful.

For a compound R_1R_2

$$R_1R_2 \longrightarrow R_1^{\cdot} + R_2^{\cdot}$$

$$R_1 + PhCH_3 \longrightarrow R_1H + PhCH_2^{\cdot}$$

$$R_2^{\cdot} + PhCH_3 \longrightarrow R_2H + PhCH_2^{\cdot}$$

$$2PhCH_2^{\cdot} \longrightarrow \text{dibenzyl}$$

The rate of initial decomposition is given by the rate of formation R_1H or R_2H. Hence one can calculate an accurate rate constant and by varying temperature, Arrehenius parameters and the bond dissociation energy can be found.

The pyrolysis of ethylbenzene by the toluene carrier method was carried out in a stirred flow reactor by C W P Crowne, V J Grigulis and J J Throssell[23]. This was a reinvestigation of a reaction studied by Szwarc on a plug flow reactor whose Arrehenius parameters were suspected of being low. It was suggested that a significant number of methyl radicals could be removed by benzyl radicals (recombination of R_1 and R_2 in the earlier reaction scheme) under the experimental conditions.

The stirred flow reactor paper assumed that mixing was complete giving a homogeneous distribution of reactants and products throughout the reaction zone. This permitted the derivation of a simple flow formula for the first-order specific rate of decomposition of ethylbenzene which included a correction for the rate of removal of methyl radicals by recombination with benzyl radicals.

The Arrehenius parameters obtained were in close agreement with values reported from later work performed with an aniline carrier.

The kinetics of the gas phase pyrolysis of poly(diflouroamino) flouromethanes have been studied by J M Sullivan, A E Axworthy and T J Houser[34] over the temperature range 463-733K in stirred flow, tubular and static reactors. The reactions of tetrakis(diflouroamino) methane, $C(NF_2)_4$. Tris (diflouroamino) flouromethane $FC(NF_2)_3$ and bis (biflouroamino) flouroamino $F_2C(NF_2)_2$ were found to be first order non chain processes with C-N bond rupture as the rate determining step in each case. Rate constants and activation energies giving a

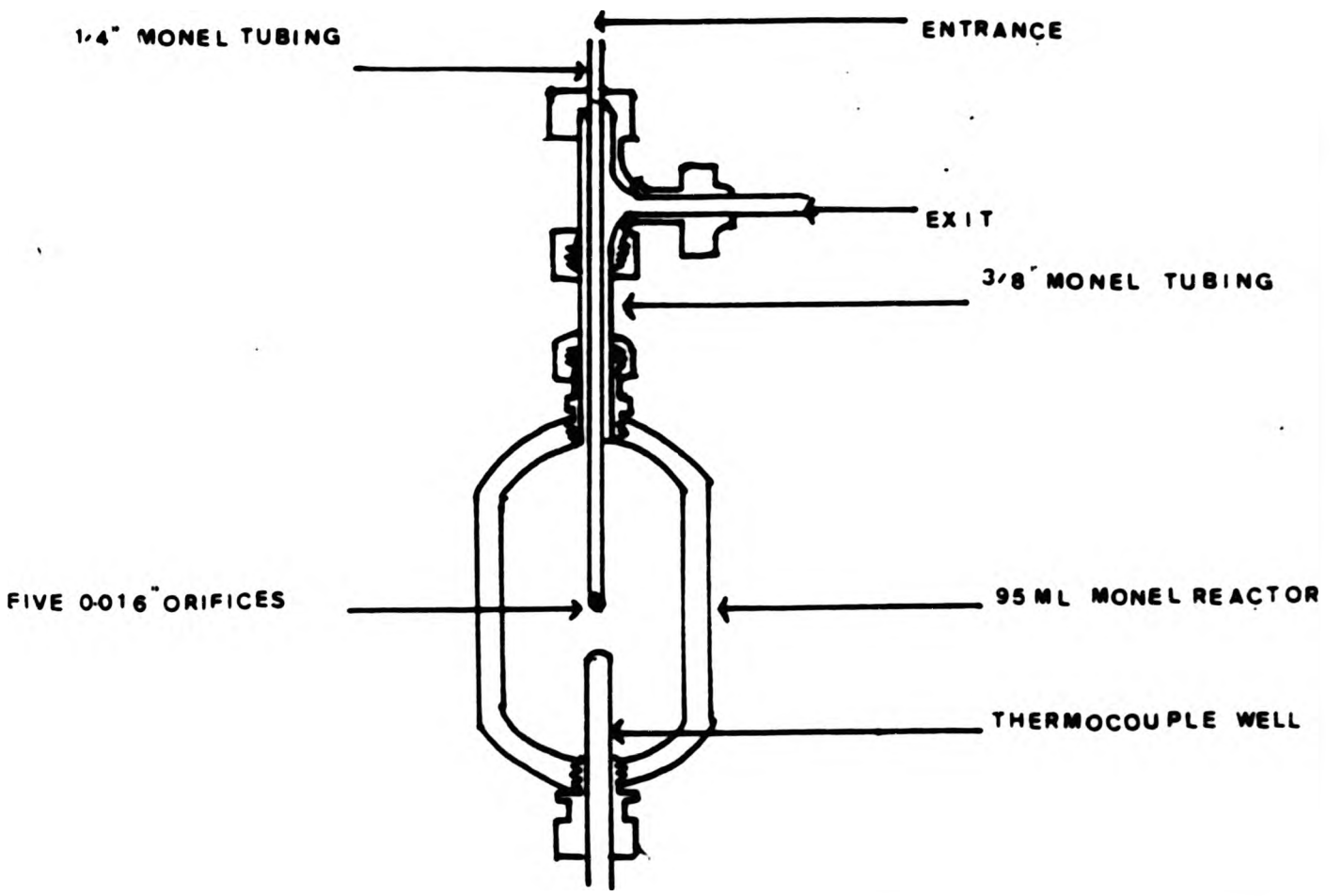

Figure 1

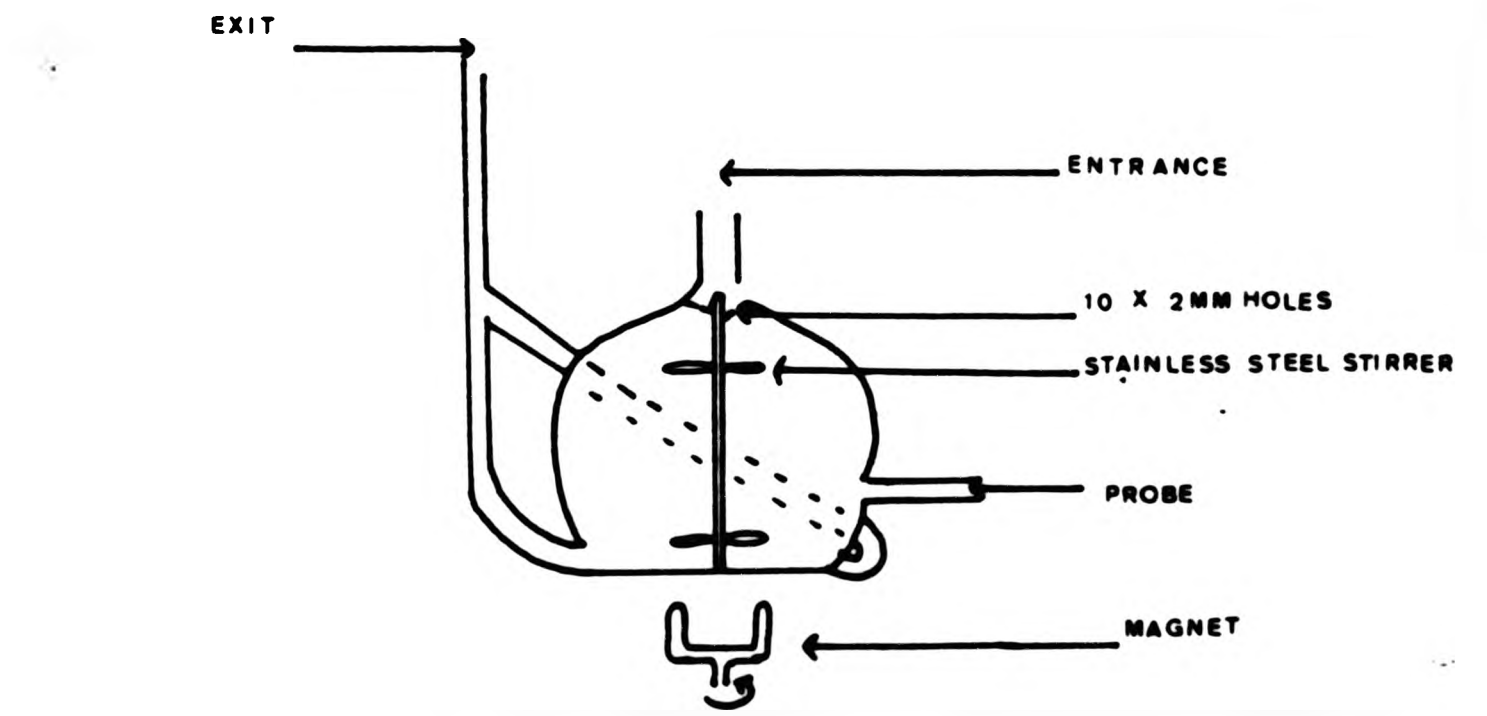

Figure 2

measurement of the bond dissociation energies for the first C-N bond were measured for each molecule.

A major portion of the data was obtained using a gas-phase, stirred flow reactor. The compound investigated was contained in a 1.5 ft^3 stainless steel tank as an approximately 1% mixture with Helium. The total pressure of the gases within the tank ranged fron 30 to 100 p.s.i. The flowrate was controlled using a Nupro fine metering valve. Any additions were mixed with helium and introduced from an auxillary tank. The reactor is illustrated in figure 1.

The reactor was heated electrically. The flow of the exit stream was measured with a soap bubble flow meter, from which the gas was vented at atmospheric pressure. The gases leaving the reactor were analysed by gas chromatography.

A stirred flow reactor system which avoided most of the difficulties encountered with static vessel experiments in combustion studies is utilised by B F Gray and P G Felton[36]. This method of studying the non-isothermal oxidation of hydrocarbons was used to determine the thermokinetic character of the low temperature oxidation of propane.

The experimental data was recorded and used to produce temperature time histories of the reaction as well as values of heat release. Accurate ignition and extinction limits were determined and the shape of the heat release curves allowed predictions of ignition and extinction characteristics under differing physical conditions. Comparison with the classical steady state methods were made throughout. A description was made of phenomena which could not be properly observed in a static reactor; the existance of a thermokinetic steady state, and investigation into a hysteresis effect with respect to the reactant temperature.

The apparatus was a novel kind of flow reactor illustrated in figure 2. This was incorporated in a subatmospheric flow line. The flow line consisted of two sections, a high pressure flow regulation system and a low pressure gas handling section. The gases flowed into the low pressure section via small orifices made from watchmaker jewwls of artificial ruby. The low pressure gases were then admitted into a mixing tube, before being passed into the stirred flow reactor. On their exit the exhaust gases passed through a trap where liquid products were condensed, the remaining gases flowed via a needle valve to a solid CO_2 trap and a rotary pump. The needle valve was used to limit the pumping rate, thus controlling the reactant pressure and the residence time.

The experimental procedure consisted of flushing with nitrogen at the starting temperature, usually 573K, the propane flow was started, the nitrogen stopped. The propane pressure was allowed to stabilise, before admitting oxygen. At this point any desired adjustments to the total pressure and residence time were made using the needle valve. The oven temperature was increased by 5K increments, with the temperature excess recorded for each temperature followed by a period for equilibriation. This procedure was repeated until the maximum operational temperature was reached. The procedure was then reversed and the temperature reduced step wise until no more appreciable heat loss was observed.

Described in the literature as a novel method of using a stirred flow reactor, A C Baldwin, I M Davidson and A V Howard[36] used their stirred flow reactor with a pulsed technique, in which a pulse of

reactant vapour was injected into a carrier gas stream, passed into a minature reactor where it was partially converted to products and then into a gas chromatograph, where the amounts of products formed and reactants undecomposed were measured.

The experimental side of the apparatus comprised of a small fused quartz spherical stirred flow reactor commected to a gas chromatograph with a storage vacuum line for reactants and samples of products. The technique is compared with conventional pyrolysis gas chromatography where a pulse of reactant is passed through a narrow tubular reactor. The authors claim that uncertainties in the concentration gradient in such a reactor preclude its use for kinetic studies beyond approximate estimates of first order rate constants. Using the pulsed stirred flow technique, accurate kinetic data could be obtained. Unlike an ordinary stirred flow reactor, a steady state does not exist, after injection the pulse is dispersed in the reactor and then steadily swept out by the carrier gas until the reactor is "empty".

Because of the difference in operation, kinetic equations were derived firstly for the time-dependance of concentration in the reactor resulting solely from the pulsed method of operation, without any chemical reaction. This required two conditions to be fulfilled:

1. Perfect pulsed behaviour, the pulse is of small volume relative to the reactor, entering it and being dispersed throughout almost instantaneously.

2. Perfect mixing, the dispersal of the pulse throughout the reactor is uniform.

The mass balance is then:

$$u(A_i(t)) - u(A_o(t)) = 0 + \frac{d}{dt} V(A_o(t))$$

u is the volumetric flow of carrier gas through the reactor.

$(A_i(t))$ and $A_o(t))$ are the concentrations of the injected compound A at the inlet (i) and outlet ($_o$) of the reactor at any time (t).

V is the volume of the reactor in cms^3.

It is a consequence of perfect mixing that $(A_o(t))$ is also the concentration at any point within the reactor, leading to:

$$(A_o(t)) = (A_o(o)) \exp(-t/T)$$

$A_o(0) = A_o/V$ $\quad T = V/u$ = residence time of reactor.

These equations based on the assumption of perfect mixing and perfect pulsed behaviour were tested experimentally by injecting a pulse of methane, where no decomposition occured and the response curve of the gas chromatograph detector was observed. There was reported good agreement between the experimental curve and the calculated points, showing that both conditions were fulfilled.

Equations were derived for a reactive pulse being introduced into the reactor, for the case of a reaction A → B occuring with order n and rate constant k.

$$\int_0^\infty k V(A_o(t))^n \, dt = (B)$$

Where (B) = number of moles B measured at the outlet giving,

$$k = \frac{B}{A_o T}$$

For equations where $n \neq 1$ and the time dependance of the concentration was not known, the rate constant could be found as long as the percentage conversion of A to B was small:

$$(B) = (A_o)^n \left(\frac{k T}{V^{(n-1)}_n} \right)$$

where a plot of Log B v Log A_o would give a straight line of slope n.

Expressions for the case, where the major decomposition route was by a first order reaction, accompanied by a concurrent minor reaction of an order other than one are also presented.

An experimental feature of the technique was that 99% of the pulse would have left the reactor after a time of 4.85T, if the retention in the chromatograph is less than this, the product would not be properly detected. On the other hand, porducts with a rentention time greater than 10T had slight tailing and some loss of resolution. The spherical reactor of fused quartz was similar in design to that used by Mulcahy and Williams but was considerably smaller. Two different vessels were used, one with an effective volume of 54.6 cms^3 and the other of 10.4 cms^3 (compared with 300cms^3 in the continuous flow reactor of Mulcahy and Williams)

The technique was tested against a known reaction; the thermal isomerization of Cyclopropane to propene. The rate constant reported by Falconer, Hunter and Trotman-Dickenson[37]

$$Log_{10} k/\ sec^{-1} = 15.45 - (274.5KJ\ mol^{-1}/2.303\ RT)$$

agrees within the bounds of experimental error with the pulsed flow results

$$Log_{10} k/\ sec^{-1} = (15.76 \pm 0.36) - 279.2 \pm 5.6)\ KJ\ mol^{-1}/\ 2.303\ RT$$

A recent paper by Benson and Weissman[38] studies chain reactions in stirred flow reactors. It begins with a comparison of the kinetics of chain reactions in stirred flow with convenional reactors. In a plug reactor, with a stationary state in every differential segment the following equation holds:

$$u_{in} + R_i = u_{out} + R_t \qquad (1)$$

Where u_{in} and u_{out} are the inflow and the outflow radical rates, R_i and R_t are the chain initiation and termination rates.

In the stirred flow reactor $u_{in} = 0$. Thus the stationary condition becomes:

$$R_1 = u_{out} + R_t \qquad (2)$$

Two extreme situations are possible,

$$u_{out} \ll R_t \qquad R_i = R_t \qquad (3)$$

$$u_{out} \gg R_t \qquad R_i = u_{out} \qquad (4)$$

By comparing the termination rates for the commonly encountered termination types (5-7) with the escape rates of radicals (8) one obtains the limits for the radical concentrations below which the escape rate becomes predominant (4).

$$R_t = k_t (R)^2 \qquad (5)$$

$$R_t' = k_t' (R)(R') \qquad (6)$$

$$R_t' = k_t'' (R)^2 (M) \qquad (7)$$

$$u_{out} = k_e (R) \qquad (8)$$

Where k_t, k_t', k_t'' are the rate constants corresponding to the particular termination steps. (R), (R') are radical concentrations and (M) is the total concentration in the system. $k_e = 1/t$ expresses the escape rate constant (in $secs^{-1}$) and t is the residence time.

In the chain reaction,

$$RH \xrightarrow{i} R^{\cdot} + H^{\cdot}$$

$$X_2 + R^{\cdot} \xrightarrow{p'} RX + X$$

$$RH + X^{\cdot} \xrightarrow{p} HX + R^{\cdot}$$

$$X^{\cdot} + X^{\cdot} + M \xrightarrow{t} X_2 + M$$

$$X^{\cdot} \xrightarrow{e} \text{out}$$

Using the whole expression for the mass balance (2) for the radicals X(10) and the reactant RH (11) one obtains the rate law (12).

$$2 k_i (RH) = k_e (x) + 2 k_t (M) (X)^2 \qquad (10)$$

$$k_e (RH)_o = k_p (X) (RH) + k_e (RH) + k_i (RH) \qquad (11)$$

$$t^2 = \frac{k_t (M)}{k_i k_p^2} \frac{(C0-C)^2}{C^3} \left[1 + \frac{k_p}{2 k_t (M)} \frac{C}{Co-C} \right] \qquad 12.$$

Where $c_o = (RH)_o$ and $c = (RH)$ are the reactant concentrations in the inflow and outflow from the reactors. k_e is the same for all the species.

While rate measurements in a conventional system or for a simplified mass balance such as can be derived for equation (3) or (4) yield only one constant, rate measurements in which (12) is valid yield two constants. Rearranging (12) and representing $t^2c^3/ (c_o-c)^2$ as a function of c/c_o-c from

$$\frac{t^2c^3}{(c_o-c)^2} = \frac{k_t (M)}{k_p^2 k_i} + \frac{1}{2k_i k_p} \frac{c}{(c_o-c)}$$

the slope $(k_i k_p)^{-1}$ and the intercept $(k_t(M)/k_p^2 k_i)$ one can obtain two elementary rate constants as a function of the third. For a known rate

constant of the propagation k_p one can obtain independantly the rate constants for the initiation k_i and the termination k_t processes.

Such information is of special interest in the study of surfact effects on chain reactions. The conventional system yields only k_i / k_t. If a wall surface modification causes a change of this ratio it cannot be known whether this change comes from a variation of k_i or k_t. Analogously an unchanged ratio can mean an independence of both k_i and k_t, of surface effects or the sam kind of dependence on the surface. The authors point out the ability of the stirred flow reactor to furnish independant data regarding the elementary rate constants of the initiation and termination steps of chain reactions provided that the condition u_{out} is realised.

Advantages amd disadvantages of a stirred flow reactor

The conventional plug flow method is limited by uncertainty in defining the mass and heat transfer conditions in the reaction tube. In this respect the stirred flow reactor offers advantages.

In a plug flow method, the gas is heated by thermal conduction from the walls as it passes, by laminar flow through the reaction tube. This method of heating results in the gas spending an appreciable time in the tube before it reaches the reaction temperature. Whereas in the stirred flow reactor the vigorous mixing inherrent in the design produces uniform composition bringing about uniform temperature. Because the reaction is occuring at the same rate everywhere in the vessel, no temperature inequalities are produced by the heat of the reaction. In the stirred flow reactor the reagents are caused to flow continuously

through a reaction vessel designed to ensure that reagents, products and carrier gas are mixed uniformly throughout its volume. When a steady state is reached the mixture which flows out of the vessel has the same composition as the contents inside the reactor. The plug flow method involves the assumption that no mixing of reactants and products occurs in the reaction tube. Experimentally it is harder to achieve a condition of no mixing than a condition of complete mixing.

Advantages of the stirred flow reactor over a static reactor include no error being involved in the time taken to admit the reactants and the lack of temperature equiliberation during the reaction. Another possible error in static reactors likely to influence the results is that which can be caused by dead space, that is by any volume containing reactants which are not heated to the reaction temperature. This might easily amount to several per cent of the total volume.

As mentioned above in the perfectly stirred condition, the concentrations of reactants, products and any intermediate species in the reactor are all maintained constant. Therefore the rate of efflux of each product and intermediate species is precisely equal to the rate at which the species is produced by the reaction at stationary concentrations of all the other species, including primarily the reactants. Since these concentrations can be determined in the effluent gas this fact is of great value in studies of complex reaction mechanisms.

Stirred flow reactors allow simple treatment of results, the time-invarient concentrations in such a system allow one to determine rates of reaction from algebraic expressions rather than differential or intergrated rate equations.

Disadvantages of all flow systems are that there is a difficulty in making accurate quantitative measurements on very small product yields in the presence of excess reactant and inert carrier. It is necessary to have a constant flow regulation to maintain a constant contact time, one consequence is that flow methods lack some of the control that is possible with the static method; it can be difficult to change one variable such is the degree of the reaction. A major disadvantage is the time consuming nature of an experiment. Critics point out the uncertainty in the extent that any particular system deviates from the assumption of complete mixing. The principle assumption in flow reactor theory is that after a short induction period reactants and products are uniformly mixed and a concentration steady state exists. This will depend not only on the design of the reaction vessel but also on the rates of the reaction occuring within the vessel. Therefore the gases entering the vessel should be mixed with those already in the vessel in a time which is small compared to the rate of reaction.

A paper submitted by J M Sullivan and T J Houser[39] investigated the mixing efficiency within a typical stirred flow reactor. The design chosen for this investigation was similar to that used in this work and first attributed to Mulcahy.

The experimental procedure was to admit from two tanks, a mixture of nitrogen and helium and pure helium. First the N_2/He mixture was allowed to flow through the reactor until the desire flowrate was achieved the first tank being closed, a needle valve controlling the

flow rate remaining at the same setting. The whole system was then purged with pure helium for several minutes. The purge was stopped and the mixture of gases passed through the reactor again, the change in gas concentration was recorded with time using the thermal conductivity cell of a gas chromatograph. According to the theory if a mixture of inert gases is allowed to pass through a stirred flow reactor the change in concentration of each component with time is given by:

$$\frac{dA}{dt} = \frac{(U)}{(V)} (A^{O} - A)$$

A^{O} = Concentration of a gas entering the reactor

A = Concentration of a gas leaving the reactor and equal to its concentration throughout the reactor

U = Volume flowrate of the gases

V = Volume of the the reactor

Integration of the above equation showed that the gases within the reactor approach a steady state according to:

$$A = A^{O} (1 - \exp(-Ut/V))$$

A set of experiments covering a wide range of flowrates were performed (48.9-2046mls min^{-1}). Two of which are reproduced in the graphs 1 and 2 overleaf.

As seen from the graph the experimentally determined concentrations of N_2 agree with those predicted by the second equation, indicating that there is essentially complete mixing within the reactor.

GRAPH 1

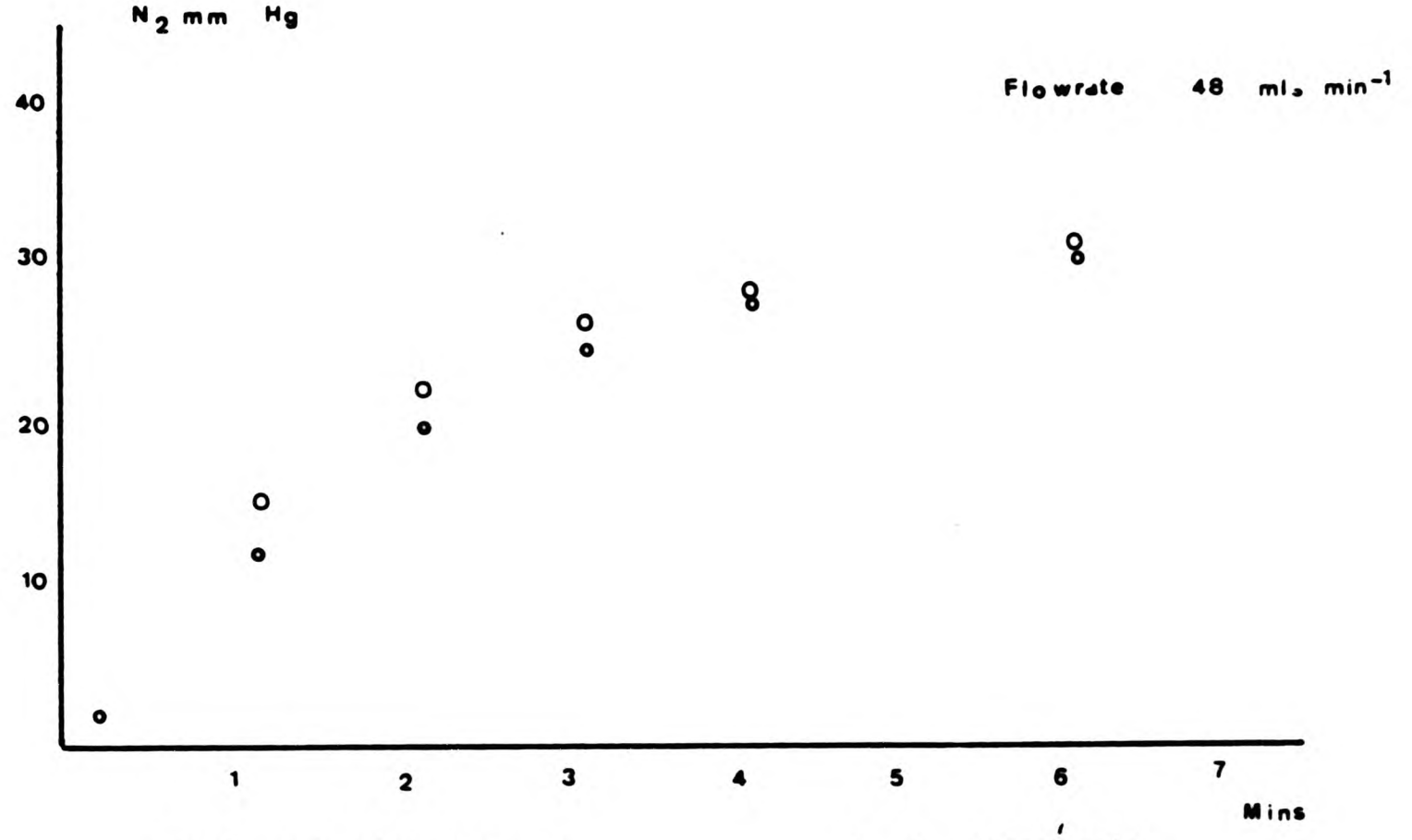

O A calculated mm Hg

o A experimental mm Hg

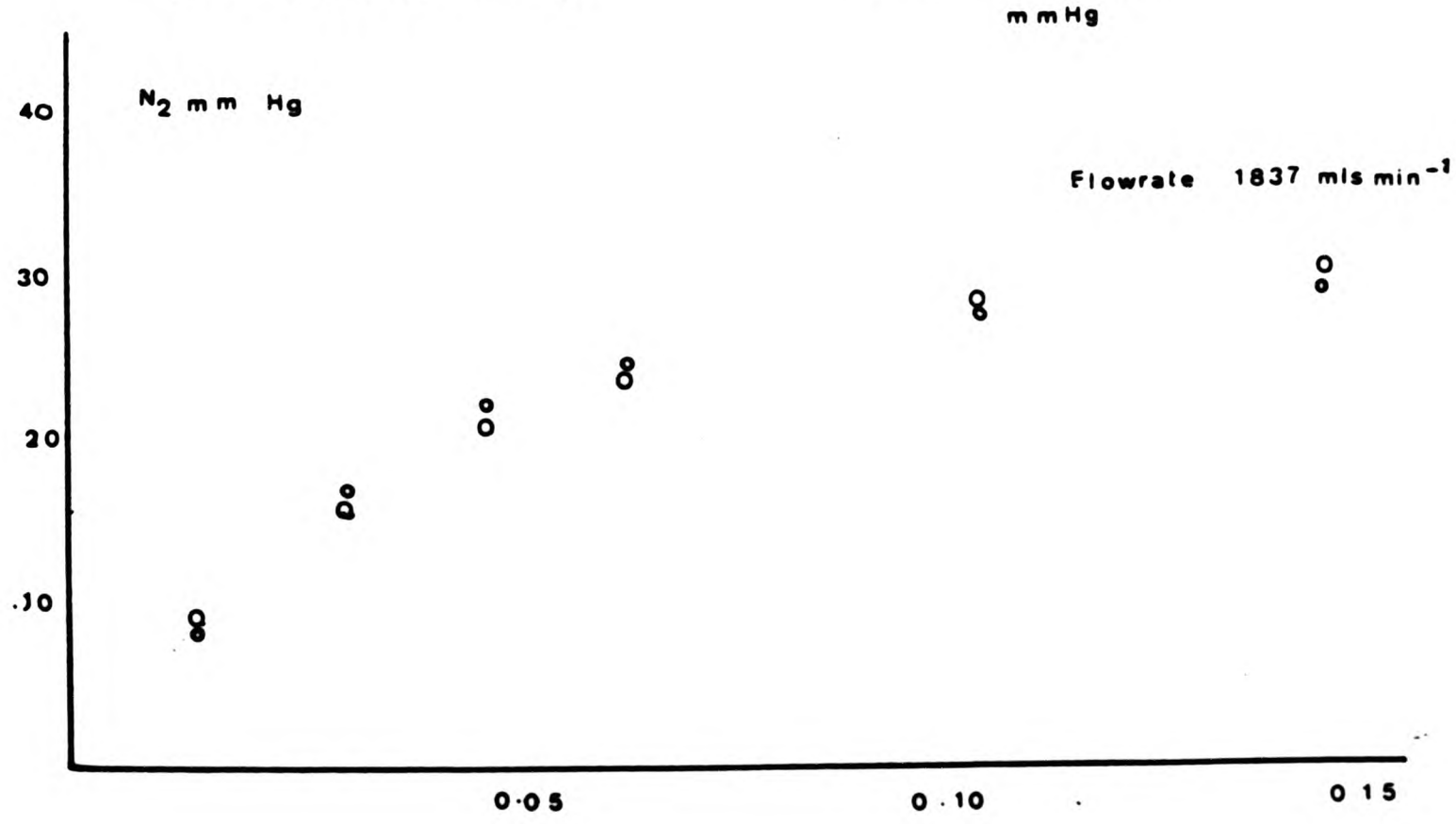

A^o = 32 mm Hg

GRAPH 2

GRAPH 3

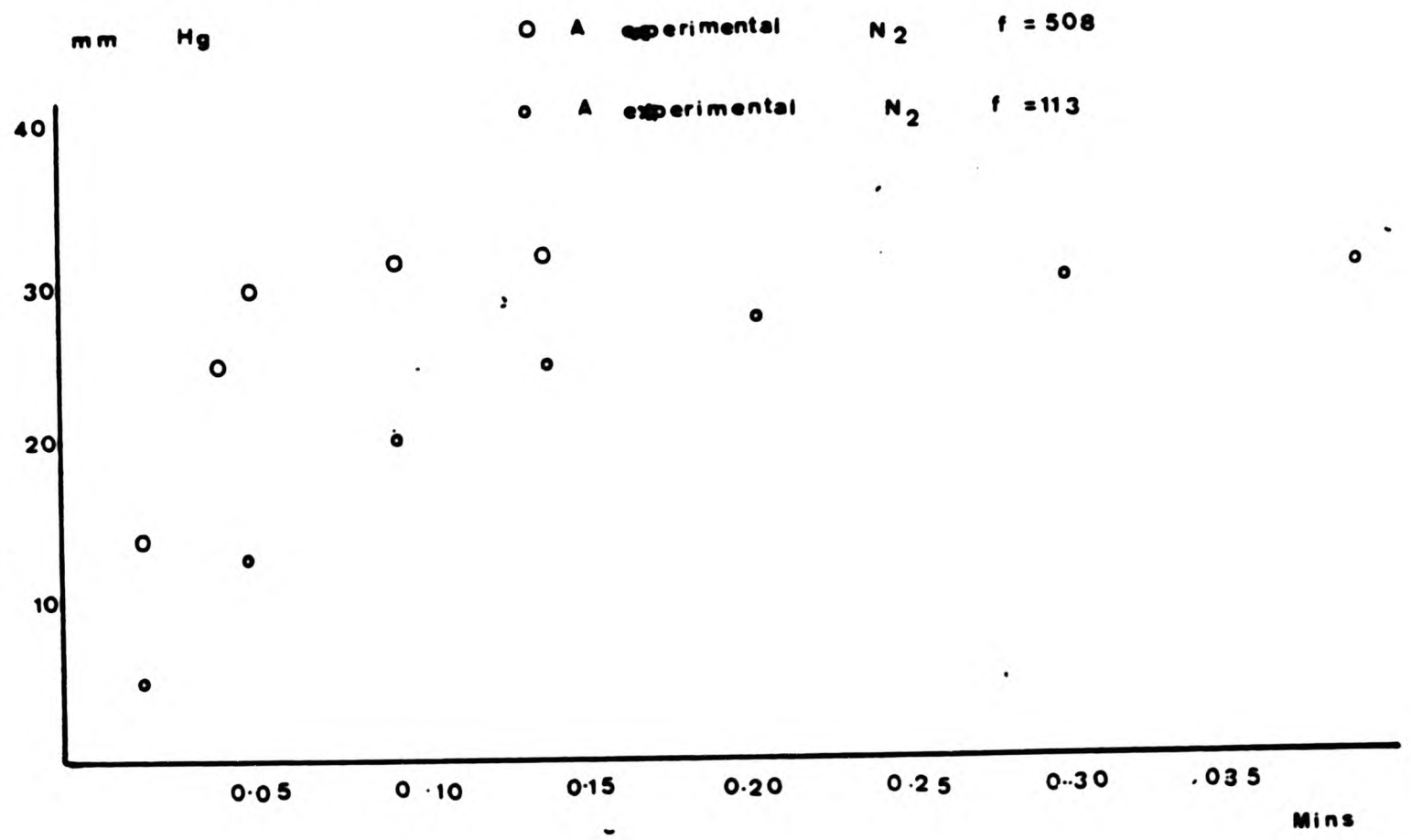

mm Hg GRAPH4

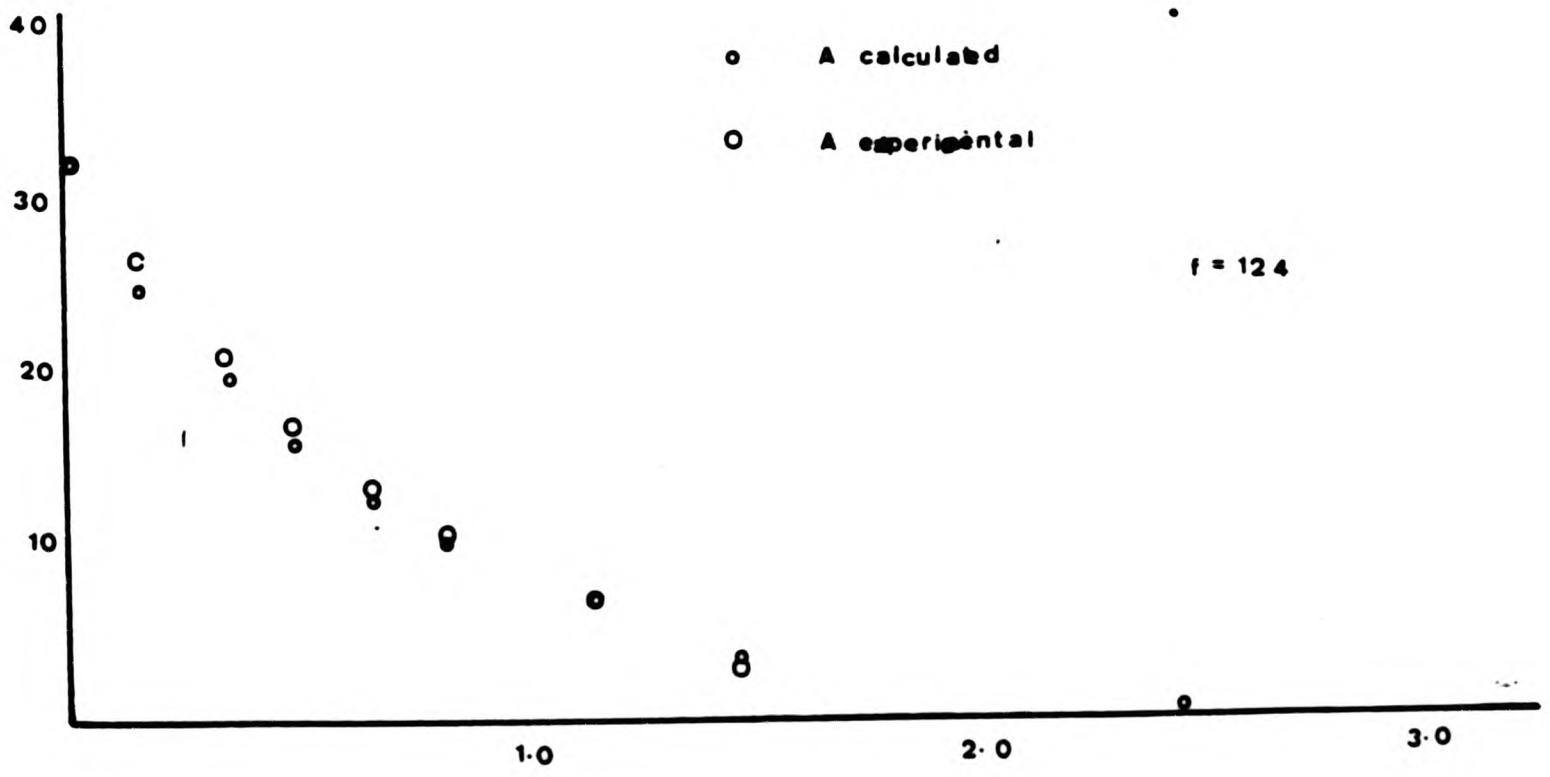

In order to confim these results, a series of experiments was conducted in which the gas mixture was allowed to by-pass the reactor and flow directly into the thermal conductivity cell. In this case there should have been little mixing and the gases might be said to exhibit "piston flow". A set of experiments were performed at different flow rates over the range 103-1050 mls min^{-1}. On set of experimental results are illustrated in the third graph, where the N_2 pressure approaches a step function at higher flow rates.

In addition complete mixing within the reactor was confirmed by a third series of experiments in which pure He was allowed to flow through the reactor, which was initially filled with a mixture of N_2 and He. In this case the concentration of nitrogen was expected to decrease with time according to the first equation for the case of A^0. The approach to a steady state would then be of the form:

$$A = A_i \exp(-Ut/V)$$

where A_i equals the initial concentration of gas in the reactor. The decrease in concentration with time predicted by this equation is similar to that found for the first order reaction rates of a single reactant, the difference being that the first order rate constant is replaced by (U/V). One set of results from these experiments is reproduced on the fourth graph. The experimental results are in good agreement with those predicted for stirred flow.

Stirred flow studies have usually centered on the pyrolysis, decomposition and measurement of bond dissociation energies of hydrocarbon and oxygenated compounds. The present work reports the

application of a flow reactor to the oxidation of aldehydes. The technique results in short reaction times, coupled with a very low percentage reaction and was hoped to effectively limit the extent of chain reactions involving free radicals.

DESCRIPTION OF APPARATUS AND EXPERIMENTAL PROCEDURE

The Apparatus

The apparatus was developed to produce a three component reaction mixture of oxygen, aldehyde and a dilutant carrier gas: nitrogen, incorporating a stirred flow reactor.

Primarily it was intended to collect any hydrocarbons produced from the reaction vessel, especially for the measurement of the C_2H_4/C_2H_6 ratio in oxidation of propanal.

.It was considered important to include in this section an estimation of errors in the hydrocarbon ratio, as well as the errors included in measuring the total hydrocarbons.

The Vacuum Line

The overall layout of the flow apparatus is shown in figure 3. The main manifold was pumped by an Edwards rotary vacuum pump, connected through a two stage mercury diffusion pump, to ensure a hard vacuum initially. In beween the two pumps was a liquid nitrogen trap, doubling as a ballast volume.

An auxillary vacuum system was used consisting of a second rotary pump to provide backing pressure, to control a McLeod gauge, a Toepler pump and a gas burette.

Low pressure in the vacuum line was measured by the McLeod gauge which also provided an absolute calibration reading for the spiral 'Bourdon' gauge, used to measure the reactant pressure immediately before entering the stirred flow reactor.

The premixed carrier gas was admitted into the vacuum line at point B, the aldehyde from a vessel connected to the flow system by ground glass ball joints.

The reaction products were trapped in a series of glass traps. During a flow experiment any non condensible gases were passed through the main rotary pump by connection at point A.

A connects to A'

B carrier Gas

C bourdon gauge

D gas standards

E gas analysis

F mcleod gauge

G flow reactor

H diffusion pumps

J manometer

'K reactant resevoir

I rotary pump

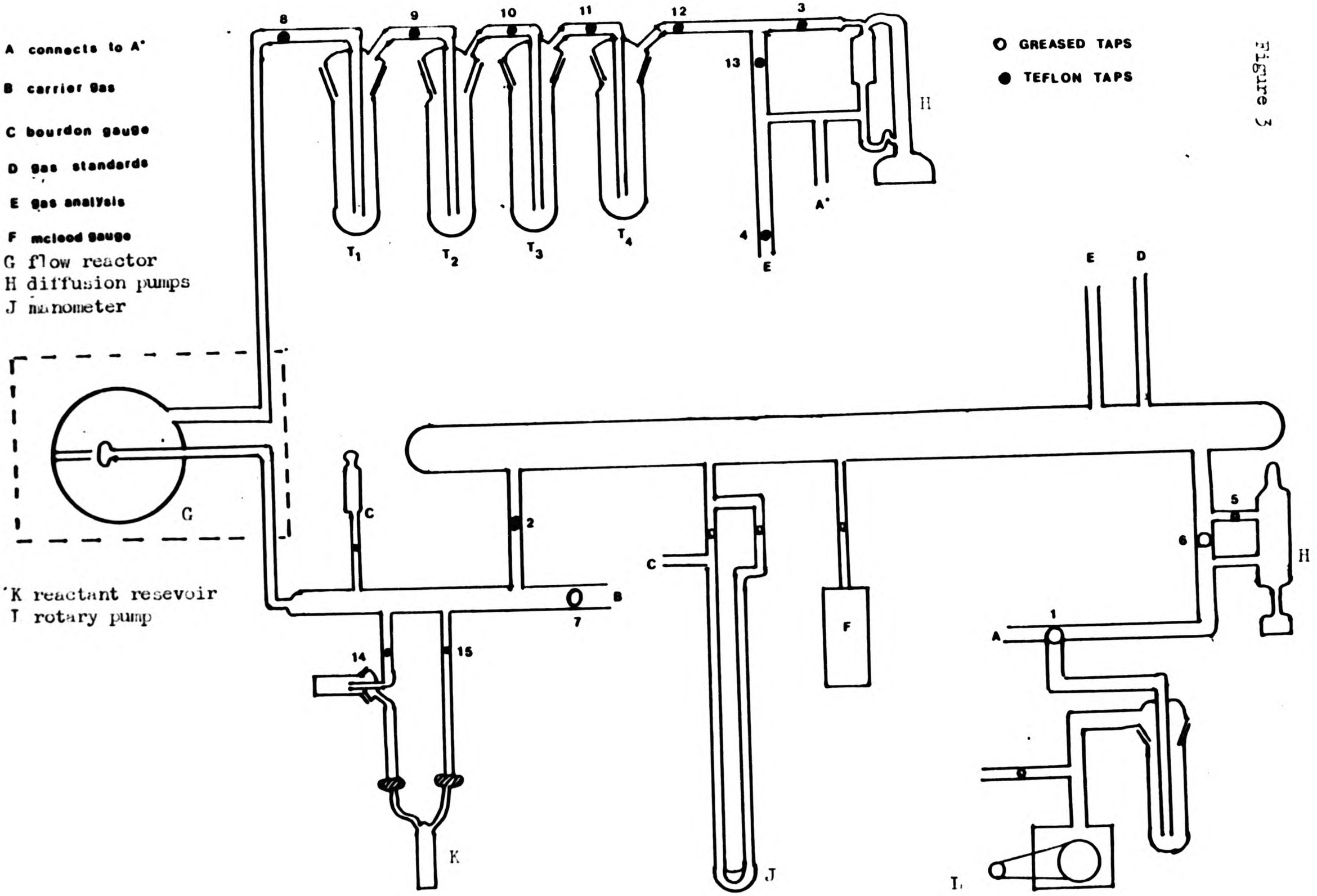

Figure 3

The Reaction Vessel

The reaction vessel, a stirred flow reactor is shown in figure 4. The design is identical to that used by Crowne, Throssell and Grigulis[1], a modified version of that used by Mulcahy and Williams[29]

The surface of the vessel used in the first experiments was left uncoated, the vessel itself was made of fused silica joined to the rest of the vacuum line by two graded seals. The volume of the vessel was taken to be that enclosed by the main sphere and this was determined by filling this part of the vessel with water and weighing it. The volume was found to be 270 cms^3.

The surface of the vessel used in later experiements was coated with Boric acid, laid by dusting the inside of the vessel with finely ground boric acid and heating in a muffle furnace. Repetition of this process five times was judged to give a good overall coating. The vessel was manufactured from pyrex glass and the volume was found to be 259 cms^3.

The Furnace

The reaction vessel was mounted horizontally inside a cylindrical refractory tube. Dimensions: 30 cms in length and 8 cms in diameter. A length of nichrome ribbon with a resistance of 55 ohms was tightly wound around the outside of this tube in such a way as to provide a uniform temperature across the reaction zone. The wound core was installed and a temperature profile was produced by moving a thermocouple along the length of the inside of the core. The core was removed and the wire turns were moved in such a way as to attain

Figure 4

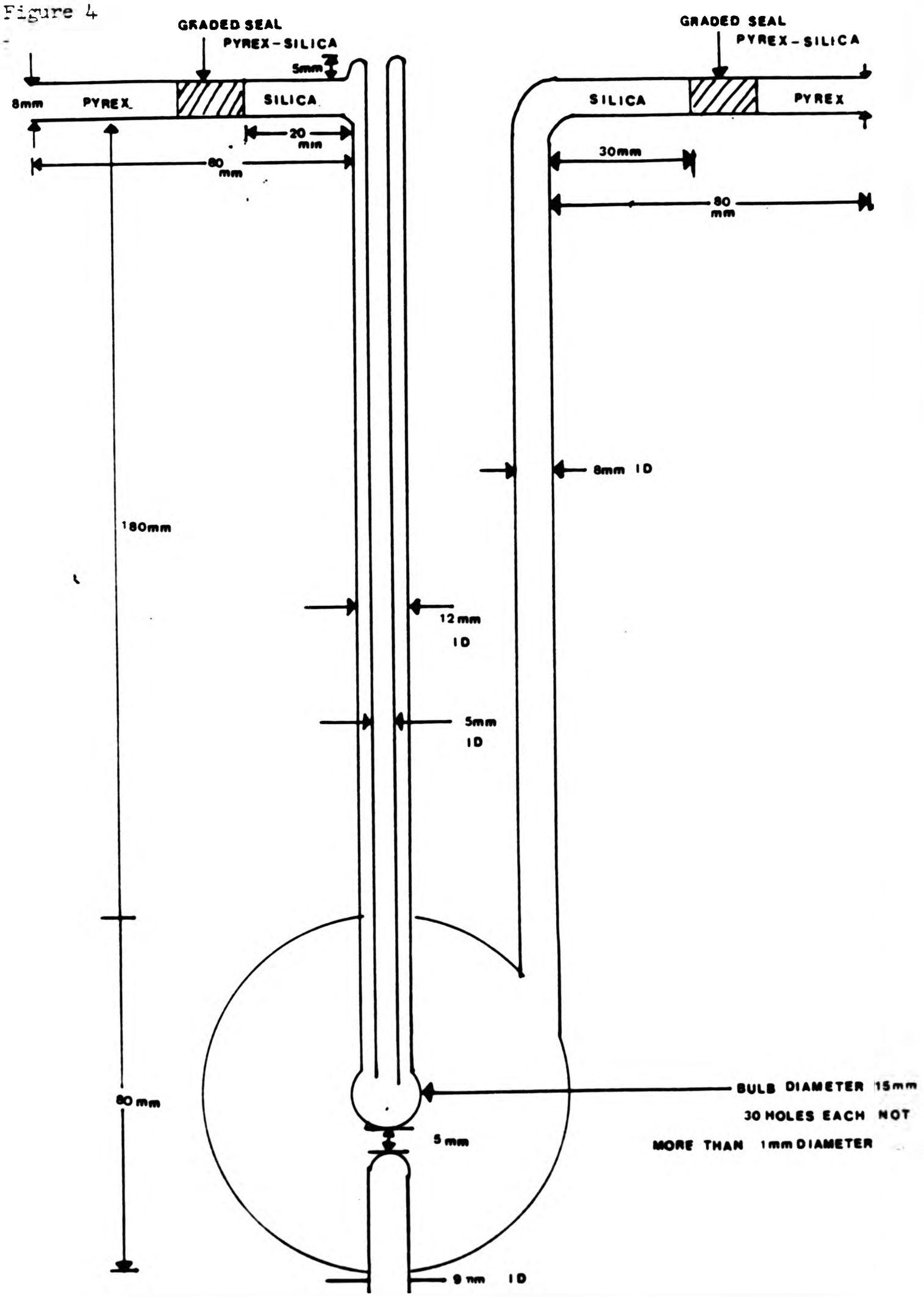
GRADED SEAL
PYREX-SILICA
5mm
8mm
PYREX
SILICA
20 min
80 mm
180mm
80 mm
8mm ID
12 mm ID
5mm ID
5 mm
9 mm ID
BULB DIAMETER 15mm
30 HOLES EACH NOT
MORE THAN 1mm DIAMETER
GRADED SEAL
PYREX-SILICA
SILICA
PYREX
30mm
80 mm

the required temperature profile. The coils were suspended in position and the core rested horizontally inside a refractory brick housing. The bricks at the rear of the housing were fashioned so that a platinum thermometer could be accommodated inside the rear of the reaction vessel, and at the fromt, so the reactant and product tubes of the stirred flow reactor were not obstructed.

Any remaining space between the cylinder and the outer bricks was filled with powdered refractory brick dust. The entire furnace and control units were supported by a Dexion framework.

The temperature was controlled by a C.N.S. Sirect proportional temperature controller, using a platinum resistance thermometer. The temperature inside the furnace was measured by a single Chromel-Alumel thermocouple, located at the centre of the stirred flow reactor situated inside the capillary running down to the central rose.

Preparation and Introduction of gases and aldehyde

The apparatus for the introduction of gases and aldehydes is shown in figure 5. Admission of gas into the vacuum line was planned to occur with a single reduction in pressure: from a low cylinder head regulator pressure into the vacuum system. The oxygen flowrate would be critical in obtaining a measurable and reproducible reaction rate. It was necessary to dilute oxygen using nitrogen. Initial experiments with separate needle valve controls for each gas gave rise to problems in the measurement of the flow rate, a simple "u" tube

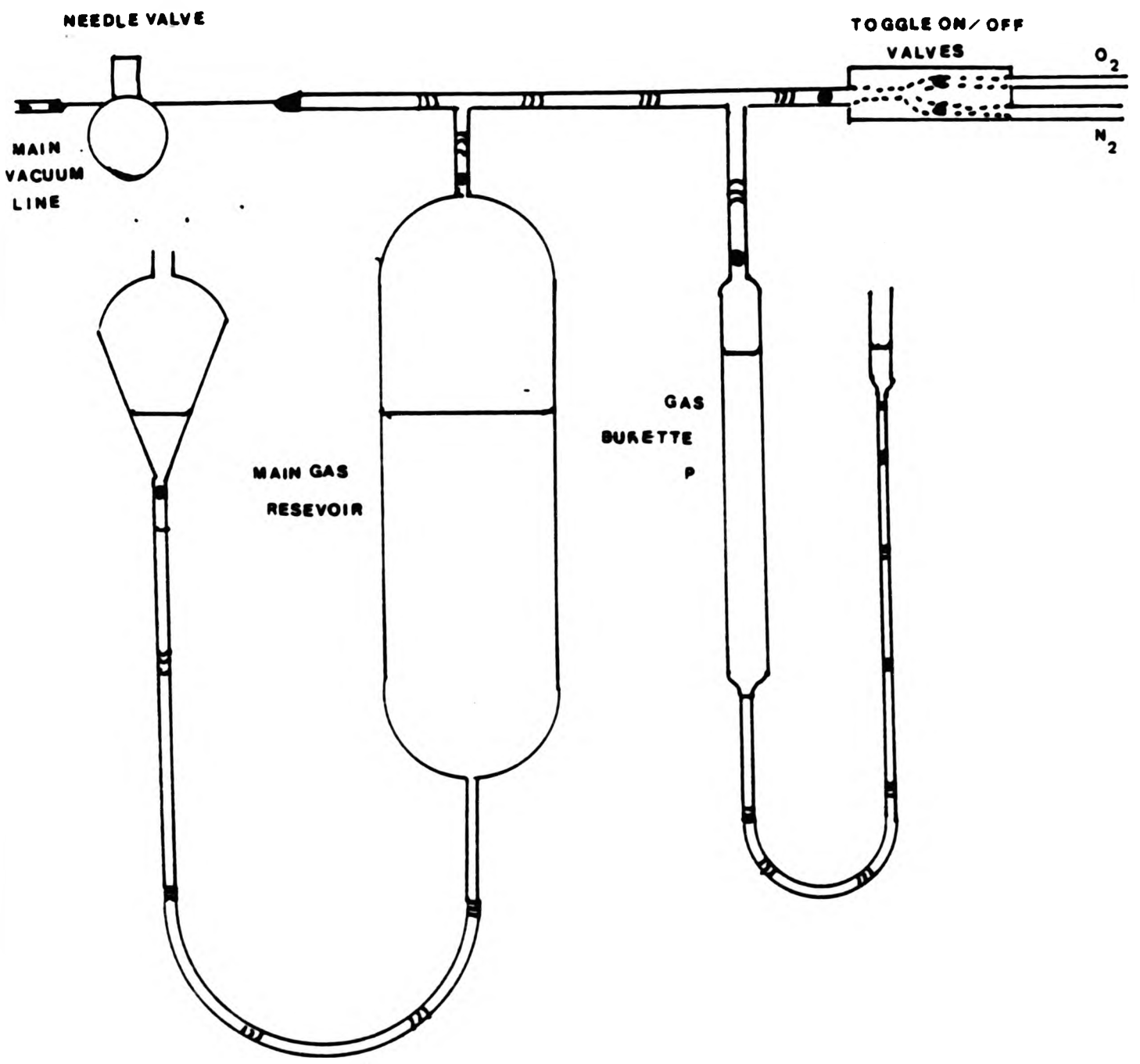
NEEDLE VALVE
TOGGLE ON/OFF
VALVES
O_2
N_2
MAIN
VACUUM
LINE
MAIN GAS
RESEVOIR
GAS
BURETTE
P

Figure 5

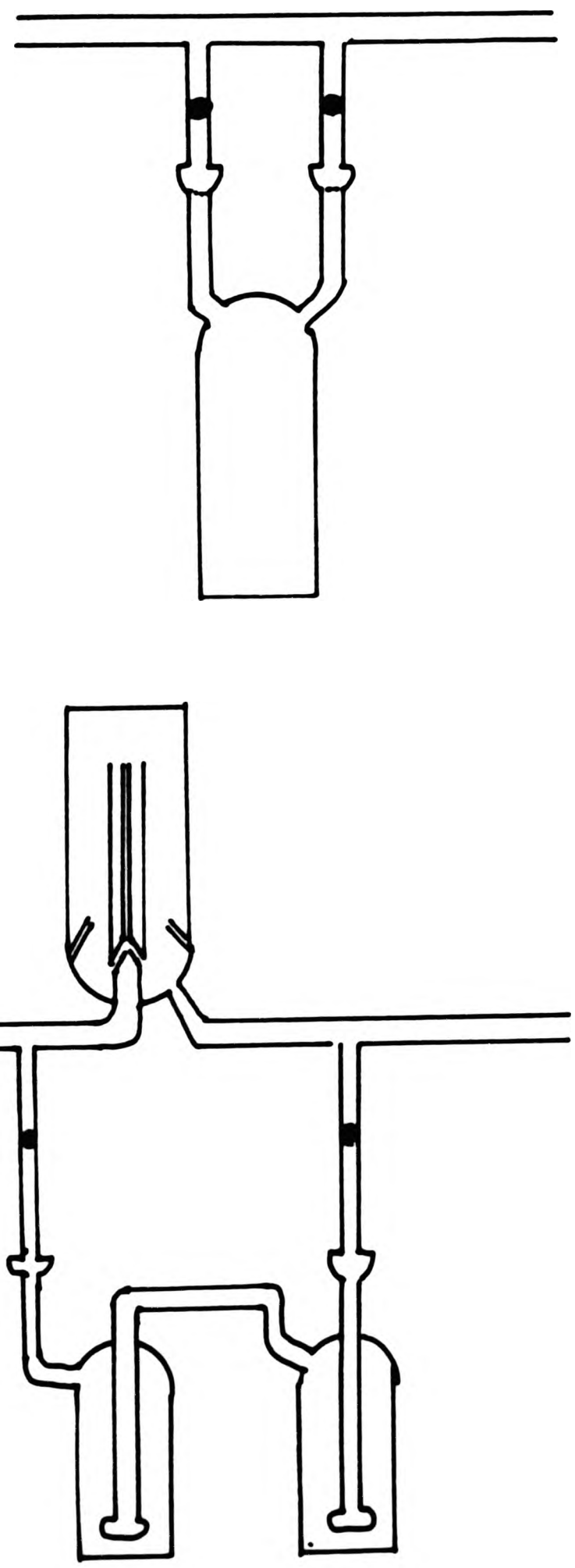

Figure 6

mannometer as a flowmeter was unsatisfactory, this approach was abandoned in favour of a method for the premixing of nitrogen and oxygen in calibrated cylinders at atmospheric pressure, the mixture of gas was bled into the vacuum system through a fine needle valve.

The introduction of aldehyde into the system was accomplished by passing the gases through the aldehyde in a set of carburetters the design of which is shown in figure 6. The amount taken up depending on the flowrate of the gases and the temperature of an external slush bath. This method proved unsatisfactory where a range of results requiring a small alteration of the aldehyde flowrate was needed.

The last modification was to leak aldehyde vapour into the system from a single vessel, which was temperature controlled using a dewar flask. Further flow restrictions could be implemented by a greaseless 'Rotaflo' tap or interchangable capillaries, before introduction of the aldehyde to the main vacuum line.

Collection and Analysis of products

During the course of a flow experiment, the effluent gases flowed from the reactor through a 'fixed' capillary and a greaseless tap into the first of a series of four traps. Each of these traps was separated from the adjacent one by a greaseless tap.

The first trap served as another capillary holder by which it was possible to alter the residence time of the species in the reactor.

After a flow experiment had finished, any condensible gas or mixture

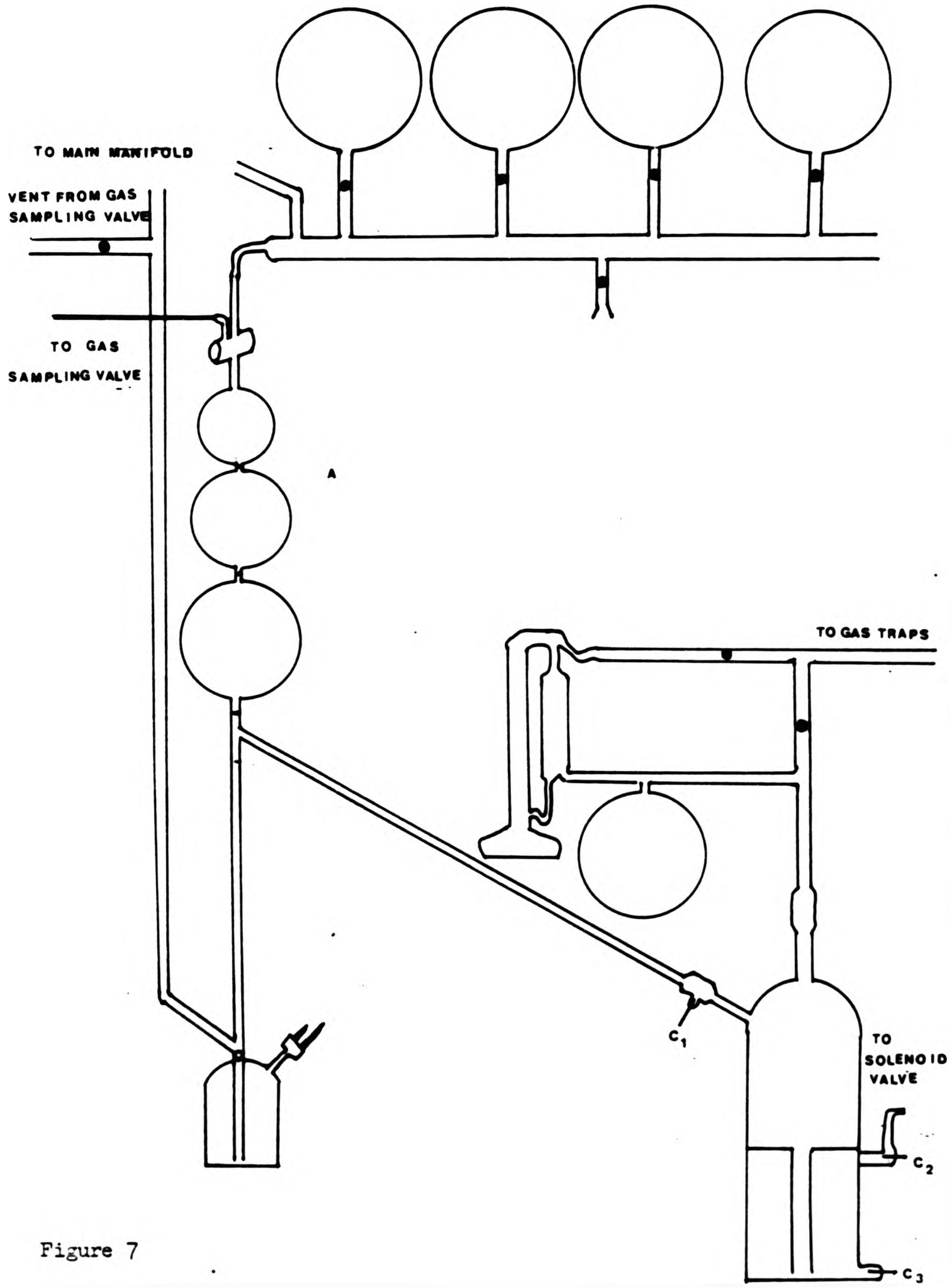
TO MAIN MANIFOLD
VENT FROM GAS SAMPLING VALVE
TO GAS SAMPLING VALVE
A
TO GAS TRAPS
C1
TO SOLENOID VALVE
C2
C3

Figure 7

of gases could be distilled off from a trap and pumped by a one stage mercury diffusion pump into a ballast volume, then transferred to an analytical gas burrette (A) by an automatic Topler pump ( ). The whole system is shown in figure 7 . The Topler pumps electrical system consisted of a relay activated by the contacts $C_1C_2$and C_3, which energised a solenoid valve, which in turn supplied, either a vacuum or air pressure to the tap leading into the lower chamber. When C_1 and C_2 were both connected air was drawn out of the lower chamber and the mercury level fell. When C_1 and C_3 were connected air was pushed back causing the mercury to rise. SW1 and SW2 are switches which simulate contact between C_1 ,C_2 and C_3.

The gas burette (A) used was made up of three bulbs of decreasing size topped by a three way tap. Between each bulb was a fiducial mark and the volume of each was determined with reference to this mark. The volumes given below were determined by filling the bulbs with mercury and weighing.

Total volume of the three bulbs	=	50.03 mms^3
Volume of top two bulbs	=	20.35 mms^3
Volume of top bulb	=	5.70 mms^3

The pressures of the gas samples collected were obtained by compressing the gas to a suitable fiducial mark and by reading the mirror scale in millimeters, on the adjacent mannometer limb. A thermometer, reading to within 0.1^{o}C was suspended alongside the gas burette (A) to measure the temperature of the gas with pressure P and volume V.

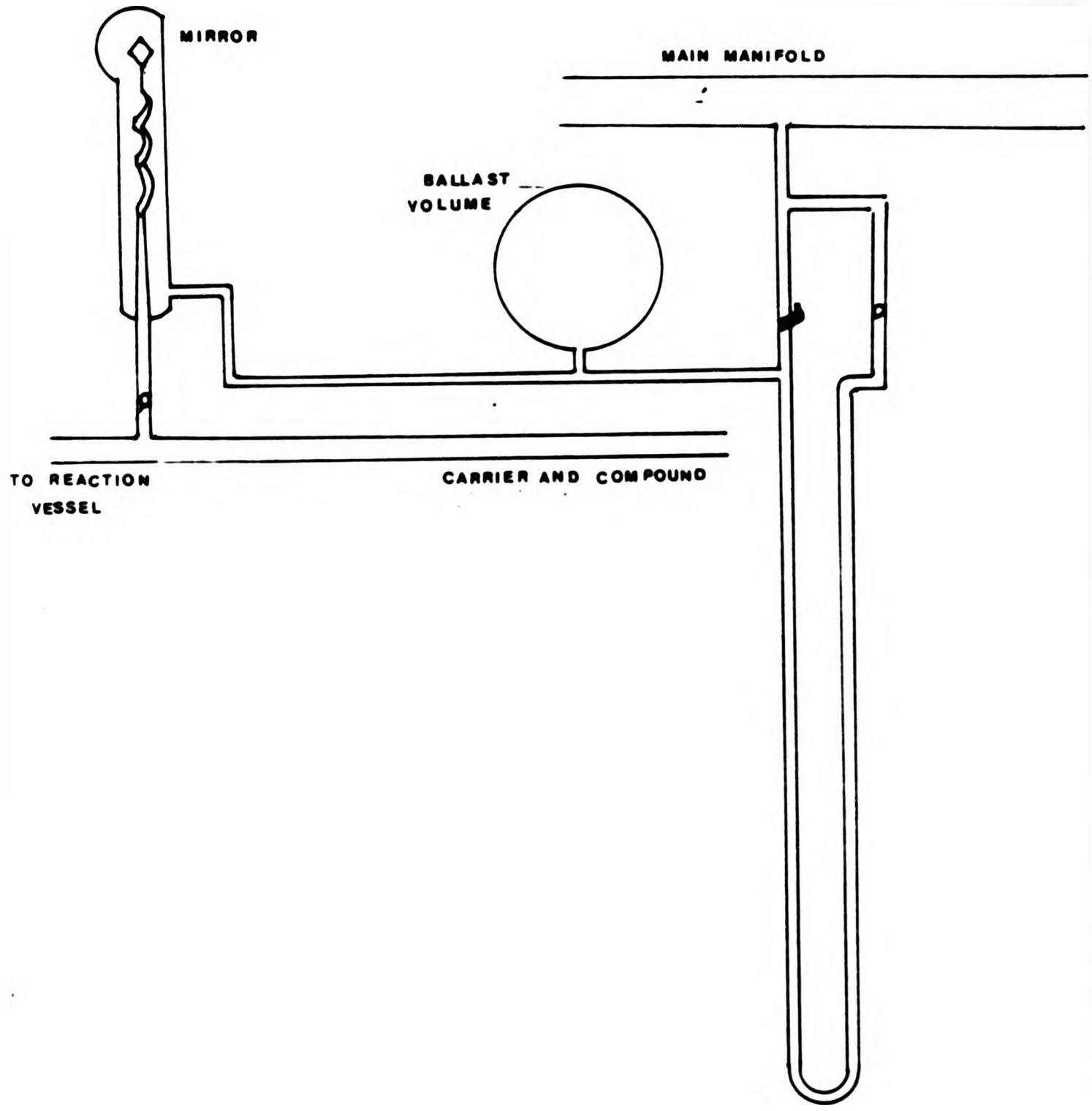
MIRROR
MAIN MANIFOLD
BALLAST VOLUME
TO REACTION VESSEL
CARRIER AND COMPOUND

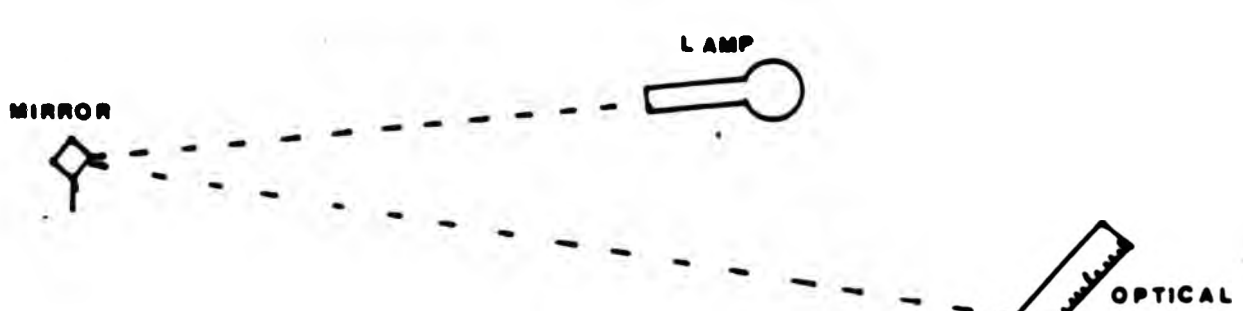
LAMP
MIRROR
OPTICAL SCALE

Figure 8

For analytical purposes pure gases could be introduced into the gas burette (A) through the three way valve from their respective storage bulbs. These bulbs could be initially filled from a 'B_{10}' cone and ground glass trap leading into the small manifold. This gas analytical system was connected to the main vacuum line at points E and E*.

Another B_{10} cone occupied the third port from the three way valve. Gas sampling bulbs were attached here and the condensible gases collected could be transferred by freezing out, to gas chromatography apparatus. This section was later improved by adding a gas sampling valve onto the three way valve and injecting into an adapted gas chromatography unit.

The Bourdon gauge

The total pressure of the reactants flowing into the reaction vessel during the course of a run, was measured using a spiral gauge backed by a wide bore mannometer, figure 6. Instead of using the Bourdon gauge to find a null point position and read the pressure directly from the mannometer. The optical scale was calibrated from the mannometer and shown to be linear up to at least 50 mms H_g (Graph 16). A statistical treatment of the calibration results in the range of 0-10 mms H_g showed a standard deviation of 0.080 mms H_g computed from twenty five results.

Procedure during a flow experiment

The gas mixing apparatus was flushed through initially with oxygen, by allowing a low pressure ($1K_g\ m^{-2}$) through the line, with the needle valve open into the main vacuum line. The preparative gas

Graph 16.1

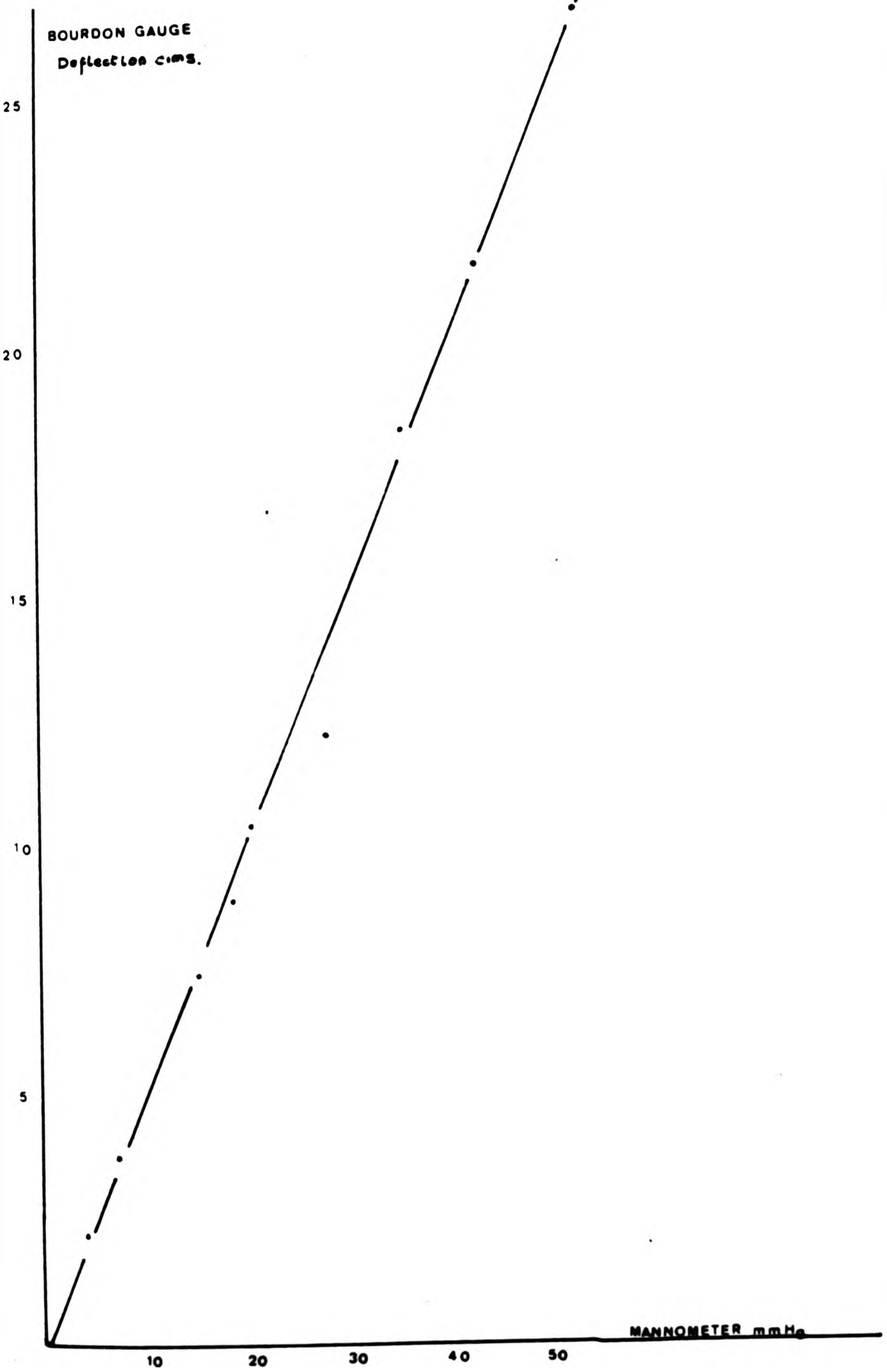
BOURDON GAUGE
Deflection cms.
25
20
15
10
5
MANNOMETER mmHg
10
20
30
40
50

burette (P) calibrated to 50 cms^3, could then be filled with oxygen and allowed to be drained into the main resevoir. The main gas resevoir: calibrated to 2500 cms^3, could then be filled to the required volume by first flushing the line and then directly metering in nitrogen.

The aldehyde sample vessel was attached to the flow line using spring clips. The aldehyde was frozen in liquid nitrogen and the vessel was evacuated by tap (15), after which the aldehyde was degassed. Air was then readmitted into the vessel before weighing and being reattached to the vacuum line. The vessel was then surrounded by a dewar flask. At this point the entire vacuum line was pumped out through the two stage mercury diffusion pump.

The product collection traps were surrounded by their respective isothermal cooling baths. These consisted of trap 1; room temperature, trap 2- Ice, trap 3; Toluene slush $-87^{o}C$ and trap 4; Liquid Nitrogen $-196^{o}C$.

The mannometer was isolated from the vacuum system and the Bourdon gauge was checked to see that the optical scale read 0mms H_g.

By closing taps 2,3,4,5 and 6 and reversing tap 1 the flow experiment was ready to commence and the mercury diffusion pump was isolated from the system and shut off.

The needle valve could now be opened to admit a predetermined flow-rate corresponding to a fixed pressure of oxygen in the reaction vessel, into the flow line from the main gas resevoir. The input pressure was checked on the Bourdon gauge and the furnace temperature was monitored until it became steady again, approximately three

minutes.

The greaseless tap (14) to the sample vessel was opened to admit aldehyde vapour into the flow line. For the first few minutes, it was necessary to adjust this tap slightly so as to provide a steady flowrate, which could be monitored by observing the Bourdon gauge.

Temperature readings were now taken at regular intervals during the course of the run, as well as recording pressure on the Bourdon gauge. The main gas resevoir was kept close to atmospheric pressure and the isothermal baths topped up with ice and liquid nitrogen.

The aldehyde flow time was usually two hours, after which the carrier gas was allowed to remain flowing for a further five minutes.

Taps 7,8,9,10,11,12, and 13 were now shut, as well as the Bourdon gauge. The dewar flask around the aldehyde vessel was removed before the remainder of the aldehyde could be frozen with liquid nitrogen, and the vessel removed for weighing.

The slush bath around trap 4 was now removed, any gas collected could now be pumped into the gas burette (A) through the one stage diffusion pump using the Toepler pump.

Careful degassing of the contents of traps 3 and 4 released the gases dissolved in the liquid aldehyde and these were also transferred to the gas burette. When no more gas was evolved the burette was adjusted to read the pressure and volume of this fraction.

Liquid products and aldehyde were collected at the bottoms of traps 2 and 3 by freezing down with liquid nitrogen. Air was now admitted to this part of the flow line and the products could be transferred and stored, or usually analysed immediately from the trap.

Analysis by gas chromatography

The analysis of any hydrocarbons during the series of experiments were performed with the aid of a flame ionisation detector. Quantitative analysis was easily performed once a response factor for each gas had been calculated. The equipment used up to run 85 consisted of a gas sampling valve, on a utility vacuum line, an aerograph oven a Perkin Elmer ionisation amplifier, a Venture MK II digital integrator and a Servoscribe potentiometric recorder. The relative percentages of the C_2's produced were worked out from the integrated peak heights and readjusted for the response factor.

Response factors were measured by preparing known amounts of standard gas samples in the vacuum line up to the gas sampling valve and recording the response for a measured pressure of sample from which a calibration graph could be constructed.

All C_2's collected from the gas burette were transferred to the vacuum line of the gas sampling valve in a round bottomed bulb of volume 140.8cm^3 fitted with a vacuum tap and a B_{10} cone.

The absolute response to the mixture inside the bulb was found by successive injections of the mixture into the column and drawing a graph of the integrated response.

Liquid products and aldehyde were collected at the bottoms of traps 2 and 3 by freezing down with liquid nitrogen. Air was now admitted to this part of the flow line and the products could be transferred and stored, or usually analysed immediately from the trap.

Analysis by gas chromatography

The analysis of any hydrocarbons during the series of experiments were performed with the aid of a flame ionisation detector. Quantitative analysis was easily performed once a response factor for each gas had been calculated. The equipment used up to run 85 consisted of a gas sampling valve, on a utility vacuum line, an aerograph oven a Perkin Elmer ionisation amplifier, a Venture MK II digital integrator and a Servoscribe potentiometric recorder. The relative percentages of the C_2's produced were worked out from the integrated peak heights and readjusted for the response factor.

Response factors were measured by preparing known amounts of standard gas samples in the vacuum line up to the gas sampling valve and recording the response for a measured pressure of sample from which a calibration graph could be constructed.

All C_2's collected from the gas burette were transferred to the vacuum line of the gas sampling valve in a round bottomed bulb of volume $140.8cm^3$ fitted with a vacuum tap and a B_{10} cone.

The absolute response to the mixture inside the bulb was found by successive injections of the mixture into the column and drawing a graph of the integrated response.

Liquid products and aldehyde were collected at the bottoms of traps 2 and 3 by freezing down with liquid nitrogen. Air was now admitted to this part of the flow line and the products could be transferred and stored, or usually analysed immediately from the trap.

Analysis by gas chromatography

The analysis of any hydrocarbons during the series of experiments were performed with the aid of a flame ionisation detector. Quantitative analysis was easily performed once a response factor for each gas had been calculated. The equipment used up to run 85 consisted of a gas sampling valve, on a utility vacuum line, an aerograph oven a Perkin Elmer ionisation amplifier, a Venture MK II digital integrator and a Servoscribe potentiometric recorder. The relative percentages of the C_2's produced were worked out from the integrated peak heights and readjusted for the response factor.

Response factors were measured by preparing known amounts of standard gas samples in the vacuum line up to the gas sampling valve and recording the response for a measured pressure of sample from which a calibration graph could be constructed.

All C_2's collected from the gas burette were transferred to the vacuum line of the gas sampling valve in a round bottomed bulb of volume $140.8cm^3$ fitted with a vacuum tap and a B_{10} cone.

The absolute response to the mixture inside the bulb was found by successive injections of the mixture into the column and drawing a graph of the integrated response.

PAGINATION
ERROR

Graph 16.11

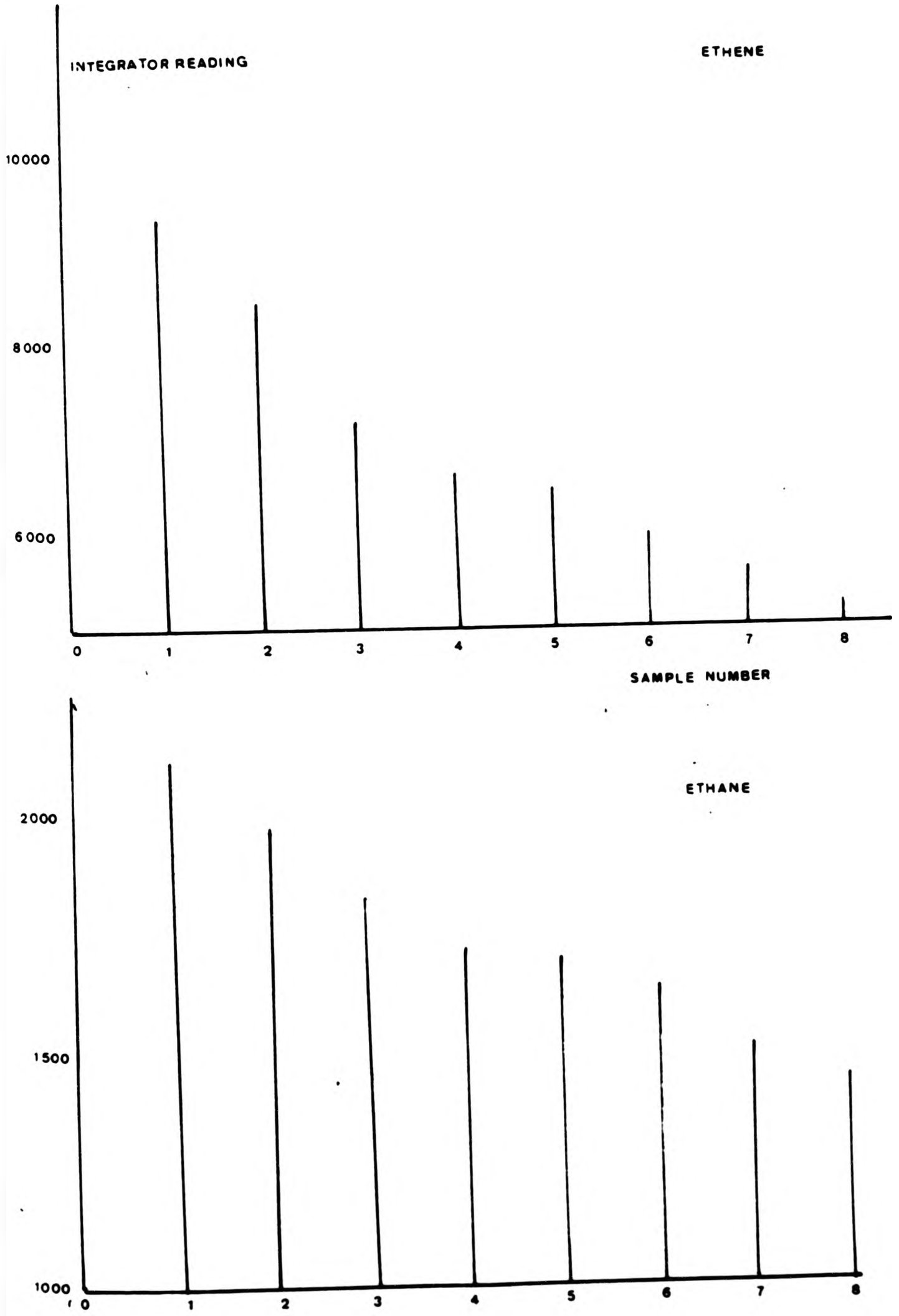
INTEGRATOR READING
ETHENE
10000
8000
6000
0
1
2
3
4
5
6
7
8
SAMPLE NUMBER
ETHANE
2000
1500
1000
0
1
2
3
4
5
6
7
8

Graph 16.111 Ethene

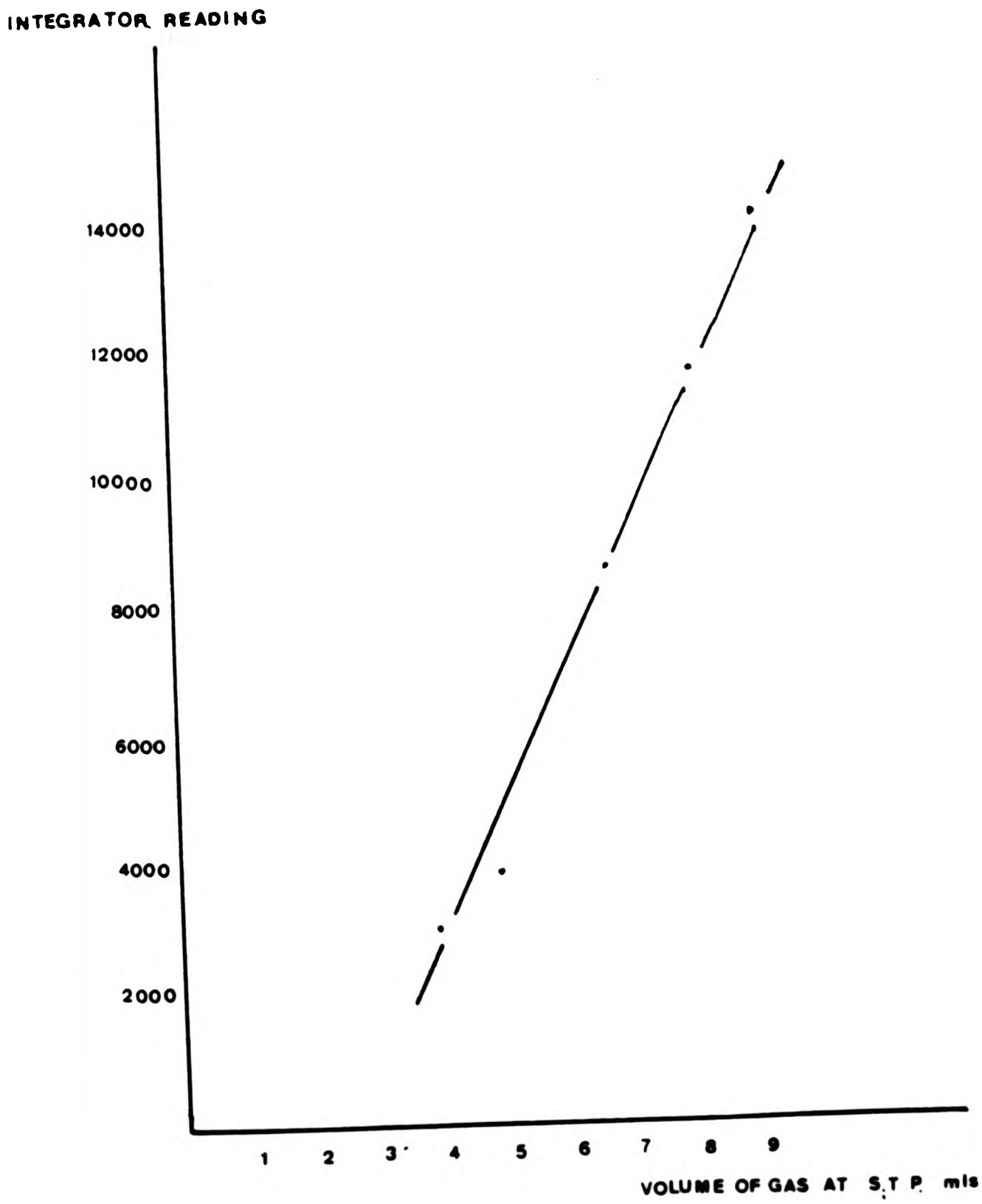

The graph could then be extrapolated (Graph 16.11) to produce a value for the response inside the bulb before the gas sample was taken.

The response could then be converted to a volume of gas S.T.P. using the data for standard gas samples. The calibration graph for a particular run is reproduced in Graph 16 III.

The introduction of new equipment which enabled a sample to be injected direct from the gas burette (A) simplified the determination of the gas collected during a run. This consisted of gas sampling valve connected to the gas burette, a Perkin Elmer 881 gas chromatograph oven and a Carlo Erba electrometer. The standard sample gases could now be introduced directly into the gas burette and a direct calibration could be achieved. This made calibration more reproducible and less time consuming.

Gas chromatographic analysis of liquid products was achieved by injecting directly a sample of the trapped liquid using a one microlitre syringe.

Standard aldehyde samples could be introduced for calibration, using the same technique. The oven used had duel column facilities, the upper column was connected to the gas sampling valve, whilst the lower column was used for analysing liquids and headspace with an injection septum.

The preparation of chromatography columns for analysis

Columns containing Porapak Q and N whether in stainless steel or P.T.F.E. tubing were packed by plugging one end of the tube with

glass fibre and filling the column using a stream of nitrogen and vibration from a portable engraver to settle the support particles as close as possible. The columns were then conditioned at the temperature of use with nitrogen passing through them.

A column of 25% W/W 3, 3 dioxypropionitrile was made by dissolving a known weight of the nitrite in dichloromethane and the solution was poured into a vacuum flask containing a weighed amount of the support. Enough dichloromethane was added to completely cover the mixture.

The bulk of the solvent was removed by gently heating the flask, whilst connected to a water pump and the remainder of the solvent was removed by standing the flask in a cool oven. A glass column was packed and conditioned as above.

Columns used

Type	Length	Internal Diameter	Support	Stationary Phase
Spiral P.T.F.E.	1 metre	2.0 mm	80-100	Poropak N
Spiral Glass	1 metre	4.0 mm	72-85	3% OV 101
Spiral Stainless Steel	1.75 "	2.0 mm	100-150	Poropak Q
Spiral Glass	1 metre	4.0 mm	70-85	25% 3,3 Dioxypropion-itrile.

Other analytical techniques

Mass spectrometry

The presence of the reaction products was confirmed by mass spectrometry. An AEl MS.10 mass spectrometer was used, which had

been installed with its own vacuum line, for the analysis of gases.

Known standards of gases could be produced and compared with the reaction products. Ethane, ethylene, ethanal, propanal, propane and propene were all detected from experimental samples collected in a sample bulb at about 2mms Hg and leaked into the mass spectrometer from a pressure of o.1 torr. Carbon monoxide could not be distinguished from nitrogen (present in the background spectra) and its presence was independently analysed by mass spectrometry.

Non condensible gases evolved during the run could be collected by inflating a sample bag from the exhause valve of the main rotary pump and collecting the carrier gas as well. Besides Carbon monoxide, hydrogen was established as a reaction product, detected in trace amounts.

Formation of Carbon monoxide

Analysis of CO as a reaction was not performed routinely. The analysis was performed twice by mass spectroscopy, its presence was measured at 0.32% of the effluent carrier gas, corresponding to a flowrate of 2.38×10^{-8} mols sec^{-1}. The corresponding flowrate of total hydrocarbons was 2.11×10^{-8} mols sec^{-1}. The ratio of the flowrate is 0.9 and the expected ratio was 1.0. We can conclude that the figures are in agreement within the region of experimental error.

Analysis of aliphatic per acids

A preliminary investigation of the low temperature, 450K, oxidation of ethanal in the flow reactor was undertaken as a feasibility study. A technique was sought to establish if any peracid were being formed, the test used was that devised by F P Greenspan and D G Mackellour[3] based

been installed with its own vacuum line, for the analysis of gases.

Known standards of gases could be produced and compared with the reaction products. Ethane, ethylene, ethanal, propanal, propane and propene were all detected from experimental samples collected in a sample bulb at about 2mms Hg and leaked into the mass spectrometer from a pressure of o.1 torr. Carbon monoxide could not be distinguished from nitrogen (present in the background spectra) and its presence was independently analysed by mass spectrometry.

Non condensible gases evolved during the run could be collected by inflating a sample bag from the exhause valve of the main rotary pump and collecting the carrier gas as well. Besides Carbon monoxide, hydrogen was established as a reaction product, detected in trace amounts.

Formation of Carbon monoxide

Analysis of CO as a reaction was not performed routinely. The analysis was performed twice by mass spectroscopy, its presence was measured at 0.32% of the effluent carrier gas, corresponding to a flowrate of 2.38×10^{-8} mols sec^{-1}. The corresponding flowrate of total hydrocarbons was 2.11×10^{-8} mols sec^{-1}. The ratio of the flowrate is 0.9 and the expected ratio was 1.0. We can conclude that the figures are in agreement within the region of experimental error.

Analysis of aliphatic per acids

A preliminary investigation of the low temperature, 450K, oxidation of ethanal in the flow reactor was undertaken as a feasibility study. A technique was sought to establish if any peracid were being formed, the test used was that devised by F P Greenspan and D G Mackellour[3] based

upon the use of ceric sulphate as a titrant for the hydrogen peroxide present, followed by an iodometric determination of the peracid present.

$$\%H_2O_2 = \frac{\text{mls of ceric sulphate} \times N \times 17}{10 \times \text{sample wt}}$$

$$\% \text{ per acid} = \frac{(\text{mls of ceric sulphate} \times N) \times \text{equiv wt of per acid}}{10 \times \text{sample wt}}$$

N = Normality of ceric sulphate

Standard per acid solutions were made up according to D Swern [42] by reaction of hydrogen peroxide with acetic anhydride. This produced a peracetic acid solution of approximately 1.0 molar.

Both synthesis and anlysis of per acid solution were successful, however the discovery of a recently published paper [43,44] concerning the oxidation of ethanal, the kinetics of which were determined in a flow apparatus at between 150-190°c led to the abandonment of further work in this direction.

Materials used

Propanal, n-butanal, and i-butanal were all supplied by British Drug Houses in 500 ml laboratory reagent bottles.

Propanal and i-butanal were found to be gas chromatography pure. The n-butanal was found to have a slight but measureable impurity by gas chromatography. This gave an identical retention time and peak shape as i-butanal.

Oxygen and nitrogen were supplied by the British Oxygen Company. Their specifications quoted were: The medical grade oxygen was not less than

99.95% pure, the major impurity being argon. The oxygen free nitrogen having impurities less than 100 p.p.m.

The standard gas samples : ethene, ethane, propane, and propene were from laboratory demonstration cylinders supplied by British Drug Houses, their indicated essay was more than 99% purity. No impurities were shown to be present when analysed by gas chromatography.

Results

The experimental results obtained in this work can be found displayed in tables of kinetic data starting on page 136. The majority of these tables show k_3/k_6 calculated in accordance with the simple mechanism put forward on page 93.

Tables 1 and 2 refer to experiments 14 to 52 and are preliminary experiments used to determine suitable parameters; residence time and reactant flowrates, so to achieve a measurable hydrocarbon flowrate for later experiments. In these two tables it should be noted that individual hydrocarbons are quoted as a percentage of the total hydrocarbons collected and that the ratio is calculated from these figures. Because of the lack of quantitative data there are no percentage decomposition of propanal or total hydrocarbon flowrate figures available. All the later experiments have hydrocarbons represented as flowrates. Table 3 refers to experiments 53 to 68 (set 5). These experiments measured hydrocarbon flowrates at a constant aldehyde flowrate and a variable oxygen flowrate to determine the order of the overall reaction with O_2 at a constant temperature and in a silica glass reactor. Table 4 includes experiments 97 to 106(set 7) and also measures hydrocarbon flowrates at a constant aldehyde flowrate with a variable oxygen flowrate for the same purpose and to examine possible surface effects. These experiments and all subsequent ones were performed in an aged boric acid vessel.

Table 5 refers to experiments 111 to 120 and 141 to 154 (sets 8 and 10). These sets measure hydrocarbon flowrates at a constant oxygen flowrate and with a variable propanal flowrate to determine the overall order with respect to propanal. Table 6 features experiments 125-140 and

160 to 170 (sets 9 and 11) and measure the temperature dependence of the hydrocarbon flowrates. Table 7 displays experiments 179-196 (set 12) and measures hydrocarbon flowrates at a constant propanal flowrate with a variable oxygen flowrate at a higher constant temperature to check the order of reaction with respect to O_2. Table 8 covers experiments 197-215 (set 13) which measured hydrocarbon flowrates at a constant oxygen flowrate with a variable propanal flowrate at a higher constant temperature again to check the overall rate reaction. Table 9 lists ethanal flowrates obtained from some of the experiments above for the oxidation of propanal. Table 10 displays experiments 222-233 (set 14.1) which measured the temperature dependance of the hydrocarbons produced from n-butanal and i-butanal. Table 11 reports experiments 234-245 (set 14b) and measure the hydrocarbon formation in pyrolysis experiments of the aldehydes.

Example of calculations (Experiment 190)

A total pressure of 189.6 mmHg was measured inside the gas burette. The partial pressures were allocated from the integrated gas chromatograph.

Peak area (integratorunits) x Response factor

Partial pressure of C_2H_6 calibrated from standard samples = 79.6 mmHg

Partial pressure of C_2H_4 calibrated from standard samples =110.0 mmHg

Volume of C_2H_4 at S.T.P. $= \frac{V_1 \times P_1}{P_{atm}}$ V_1 = volume of burette = 20.35 mls

P_1 = partial pressure calculated for ethene

$V_{S.T.P.}$ = 2.94 mls

C_2H_6 $V_{S.T.P.}$ = 2.13 mls

C_2H_4 flowrates = $\frac{V_{S.T.P.}}{22400 \times t}$ moles sec^{-1} t = 7200 seconds

t = duration of reactant flowrate, the vacuum system having been purged for five minutes either side with carrier gas to bring the system to equilibrium and to collect reaction products.

f C_2H_4 = 1.82×10^{-8} moles sec^{-1} fC_2H_6 = 1.32×10^{-8} moles sec^{-1}

Propanal flowrate = $\frac{P_{wt}}{M_{wt} \times t}$ moles sec^{-1} P_{wt} = 4.36 grams

Molecular weight =58.1

P_{wt} = weight loss of propanal in the reactant carburettor.

Carrier gas mixture = 55mls O_2 in 1100mls N_2

Oxygen flowrate= $\frac{55}{22400 \times 7200}$ = 3.41×10^{-7} moles sec^{-1}

corrected to S.T.P. = 3.13×10^{-7} moles sec^{-1}

Nitrogen flowrate = 6.26×10^{-6} moles sec^{-1}

Calculation of residence time

Total volume flowing into reactor = 1100(carrier) x 273 + 1683 (propanal)
= 2700 mls

Total volume passed in two hours, corrected at reactant temperature and pressure. (Reactant pressure = 10mmHg, temperature = 773K, reactor volume V = 259 mls)

$$u = \frac{2700 \times 760 \times 773}{10 \times 273}$$ Residence time $\frac{V}{u}$

$$t = \frac{259 \times 10 \times 273 \times 7200}{2700 \times 760 \quad 772} = 3.21 \text{ seconds}$$

Percentage decomposition of propanal in terms of total hydrocarbons

$$\frac{f\ (C_2H_4 + C_2H_6)}{f\ \text{propanal}} \times 100 = \frac{3.14 \times 10^{-8}}{1.04 \times 10^{-4}} \times 100 = 0.30\%$$

Estimation of errors

The flowrate of mixtures of oxygen and nitrogen was controlled by a needle valve. The pressure of gas leaving the valve was held constant in the range 0 to 25 mmHg, to better than ± 0.1 mmHg during a run. This was established in preliminary, experiments, to determine the total volume of carrier required for a kinetic run.

The propanal flowrate was monitored during an actual run by observing the pressure in the carburettor using a glass spiral Bourdon gauge with an optical lever. This gauge had been previously calibrated and showed a linear response with pressure over the range 0-50 mms Hg (graph 16I)

The total input pressure was monitored on the Bourdon gauge, however because the permanent gas flow had previously been shown to be very steady any fluctuations in the optical reading r , were attributed to the flowrate of the propanal generated from its thermostatted source. The partial pressure of propanal was held constant in the range 0 to 10mmHg to - 0.25 mm Hg .

The errors involved in measuring the flowrate of hydrocarbons using gas chromatography were thought to be:

a) Incomplete recovery of total C'2s from the trap.

b) Possible addition of dissolved gas or other vapour to the hydrocarbon fraction in the burette so that the total pressure exceeds the true value.

c) Errors in the fixed volume of the burette.

d) Errors in measuring pressure of gas trapped in burette (Mercury level parallax, temperature correction for room temperature)

e) Gas chromatography errors (1) Measuring peak areas
(2) Determining response factors

Three recovery experiments were performed to investigate the size of the errors contributed by a) and b) which involved introducing a known amount of C'2s into the vacuum line, trapping it with excess propanal and then degassing the C'2s from the trap to the gas burette via the toepler pump, this followed the procedure outlined in the later part of the experimental section. The total amount recovered was checked by using the gas burette, and the composition by gas chromatography. In all the experiments a positive deviation was shown, the maximum recovery was 106%. The recovery in all cases being over 100% indicates a systematic error. The most probable explanation is that the method resulted in the addition of carrier gas or some non-condensible dissolved product from the traps.

The error in determining peak heights was calculated by repeated injections of a standard mixture over a certain pressure range. The error involved in measuring the amount of gas in the burette over the range 0 to 10 mls at S.T.P. was 4.0%. Figure 16III shows a typical calibration graph from a mixture of total hydrocarbons.

To quantify the components in an unknown gas mixture, a relative response factor was used. Although this included a percentage pressure error, the maximum error involved in the pressure measurement over the experimental range was 1.5% and the error involved in measuring the relative peak areas was 4%.

The errors involved in calibrating the gas burette with weighed mercury and fluctuations in room temperature were considered negligible compared with the above sources of errors.

Combining the errors for a measurement of the $f(C_2H_4/C_2H_6)$ ratio, it is assumed that the error for the associated relative response factors will cancel out.

$$\text{Percentage error in } \frac{fC_2H_4}{fC_2H_6} = (2 \times (0.4)^2)^{\frac{1}{2}} = 5.6\% \text{ (6\% approx)}$$

The graphs illustrating variation in relative rates of C'2 formation (eg graph 13.1: C_2H_4 v O_2/ propanal) have error bars for measurement of the hydrocarbon ratio. Single hydrocarbon flowrates used in determining orders of reaction (eg graph 12.ii: $\text{Log}_{10} fC_2H_4$ v $\log_{10} f\ O_2$) include error bars calculated for the individual flowrate which was calculated as 6%. The error calculated for the total flowrate of hydrocarbons was 8%. The majority of these graphs only have two error bars shown, because the errors are calculated as percentages , the ones drawn usually cover the spread of the data represented.

Graph 15.1 has two error bars representing the scatter on a number of repeat experiments. The size of these error bars were determined graphically from 7.1 and 13.1. These are plotted with a number of single experimental points which have their error bars calculated as in the example over the page. It is satisfying to see the similarity between the two different types of error determination. The individual experiments shown on graph 15.1 were performed at constant reactant pressures with variation in temperature, so there will be no change in the fractional errors for propanal or the carrier.

Run 126, Temperature = 712K, $1/T = 1.40 \times 10^{-3}$

partial pressures; propanal = 4mmHg, carrier =6mmHg

Run 140 Temperature = 783K, $1/T = 1.28 \times 10^{-3}$

partial pressures; propanal = 4mmHg, carrier =6mmHg

$$\frac{k_3}{k_6} = \frac{fC_2H_4 \quad [\text{propanal}]}{fC_2H_6 \quad [\ O_2\ ]}$$

Fractional error in rate constant determination $= \frac{\Delta x}{x}$

Fractional error in propanal $= \frac{0.25}{\text{nPropanal/mmHg}}$, in oxygen $= \frac{0.10}{\text{pOxygen/mmHg}}$

$$\frac{\Delta x}{x} = \left((0.06)^2 + \frac{(0.25)^2}{(4)} + \frac{(0.10)^2}{(6)}\right)^{\frac{1}{2}} = 0.085 = 8.5\%$$

Run 126 $\frac{k_3}{k_6} = 68.56 \pm 5.8$ Run 140 $\frac{k_3}{k_6} = 36.5 \pm 3.1$

The rate constant ratios obtained from graphs 7.1 and 12.1 were

$\frac{k_3}{k_6}$ (710) $= 66.7 \pm 5.0$ and $\frac{k_3}{k_6}$ (773) $= 44.0 \pm 3.0$ respectively.

DISCUSSION OF RESULTS

Determination of the order of reaction

The flowrate f_i in the effluent stream is related to the concentration in the reactor by:

$$f_i = \frac{V[i]}{t}$$

where [i] = The concentration of species i in the effluent stream in moles l^{-1}.

V = Volume of the reactor (dm^3)

t = Residence time (seconds)

After a brief initial non-stationary state period

$\frac{dn_i}{dt} \longrightarrow 0$ for all i thus; $f_i^{\circ} - f_i = V \frac{d[i]}{dt}$ is the condition for the steady state, the summation being over all chemical processes.

$f_i^{\bullet}$ = the flowrate of species in the influent stream.

$fC_2H_6 = V \frac{d[C_2H_6]}{dt}$ and the rate of production of ethane is:

$$\frac{d(C_2H_6)}{dt} = [C_2H_5CHO]^n [O_2]^m$$

$$fC_2H_6 = V \frac{d(C_2H_6)}{dt} = V k (C_2H_5CHO)^n [O_2]^m$$

Where k is the rate constant, V is the volume lf the reaction vessel and n = the kinetic order of reaction with respect to propanal substituting propanal flowrate for concentration:

$$fC_2H_6 = k (t.fC_2H_5CHO)^n [O_2]^m$$

At a constant temperature: and $[O_2]$

$$\text{Log } C_2H_6 = n \log fC_2H_5CHO + \text{Log } K$$

where K contains all the terms except fC_2H_5CHO in the previous expression. Hence a plot of Log fC_2H_6 v Log fC_2H_5CHO should give a straight line of slope n, thus giving the order of reaction with respect to propanal.

In fact, $f^oC_2H_5CHO$ has been plotted instead of fC_2H_5CHO, the same approximation is also made with oxygen flowrates in determining reaction order with respect to oxygen. The propanal flowrate is very high compared to other species, however the oxygen flowrate is quite low, but the substitution will remain valid as long as the percentage decomposition remains so low that $f^o{}_{O_2} \simeq f_{O_2}$.

Table 4.1 : KINETIC ORDERS OF REACTION WITH RESPECT TO VARIATION IN OXYGEN OR PROPANAL

	This work			Baldwin's work [1]		
	C_2H_4	C_2H_6	Total Hydrocarbons	low pressure	high pressure	
Oxygen						
Silica vessel (713)	1.2 ± 0.2	0.0 ± 0.2	0.9 ± 0.2			
Boric vessel (713)	1.52 ± 0.1	0.25 ± 0.1	0.90 ± 0.1	0.9	0.11	0.35*
Boric Vessel (773)	1.30 ± 0.1	0.8 ± 0.1	1.0 ± 0.1			
Propanal						
Boric vessel (713)	$2.3(2.6) \pm 0.2$	$1.2(1.5) \pm 0.2$	$1.2(1.6) \pm 0.2$	1.5	2.5	1.50*
Boric vessel (773)	1.7 ± 0.1	0.2 ± 0.1	0.8 ± 0.1			

* Baldwin's orders of reaction are quoted for the maximum rate of reaction and initial rate

Comparing these kinetic orders of reaction for the formation of C_2H_4, C_2H_6 + total C_2's obtained by either the variation of propanal or oxygen flowrates, the most immediate fact is they are clearly seen to change. The most marked difference is the increasing dependance of the rate of production of C_2H_6 on fO_2 as the temperature is raised. This is illustrated by graphs 7.111 and 12.111. In the variation of f propanal and its effect on the rate of C_2H_6 formation, the order decreases as the temperature is raised, shown by comparison of graph 13.111 with 10.111. Ideally for the measurement of kinetic parameters for radical -molecule reactions the mechanism and hence the order should not change, however the experiments suggest a change in the mechanism between 710K and 773K, this could result in changing pathways to the formation of C_2H_4 and C_2H_6.

The order of the reaction for the production of total C_2s was not determined with precision but the result could be expressed approximately as:

$$r\ C_2\text{'s} = [P]^{0.8-1.2}\ [O_2]^{1.0}$$

over the temperature range studied and this is what might be expected for a pyrolytic oxidation involving chain carriers derived from propanal. The acceptance of this result reinforces the belief that C_2H_4 and C_2H_6 have a common precursor in the $C_2H_5^{\bullet}$ radical. This was assumed in Baldwin's mechanism which was reviewed in an earlier chapter and the kinetic analysis later on is based on this assumption.

Boric coated vessels reduced the rate of reaction without apparently changing the order. This would suggest a heterogeneous component, either a reduced heterogeneous initiation or enhanced destruction of chain carriers. The former would seem to be indicated as it is believed that the coating improves the inert character of the wall with respect to radicals[1].

In the glass reactor where the fC_2H_6 is independant of f O_2 at 713K it would appear there is no reaction by oxygen or a derived radical such as HO_2 to produce C_2H_5 radicals. However the observation that f $C_2H_4 \propto$ f O_2,[1.2] at 713K suggests some participation by oxygen containing radicals that might arise from the reaction with propanal on HO_2 formed by:

$$C_2H_5 + O_2 = C_2H_4 + HO_2$$

The more marked dependance of rate on oxygen concentration (both C_2H_6 and especially C_2H_4) in the coated vessel would indicate that the radicals involved in the oxidative mechanism were being produced more efficiently. Increasing the temperature to 773K results in $fC_2H_6 \propto$ f $O_2^{0.8}$ while f $C_2H_4 \propto$ f $O_2^{1.3}$, graphs 12.11 and 12.11 respectively, this could be interpreted as an increase in the oxidation relative to pyrolytic pathways possibly including the bimolecular initiation reaction:

$$C_2H_5CHO + O_2 = C_2H_5C^{\bullet}O + HO_2$$

The order with respect to propanal was very high at lower temperatures

and these results exhibit a large scatter (Graphs 10.2 and 10.3) an indication of the extreme sensitivity of the reaction rate to propanal concentration.

Baldwin's results[1] See Table 1, at 713K and p O_2 = 30mmHg led to an order for the initial rate in aldehyde being 1.5. The order at the maximum rate varied from 1.5 at low aldehyde to 2.5 at an aldehyde pressure greater than 10mmHg, the total static pressure was maintained at 60 mmHg. The dependence of reaction rate on oxygen pressure was reported as being much smaller, as found in the present work. With the aldehyde pressure fixed at 4mmHg and oxygen pressures in the range 4-56 mmHg, orders of 0.11 and 0.35 were obtained for the maximum and initial rate respectively. An apparent order of 0.9 was obtained for the maximum rate up to 0.6 mmHg.

In this work, order investigations were carried out at a total pressure of 10 mmHg in the reactor vessel and with a constant O_2 flowrate, the propanal partial pressure was varied from 0.5 to 8.0 mmHg. In determining the oxygen dependence the percentage oxygen in the carrier gas flowrate was varied from 0% to 10% (0.0 to 0.6 mmHg) and 0% to 25% in earlier experiments (0.0 to 1.5 mmHg)

Formation of C_2H_4 and C_2H_6

The mechanism in chapter 1 quoted from Baldwins papers, assumes that both ethene and ethane are primary products being formed by the elementary reactions involving the C_2H_5 radical

$$C_2H_5^{\cdot} + O_2 = C_2H_4 + HO_2 \qquad (3)$$

$$C_2H_5^{\cdot} + C_2H_5CHO = C_2H_6 + C_2H_5CO^{\cdot} \qquad (6)$$

These lead to the flow rate of reactions.

$$fC_2H_4 = \frac{V\, d[C_2H_4]}{dt} = V k_3 [C_2H_5^{\cdot}] [O_2]$$

$$\text{and } fC_2H_6 = \frac{V\, d[C_2H_6]}{dt} = V k_6 [C_2H_5^{\cdot}]\ C_2H_5CHO$$

By eliminating $[C_2H_5^{\cdot}]$ the following relationship is obtained

$$\frac{f\,C_2H_4}{fC_2H_6} = \frac{k_3\ [O_2]}{k_6 [C_2H_5CHO]} \qquad (i)$$

Reaction 6 has been studied in a number of systems and values of k_6 [16] may be calculated from:

$$\log k_6 = 8.1 - 5900 \text{cals}/2.3\ RT$$

eg $k_6 = 2.67 \times 10^6$ 1 mol^{-1} sec^{-1} at 773K.

It follows that if (3) and (6) are the only sources of C_2H_4 and C_2H_6 respectively, a study of the relative flowrates of C_2H_4, C_2H_6 at measured reactant oxygen and propanal flowrates leads to a value for k_3.

Initial studies were performed in a silica glass reactor around 710K.

These gave R_3/R_6 ratios of 56(set 1), 52(set 2), 69 (set 4) and 66(set 5). These results represent a series of mixtures with varying amounts of oxygen while the propanal flowrate was held constant. The residence and total pressure were changed for each set.

Later experiments were performed in an aged boric acid coated vessel used to give reproducible rate measurements. The two sets of results 12 and 7 produced R_3/R_6 ratios of 44 ± 3.0 and 66.7 ± 5 for temperatures of 773K and 710K respectively. The results plotted according to equation (I) formed a good straight line and were obtained at a constant total pressure and flowrate of propanal, with a variation in oxygen composition (Graphs 12.I and 7.I).

Three other sets of results: 13 (8 and 10) gave initial R_3/R_6 ratios of 41 ± 9 and (76 ± 5) for temperatures of 773K and 710K respectively. The points on the graphs were more scattered than for sets 7 and 12. They represent a series of mixtures at the same total pressure as before and constant flowrate of oxygen, with variation in propanal flowrate. The greater scatter is expected in view of the more marked dependence of rate on f propanal. A 'high order' in propanal indicates a marked sensitivity of rate to propanal concentration. (Graphs 13.I and 10.I)

Results 1 and 5 (Graphs 1.I and 5.I) show an interesting trend in that with higher oxygen concentration there is a definite curvature representing a positive deviation in the C_2H_4/C_2H_6 ratios vs O_2/ propanal. The R_3/R_6 ratio was subsequently calculated from measurement

of the initial slope, this behaviour is interpreted as an indication of degenerate branching, these experiments contained a higher oxygen concentration and showed a higher percentage decomposition.

The reaction:

$$H_2O_2 \longrightarrow 2OH^{\cdot}$$

becomes more extensive and $OH^{\cdot}$ being a less selective radical than HO_2 could provide other routes to C_2H_4.

A comparison of results in silica glass with those in a boric acid coated vessel at equivalent pressures, temperatures, and flowrates is possible with the results of sets 5 and 7. The initial C_2H_4/C_2H_6 ratios were the same although total product flowrates were higher in the silica glass vessel, than in the aged boric acid vessel.

The close agreement on the k_3/k_6 ratio lends support to the assumption that changes in the mechanism involving wall effects do not appear to influence the relative rates of production of C_2H_4 and C_2H_6.

The flow reactor results may be compared with those obtained by Baldwin and co-workers in a static reactor, at higher oxygen and a much larger total pressure. They obtained a value of 41 ± 5 at 713K for k_3/k_6 in an aged boric acid coated vessel. An adjusted value of 62 from 42 is calculated for the measured ratio in an aged KCl coated vessel. The correction was made for a heterogeneous reaction producing both C_2H_4 and CH_3CHO that was adjudged to be effectively independent of the chain process, and occuring on the surface of the KCl coated vessel.

Using the graphical results produced in sets 12 and 7 the rate constants $k_3 = 1.2 \pm (0.1) \times 10^8$ l mol^{-1} sec^{-1} at 773K and $k_3 = 1.3 \pm 0.1 \times 10^8$

of the initial slope, this behaviour is interpreted as an indication of degenerate branching, these experiments contained a higher oxygen concentration and showed a higher percentage decomposition.

The reaction:

$$H_2O_2 \longrightarrow 2OH^{\cdot}$$

becomes more extensive and $OH^{\cdot}$ being a less selective radical than HO_2 could provide other routes to C_2H_4.

A comparison of results in silica glass with those in a boric acid coated vessel at equivalent pressures, temperatures, and flowrates is possible with the results of sets 5 and 7. The initial C_2H_4/C_2H_6 ratios were the same although total product flowrates were higher in the silica glass vessel, than in the aged boric acid vessel.

The close agreement on the k_3/k_6 ratio lends support to the assumption that changes in the mechanism involving wall effects do not appear to influence the relative rates of production of C_2H_4 and C_2H_6.

The flow reactor results may be compared with those obtained by Baldwin and co-workers in a static reactor, at higher oxygen and a much larger total pressure. They obtained a value of 41 ± 5 at 713K for k_3/k_6 in an aged boric acid coated vessel. An adjusted value of 62 from 42 is calculated for the measured ratio in an aged KCl coated vessel. The correction was made for a heterogeneous reaction producing both C_2H_4 and CH_3CHO that was adjudged to be effectively independent of the chain process, and occuring on the surface of the KCl coated vessel.

Using the graphical results produced in sets 12 and 7 the rate constants

$k_3 = 1.2 \pm (0.1) \times 10^8$ 1 mol^{-1} sec^{-1} at 773K and $k_3 = 1.3 \pm 0.1 \times 10^8$

$1\ mol^{-1}\ sec^{-1}$ at 710K were obtained. Baldwin obtained a value of

$k_3 = 8.2 \times 10^7\ 1\ mol^{-1}\ sec^{-1}$ at 713 K[1]

Temperature variation

The two sets of results 9 and 11 were combined to produce a detailed investigation of C_2 hydrocarbon formation in the oxidation of propanal between 712 and 783K. Both sets of results agree giving reproducible data points and a linear plot for the graph (11.IV)

$$\text{Log} \quad (fC_2H_4 \quad + \quad C_2H_6) \quad v \quad 1/T \qquad \text{(1I.IV)}$$

This plot would become significant if the rate equation formulated earlier for the production of C_2 holds true as the reactant mixture composition is constant.

$$f\ C_2 = K_{expt.} V\ [\text{Propanal}]^{0.8-1.2} [O_2]^{1}$$

If $(P)^x\ (O_2)^y$ are constant throughout the experiments then the temperature dependance of C_2 gives an apparent E_a for the overall pyrolytic oxidation. An activation energy of $115^{\pm 8}$KJ was calculated from the slope of graph 11.IV. Baldwin and his co-workers measured an apparent activation energy for the maximum rate of reaction of 125 KJ bewteen 698 K and 773 K with orders of 1.5 and 0.2 with respect to aldehyde and oxygen at 713 K. He observed a region of a negative temperature coefficient between 610 K and 673 K and chose the temperature of 713 K as a compromise between a low temperature where the contribution from the 'low temperature' mechanism would be significant and a higher temperature where the rapid decomposition rate of H_2O_2 would give reaction rates too high for accurate measurement.

The overall activation energy when compared with that by Baldwin does provide evidence that the mechanism is similar to that occuring in the static reactor, referring back to the table on page 89. It is worth

bearing in mind that the order with respect to reactants for the production of hydrocarbons was not determined by Baldwin. for the initial rates at low pressures .The initial rate orders would be expected to be less than those determined for maximum rate and might approach our findings.

The experiments (series 7) and (series 12) at 713 K and 773 K respectively, examined the effect of oxygen and propanal on reaction rate, they provided a number of values for fC_2H_4/ f C_2H_6 vs f oxygen/ f propanal. The slope m gave an averaged value assuming equation (i) is valid for k_3/k_6 from which the data constant k_3 was evaluated. (Graphs 7.I and 12.I)

Two points each representing an average value for Log k_3/k_6 for variation with oxygen at 713 K and 773 K are plotted on the graph of Log k_3/k_6 vs 1/T, graph (15.I). These points include error bars to indicate scatter from the two sets of repeated experiments. Alongside this data are displayed points generated from single experiments at chosen temperatures, investigating temperature variation (results 11 & 9)

$$\log \frac{k_3}{k_6} = \text{Log } \frac{A_3}{A_6} - \frac{E_3}{2.3\ RT} - \frac{(-E_6)}{RT}$$

$$= \text{Log } \frac{A_3}{A_6} + \frac{1}{2.3\ RT}\ (E_6 - E_3)$$

for a graph of Log $\frac{k_3}{k_6}$ vs $\frac{1}{T}$ slope $= \frac{E_6 - E_3}{2.3\ RT}$ $+E_3 = (R \times \text{slope} \times 2.3) + E_6$

Slope = 1415 ± 350

E_3 = -2450 ± 613J

The negative value indicates that v the temperature dependence of k_3/k_6 is too large to be accounted for by the mechanism assumed. Baldwin's calculated value for E_3 is 16.20 KJ mol^{-1} (27)

A theoretical plot 15(II) can be drawn for k_3/k_6 vs 1/T using the two known rate parameters.

$$\text{Log } k_3 = 8.93 - \frac{16200}{2.3\ RT} \quad \text{Baldwin (estimate)}$$

$$\text{Log } k_6 = 8.1 - \frac{24660}{2.3\ RT} \quad \text{Trotman-Dickenson}$$

The gradient of this plot is +430 which is very much smaller than that of the experimentally produced line.

The steeper temperature dependence could be accounted for by the introduction of a peroxy radical intermediate, assumed to be prominent only in the low temperature oxidation of alkanes.

There is data for estimated values of Keq. for the gas phase association:

$R^{\cdot} + O_2 \rightleftharpoons RO^{\cdot}_2$ which indicates that it does take place at 700 K(9).

We now assume that reaction (3) becomes:

$$C_2H_5^{\cdot} + O_2 \rightleftharpoons C_2H_5OO^{\cdot} \xrightarrow{k_3'} C_2H_4 + HO_2^{\cdot}$$

replacing the direct bimolecular reaction.

A similar peroxy radical is used in the mechanism for the high temperature oxidation of acetaldehyde by Baldwin(21) and has not been entirely ruled out from the oxidation of propanal(4) in the same temperature ranges, though it is not strongly favoured.

The relative rates of formation of C_2 hydrocarbons on this assumption are:

$$\frac{r\ C_2H_4}{r\ C_2H_6} = \frac{k'_3[C_2H_5OO^{\cdot}]}{k'_6[C_2H_5^{\cdot}][C_2H_5CHO]} = \frac{k'_3\ K[C_2H_5^{\cdot}][O_2]}{k'_6[C_2H_5^{\cdot}][C_2H_5CHO]}$$

k_3 has been replaced by k'_3K, the temperature dependance of rC_2H_4/rC_2H_6 now included the temperature dependance of K;

$$\frac{d\ rC_2H_4}{d\left(\frac{1}{T}\right)rC_2H_6} = \frac{(\ln k'_3K)}{k_6} = (-E'_3 - + E_6)/R$$

Benson suggests[9] $\Delta H = -117$KJ for the association producing the peroxy radical, this has been modified by Baldwin[27] $\Delta H = -113$KJ.

Now $\Delta H = \Delta U + \Delta nRT$ taking an average temperature of 750 K and n = -1.

$$\Delta U = 113 + 623 = 119.2\ KJ$$

Graph 15(I) gives $(-E_3 - \Delta U + E_6) = 27.1$ KJ

$$E'_3 = 119.2 + 24.6 - 27.1$$

$$= 116 \pm 25\ KJ.$$

At first this might seem to be rather high, although it is not dissimilar to that calculated by Baldwin[27] for the activation energy of the reaction:

$$C_2H_5OO^{\cdot} \longrightarrow C_2H_4OOH \qquad (16)$$

which Baldwin calculated to be 114.5 KJ mol^{-1} and must involve a similar transition state.

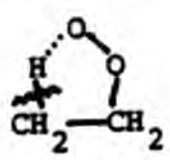

c.f.

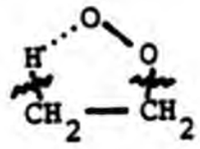

A_3' was determined by averaging the data used for the two experimental sets plotted on graph 15(7 and 12). A single estimation for each A_3' was used to calculate the mean value.(Shown below for experiment 196)

Temperature = 773 K ($1/T = 1.29 \times 10^{-3}$) Volume V=).259 dm^3

$fC_2H_6 = 2.30 \times 10^{8}$ moles sec^{-1}, $fC_2H_4 = 2.77 \times 10^{-8}$ moles sec^{-1}

$f\ O_2 = 54.0 \times 10^{-8}$ moles sec^{-1}, $O_2 = 7.10 \times 10^{-6}$ moles dm^3

$fC_2H_5CHO = 1020 \times 10^{-8}$ moles sec^{-1}

The concentration of $C_2H_5^{\cdot}$ can be estimated from the flow equation for C_2H_6.

$fC_2H_6 = V k_6 [C_2H_5^{\cdot}][C_2H_5CHO]$ $\quad C_2H_5^{\cdot} = 1.85 \times 10^{-9}$ moles dm^3

Together with Benson's data for the temperature dependance of K which extrapolated gives $K_{773} = 0.7\ atm^{-1}$, and $K_{710} = 1.4\ atm^{-1}$) we can now estimate a value for the concentration of the peroxy radical .

$$C_2H_5 + O_2 \rightleftharpoons C_2H_5O_2^{\cdot} \qquad C_2H_5O_2 = K [C_2H_5][O_2]$$

$K_p = K_c (RT)^n$ $\quad K_{c\ 773} = 40.7$ mols dm^3

$[C_2H_5O_2^{\cdot}] = 40.7 \times 1.85 \times 10^{-9} \times 7.10 \times 10^{-6} = 5.35 \times 10^{-13}$ moles dm^{-3}

k_3' can be obtained using the flow equation for $fC_2H_4 = V k_3' [C_2H_5OO^{\cdot}]$

$$k_3' = 2.0 \times 10^{5}\ sec^{-1} = A_3' \exp \frac{(-116000)}{(8.31 \times 773)}$$

$$A_3'\ (196) = 1.40 \times 10^{+13}$$

An average value for the experimental sets to obtain a "best" value was $1.00 \times 10^{+13}$ sec^{-1}. This is close to Baldwin's value[27] for $A_{16} = 10^{13.31}$ for the intra-radical proton transfer (see above), which would be expected if the transition states were similar.

Baldwin notes that Benson suggests a value of $10^{12.1}s^{-1}$ for a 1.5p transition which has been used in the absence of any experimental determination to calculate activation energies from single values of rate constants. Walsh had suggested [27] that the A factors for such transfers should decrease with increase in ring size in the transition state and that although a value of $10^{12.1}sec^{-1}$ is reasonable for a 1.5p transition, the value for a 1.4 transfer should be higher by a factor of about 10. Although in this it should be noted that the level of $C_2H_5OO^{\cdot}$ is calculated at four orders of magnitudee below that of $C_2H_5^{\cdot}$.

There is also thermochemical evidence in favour of an intermediate peroxide if the heats [8] of reaction are compared for:

$$\Delta H_3 = \Delta H_f C_2H_4\ (+52.3) + \Delta H_f HO_2 (+20.9) - \Delta H_f C_2H_5^{\cdot}\ (+110.8)$$

$$= -37.6\ KJ\ mol^{-1}.$$

$$\Delta H_3' = \Delta H_f C_2H_5OO^{\cdot}\ (+7.52) - \Delta H_f C_2H_5^{\cdot}\ (+110.8)$$

$$= -103.2\ KJ\ mol^{-1}$$

Reaction (3) although exothermic, is less so than the competitive foramtion of the peroxide.

Degenerate Branching

It has been suggested [1] that the bulk of ethene and ethane are formed by the elementary steps:

$$C_2H_5^{\cdot} + O_2 = C_2H_4 + HO_2^{\cdot} \quad (3)$$

$$C_2H_5 + C_2H_5CHO = C_2H_6 + C_2H_5CO^{\cdot} \quad (6)$$

and that autocatalysis results from formation of $OH^{\cdot}$ radicals by the decomposition of hydrogen peroxide and the subsequent attack on propanal;

$$H_2O_2 + M = 2OH^{\cdot} + M \quad (7)$$

$$OH^{\cdot} + C_2H_5CHO = C_2H_5CO^{\cdot} + H_2O \quad (8)$$

This results in the formation of more of the chain carrier $C_2H_5^{\cdot}$. $OH^{\cdot}$ radicals would be expected to interfere with the calculation of k_3 if reaction 3 was replaced by:

$$OH^{\cdot} + C_2H_5^{\cdot} = H_2O + C_2H_4 \quad 3(a)$$

$$O_2 + C_2H_5^{\cdot} = HO_2^{\cdot} + C_2H_4 \quad (3)$$

$$HO_2^{\cdot} + C_2H_5^{\cdot} = HO_2^{\cdot} + C_2H_4 \quad 3(b)$$

As reactions (a) and (b) are radical-radical (3) would be expected to predominate at low conversions.

As well as introducing an autocatlaytic character to the mechanism via (7) and (8) OH might also introduce an alternative pathway to C_2H_4 as the OH radical is far less selective in hydrogen abstraction than $HO_2^{\cdot}$. One can envisage hydrogen abstraction at a point other than the weak aldehydic C——H bond ie:

$$OH^{\cdot} + C_2H_5CHO = H_2O + CH_2^{\cdot}—CH_2CHO = C_2H_4 + CHO\ (2p^1)$$

Using equation (2p') a modified equation, relating the flowrates for the formation of C_2H_4 and C_2H_6 can be written

$$fC_2H_4/fC_2H_6 = \frac{k_3[C_2H_5^{\cdot}][O_2] + k_{2p}[OH^{\cdot}][C_2H_5CHO] + k'[R][C_2H_5CHO]}{k_6[C_2H_5^{\cdot}][C_2H_5CHO]}$$

The activation energy for the reaction 2p' is expected to be greater than that of reaction (8). Then as the temperature increases there will be a greater contribution via this alternative route to the flowrate of ethene. The ratio fC_2H_4/fC_2H_6 will rise more steeply than expected, this behaviour is observed on graph 15. The above explanation of this is only valid if the concentration of $OH^{\cdot}$ radicals is a comparable order of magnitude with $C_2H_5^{\cdot}$ radicals, so as to make the second term significant. The second term represents the consequence of the product H_2O_2 decomposition and is part of the degenerate branching mechanism, but as $OH^{\cdot}$ is not a chain carrier; ie not regenerated in the decomposition of the aldehyde, the fraction of ethene from this route will be strictly proportional only to the fraction of H_2O_2 decomposed. A theoretical check can be made on the amount of H_2O_2 decomposed by assuming that $H_2O_2 \equiv \Sigma C_2$'s and using equation (13) and it's known rate parameters(*1)

$$H_2O_2 + M \longrightarrow 2OH^{\cdot} + M \qquad (13)$$

$$k_{13}\ (dm^3 mols\ sec^{-1}) = 3.19 \times 10^{14} \exp \frac{(-196KJ)}{(8.31\ T)} \qquad (M = N_2)$$

Using coefficients for O_2, H_2O and H_2O_2 relative to N_2 = 0.78, 5.4,4.0, respectively, an arbitary coefficient of 4 for C_2H_5CHO.

The percentage decomposition of propanal in terms of the flowrate of hydrocarbons for run 196 was 0.49% (run 97 = 0.042%)

$$fH_2O_2 = f\ propanal \times 0.0049 = 5.00 \times 10^{-8}\ mols\ sec^{-1}$$

$$[H_2O_2] = t\ fH_2O_2/V = 3.36 \times 5.0 \times 10^{-8} / 0.259 = 6.48 \times 10^{-7}\ mols\ dm^{-3}$$

$$\frac{-d\ H_2O_2}{dt} = k_{13}[H_2O_2][M]\ r = 16.38 \times 6.48 \times 10^{-7} \times 8.93 \times 10^{-3} = 9.5 \times 10^{-6}$$

The corresponding reduction in fH_2O_2 is Vx r= 2.45×10^{-8} mols sec^{-1} which gives a fractional decomposition of $2.45 \times 10^{-8}/5.0 \times 10^{-8}$ $\simeq$ 50% this represents the limit of expected decomposition at the higher temperature (773K). A similar calculation for a low decomposition of propanal at the lower temperature (run 97, 710K) indicated only 0.25% H_2O_2 decomposed by the gas phase decomposition path. Over the spread of decomposition and temperature covered in these experiments the range of the homogeneous decomposition calculated is larger than expected towards the higher limit and indicates a possible major contribution to the ethene formed. Unfortunately , in the experimental work there was no H_2O_2 detected. It may well be that it was decomposed heterogeneously to $H_2O_2 + O_2$ or associated with aldehyde[11].

The third term represents a chain carrier radical $R(HO_2^{\cdot}$ or $C_2H_5^{\cdot})$ abstracting $H^{\cdot}$ from the alkyl group.

$$R^{\cdot} + C_2H_5CHO \rightarrow CH^{\cdot}-CH_2CHO + RH$$

$$CH_2^{\cdot}-CH_2CHO \rightarrow C_2H_4 + CHO \rightarrow C_2H_4 + CO + H^{\cdot}$$

Trace amounts of H_2 were found, also ethanal figures reflecting attack on alkyl groups, but the results here do not indicate a great deal of difference over the temperature range which would be encouraging for a simple mechanism. There is a possibility of adding a fourth term for ethene production, arising from the pyrolytic mechanism.

$$C_2H_5^{\cdot} \rightarrow C_2H_4 + H^{\cdot} \quad \text{and}$$

$$C_2H_5^{\cdot} + C_2H_5^{\cdot} \rightarrow C_4H_{10} \quad \text{or} \quad C_2H_4 + C_2H_6$$

The steepness of graph 15 may therefore be accounted for by the intrusion

of one of several of these alternative pathways to ethene. This also applies to the positive deviations on earlier graphs (1.1 and 5.1).

Formation of Ethanal

Ethanal was measured in small quantities throughout the work performed on the oxidation of propanal. The results suggests the amounts proportional to the flowrate of oxygen. At low flowrates of oxygen, no traces of ethanal were discovered. The lower limit of detection was of the order 1.00×10^{-9} moles sec^{-1}.

For a number of the experiments where the flowrate of oxygen was constant at 3.1×10^{-7} mols sec^{-1} the ethanal flowrate was about $3.0 \times 10^{-9} \pm 0.9$ moles sec^{-1}. Typical flowrates for C_2H_4 were 1.37×10^{-8} to 1.97×10^{-8} moles sec^{-1}. The ratio fCH_3CHO/C_2H_4 was approximately 0.2 ± 0.1. This result is broadly in agreement with Baldwin's findings[1]. His proposal was that ethanal arises from attack on propanal at the secondary position in the $C_2H_5^{\cdot}$ group.

$$HO_2^{\cdot} + CH_3CH_2CHO \longrightarrow CH_3CHCHO + H_2O_2$$

$$CH_3CHCHO + O_2 \longrightarrow CH_3\underset{\overset{\cdot}{O}-O}{CH-CHO} \rightarrow CH_3CHO + CO + OH$$

The results can only be considered to be semi-quantitative because of the difficulty in sampling the aldehyde from the liquid trap due to the vast excess of propanal.

The oxidation of Isobutanal

The oxidation of isobutanal was studied at fixed aldehyde and oxygen flowrates and at two different temperatures (Graph 14.I results 14,222-228).

Propene the major reaction product was detected in all the experiments. Propane was detected only in trace amounts at 715K; less than 7.0×10^{-11} moles sec^{-1}. at higher temperatures a value for the ratio fC_3H_6/fC_3H_8 was obtained.

If as above in the case of propanal, propane and propene like ethane and ethene are primary products being formed by the elementary reactions[9]

$$i\text{-}C_3H_7 + O_2 = C_3H_6 + HO_2 \qquad (1i)$$

and $$iC_3H_7 + iC_3H_7CHO = C_3H_8 + iC_3H_7CO \text{ or } i\text{-}C_3^{\cdot}H_6CHO \qquad (4i)$$

the product flowrate equations are:

$$fC_3H_6 = V \frac{d[C_3H_6]}{dt} = V k_1 [i\text{-}C_3H_3][O_2]$$

$$fC_3H_8 = V\ d[C_3H_8] = V k_4 [C_3H_7][iC_3H_7CHO]$$

By eliminating C_3H_7 the following relationship is obtained:

$$\frac{fC_3H_6}{fC_3H_8} = \frac{k_1 [O_2]}{k_4 [C_3H_7CHO]} \qquad (I)$$

A value of k_4 may be obtained from a modified equation in the literature produced by Baldwin and Walker[46] based on earlier work by Kerr and Trotman-Dickenson who considered the increase in yield of C_3H_6 at higher temperatures due to the decomposition of the $CH_3CH(CH_2)CHO$ radical, formed by $i\text{-}C_3H_7$ attack at the primary

C_H positions in $i\text{-}C_3H_7CHO$. The rate constant k_4 used represents a combination of these reactions

$$i\text{-}C_3H_7^{\cdot} + i\text{-}C_3H_7CHO \longrightarrow C_3H_8 + (CH_3)_2 CH\,C^{\cdot}O \qquad (4a)$$

$$i\text{-}C_3H_7^{\cdot} + i\text{-}C_3H_7CHO \longrightarrow C_3H_8 + (CH_3)_2 C^{\cdot}CHO \qquad (4b)$$

$$i\text{-}C_3H_7^{\cdot} + i\text{-}C_3H_7CHO \longrightarrow C_3H_8 + CH_3CH(C^{\cdot}H_2)CHO \qquad (4c)$$

$$\text{Log } (k_{4a} + k_{4b})/\ dm^3 mol\ sec^{-1} = 8.05 - (8080\ cal\ mol^{-1}/2.3RT)$$

$$\text{Log } (k_{4c})/dm^3\ mol\ sec^{-1} = 7.95 - (11280 cal\ mol^{-1}/2.3RT)$$

$$(k_4 = k_{4a} + k_{4b} + k_{4c}) \simeq 7.0 \times 10^5\ dm^3\ mol\ sec^{-1} \qquad (46)$$

Although not enough data was collected to produce a graphical study and only trace amounts of propane were detected at 715K, a rough estimate can be made using the above value of $C_3H_6/C_3H_8 = 4.5 \pm 0.4$ obtained at 772K. Using expression (I) a value of 135.8 is obtained for k_1/k_4 which produces the rate constant k_1 of $9.5 \times 10^7\ dm^3\ mol^{-1}\ sec^{-1}$ at 772K. which is comparable with the value obtained by Baldwin of 1.27×10^8 at 715K.

Our rate constant is less than that obtained by Baldwin, even though the temperature is 57K higher. Comparison with propanal oxidation leads to the suggestion of another peroxy radical intermediate present in the mechanism and using Benson's data[45] for the equilibrium constant K we can form the equation below

$$iC_3H_7 + O_2 \overset{K}{\rightleftharpoons} iC_3H_7OO \qquad k' = C_3H_6 + HO_2$$

$$\frac{rC_3H_6}{rC_3H_8} = \frac{k_1\,(iC_3H_7OO)}{k_4\,(iC_3H_7)\,(iC_3H_7CHO)} = \frac{k'_1 K\,(iC_3H_7)\,(O_2)}{k_4\,(iC_3H_7)\,(iC_3H_7CHO)}$$

K_P = 0.85 atm^{-1} K_c = 54 1 mol^{-1}.

Substitution of the experimental values to the equation produces a rate constant of k'_1 = 2.0 x 10^6 sec^{-1}. at 772K.

Small traces of C_2H_4 were found in the course of this work, in the high temperature region. The assumption had been made by Baldwin that it was a secondary product from the decomposition of propanal or propene oxide. These products in our work remained undetermined.

An alternative route to produce ethene would be the alkyl radical decomposition.

$$iC_3H_7 \longrightarrow C_2H_4 + CH_3 \qquad (7i)$$

Oxidation of n-Butanal

Ethene was detected as the major product from the oxidation of n-butanal, the experimental conditions were the same as those for isobutanal. Propene was obtained as a trace product in all the experiments. Baldwin had found propene as the major reaction product in an early oxidation of n-butanal[19]. The formation of C_2H_4 rather than propene as the major product points to another reaction competing successfully against the oxidation reaction under our experimental conditions.

$$nC_3H_7 + O_2 = C_3H_6 + HO_2 \qquad (3n)$$

$k_3 = 6.4 \times 10^7$ l mol^{-1} sec^{-1} at 753K Baldwin[12]

This competition could either be due to the rapid unimolecular decomposition of nC_3H_7 [4]

$$nC_3H_7 \longrightarrow C_2H_4 + CH_3 \qquad k = 1 \times 10^5 \text{ sec}^{-1} \quad 753K$$

or the bimolecular pyrolysis reaction as given by Laidler and Lin[47]

$$nC_3H_7 + M \longrightarrow C_2H_4 + CH_3 + M$$

$k = 3.47 \times 10^{13} \exp(-131KJ/RT)$ sec^{-1}

Unfortunately no methane was recovered as a reaction product.

The thermal decomposition of aldehydes

Pyrolysis in the absence of oxygen in the system was studied because of the low flowrate of oxygen in the oxidation experiments, and a comparison made of the major products.

In the propanal decomposition analysis of light hydrocarbons showed C_2H_6 as the major product with a much reduced flowrate of C_2H_4.

The ratio of C_2H_6 to C_2H_4 varied from 25.2 at lower temperatures to 9.6 at 772K. The flowrates of ethane were seen to be only slightly smaller than that obtained in oxidation experiments under equivalent conditions:

$$C_2H_6 \text{ (pyrolysis) @ 772K} = 6.6 \times 10^{-9} \text{ mols sec}^{-1}$$

$$C_2H_6 \text{ (Oxidation) @ 772K} = 1.0 \times 10^{-8} \text{ mols sec}^{-1}$$

The elementary reaction in both cases for the formation of C_2H_6 is presumed to be the same:

$$C_2H_5^{\cdot} + C_2H_5CHO = C_2H_6 + C_2H_5CO^{\cdot}$$

The flowrates of ethene are seen to be over an order of magnitude smaller in pyrolysis for corresponding temperature and propanal flowrates:

$$C_2H_4 \text{ (pyrolysis) @ 772K} = 6.9 \times 10^{-10} \text{ mols sec}^{-1}$$

$$C_2H_4 \text{ (Oxidation) @ 772K} = 1.9 \times 10^{-8} \text{ mols sec}^{-1}$$

The formation of ethene in the pyrolysis system is probably via unimolecular decomposition of the $C_2H_5^{\cdot}$ radical.

$$C_2H_5^{\cdot} = C_2H_4 + H^{\cdot}$$

$$\text{or } C_2H_5^{\cdot} + C_2H_5^{\cdot} = C_4H_{10} \text{ or } C_2H_4 + C_2H_6$$

No trace of ethanal was discovered which was to be expected, because its formation in the oxidation of propanal is considered via attack on an oxygen molecule by secondary CH_3CHCHO radical.

Thermal decomposition experiments were also performed for i-butanal and n-butanal, with both aldehydes the major products measured were the same as those in oxidation, however no trace of C_2H_4 was detected in the decomposition of iso-butanal.

Graph 1.1 Relative percentage rate of formation in a silica reactor at 710K.

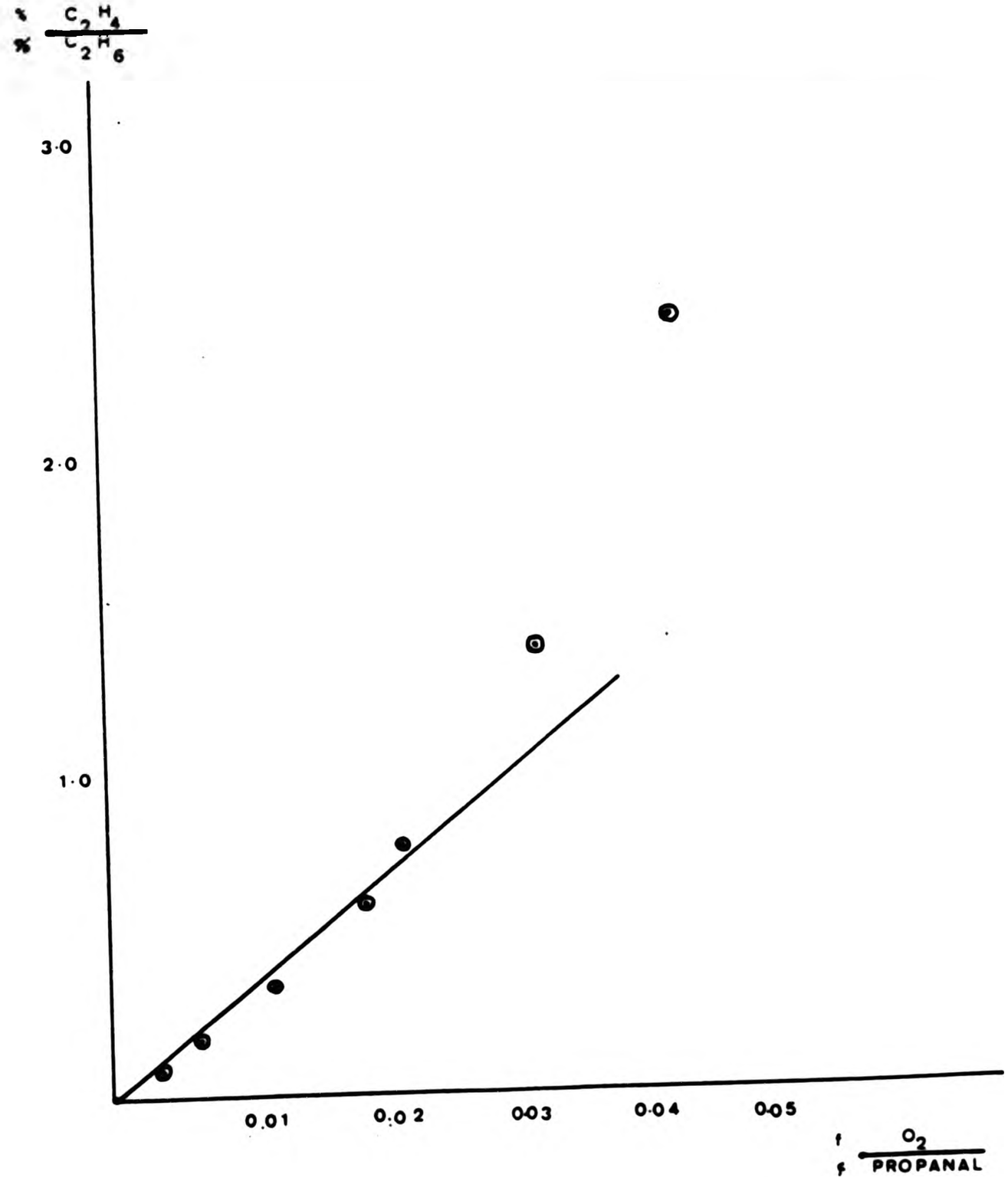

Graph 4.1 Relative percentage rate of formation in a silica reactor at 713K.

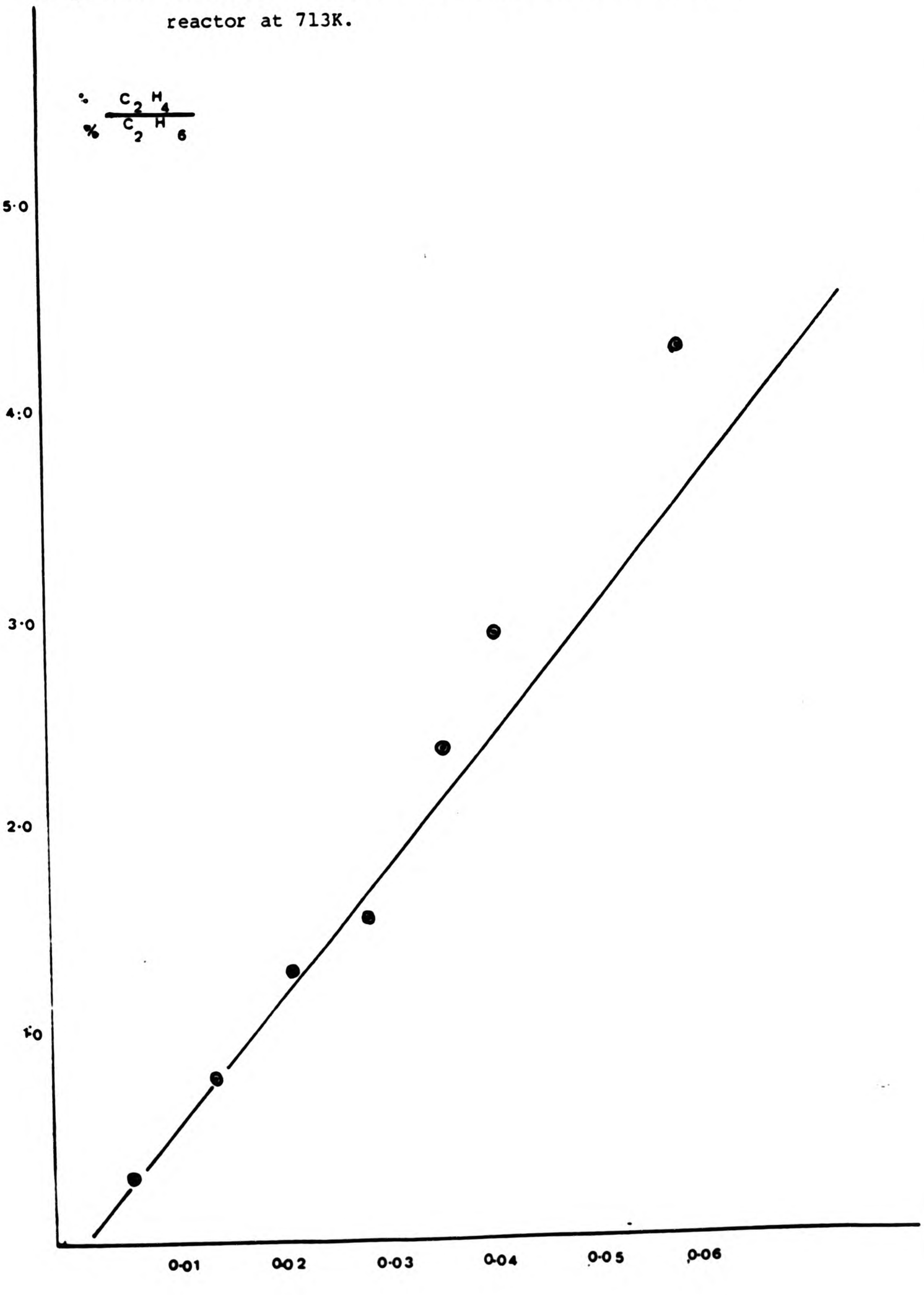

Graph 5.1. Relative rate of formation of hydrocarbons in a silica glass reactor at 713K.

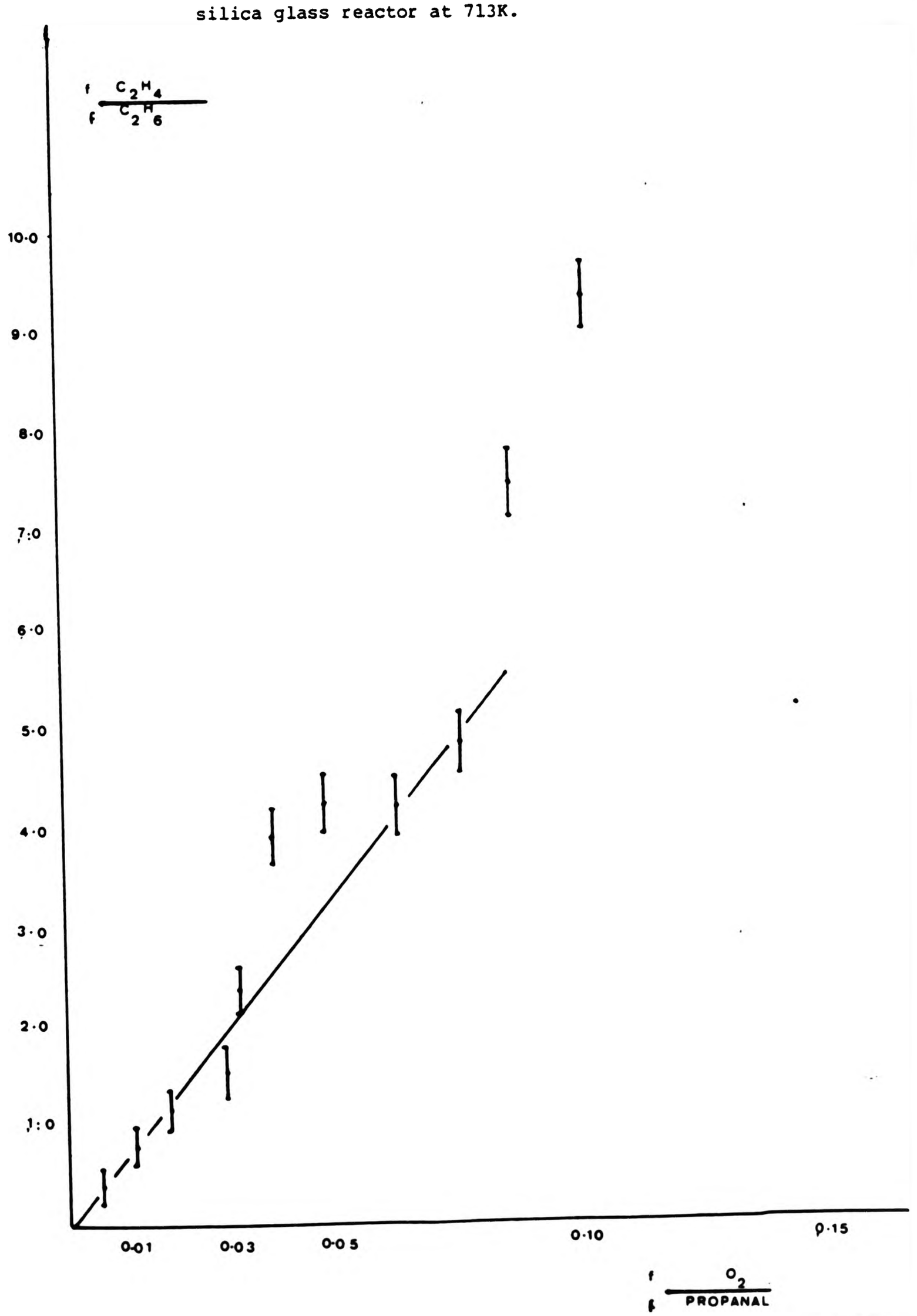

Graph 7.1. Relative rate of formation of hydrocarbons at 713K in an aged boric acid vessel.

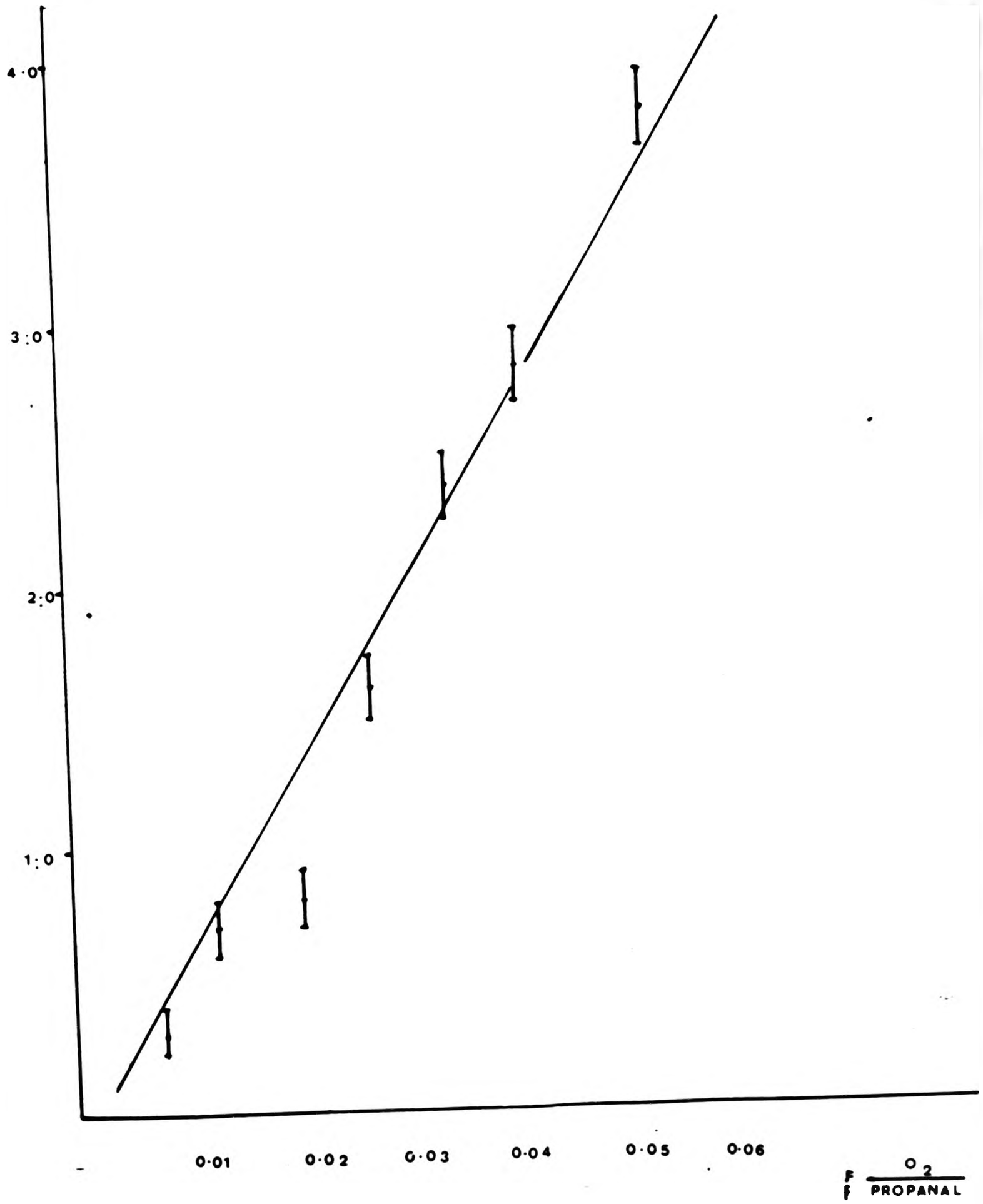

Graph 7.1. Relative rate of formation of hydrocarbons at 713K in an aged boric acid vessel.

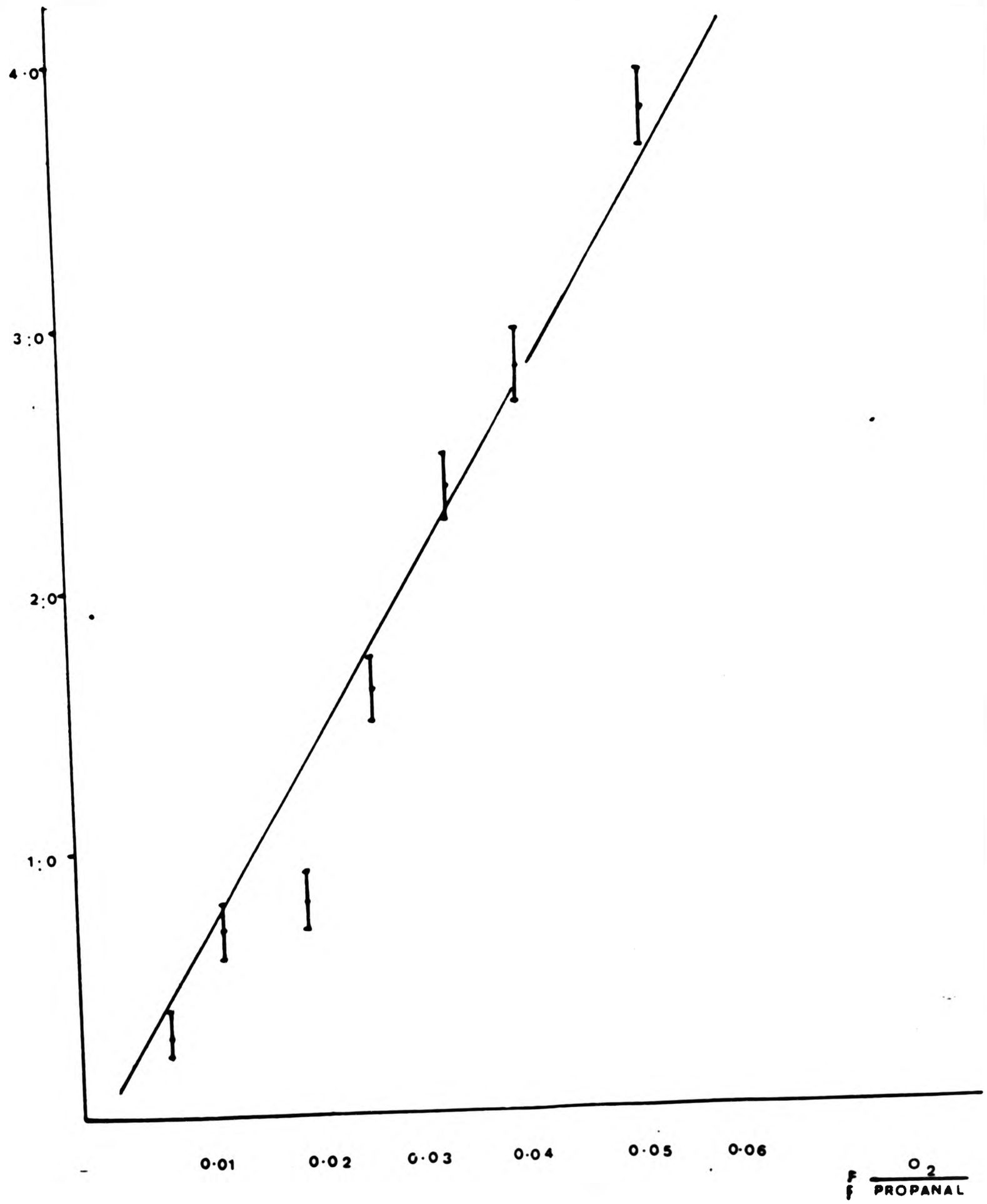

Graph 7.11. Used in determination of the order of C_2H_4 with respect to oxygen at 713K.

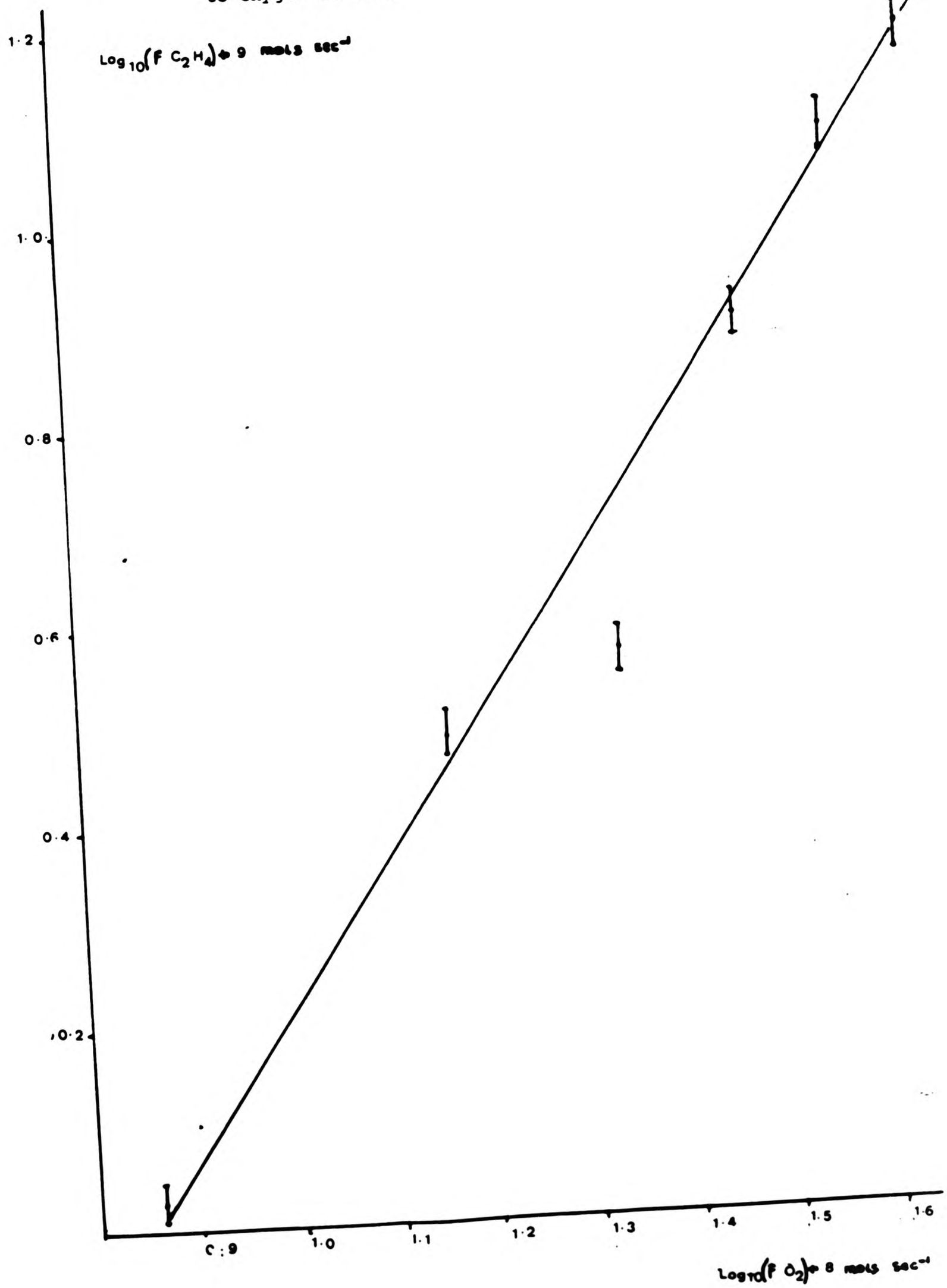

Graph 7.111. Used in determination of the order of C_2H_6 with respect to oxygen at 713K.

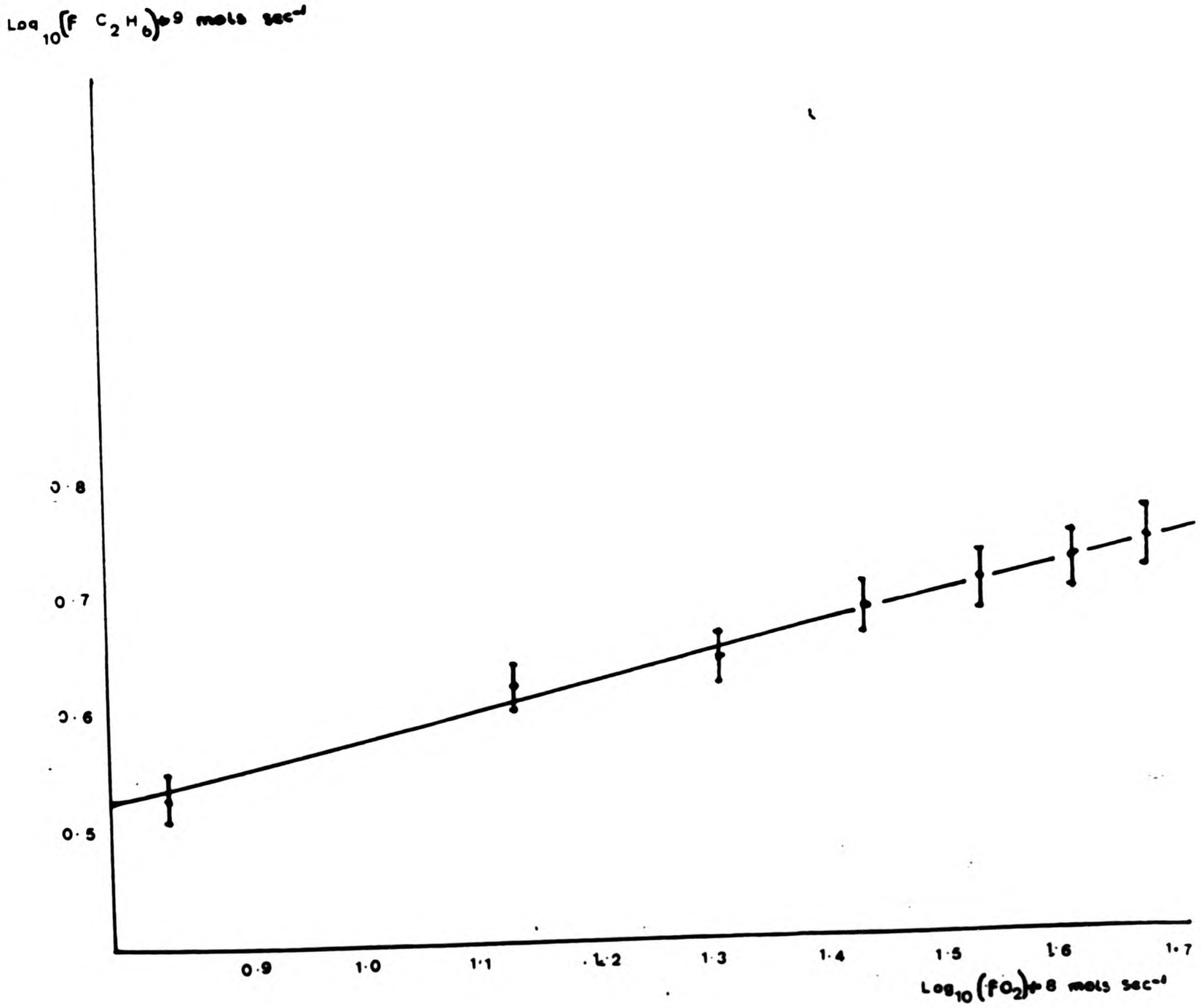

Graph 7.IV Used in the determination of the order of total hydrocarbons with respect to oxygen at 713K.

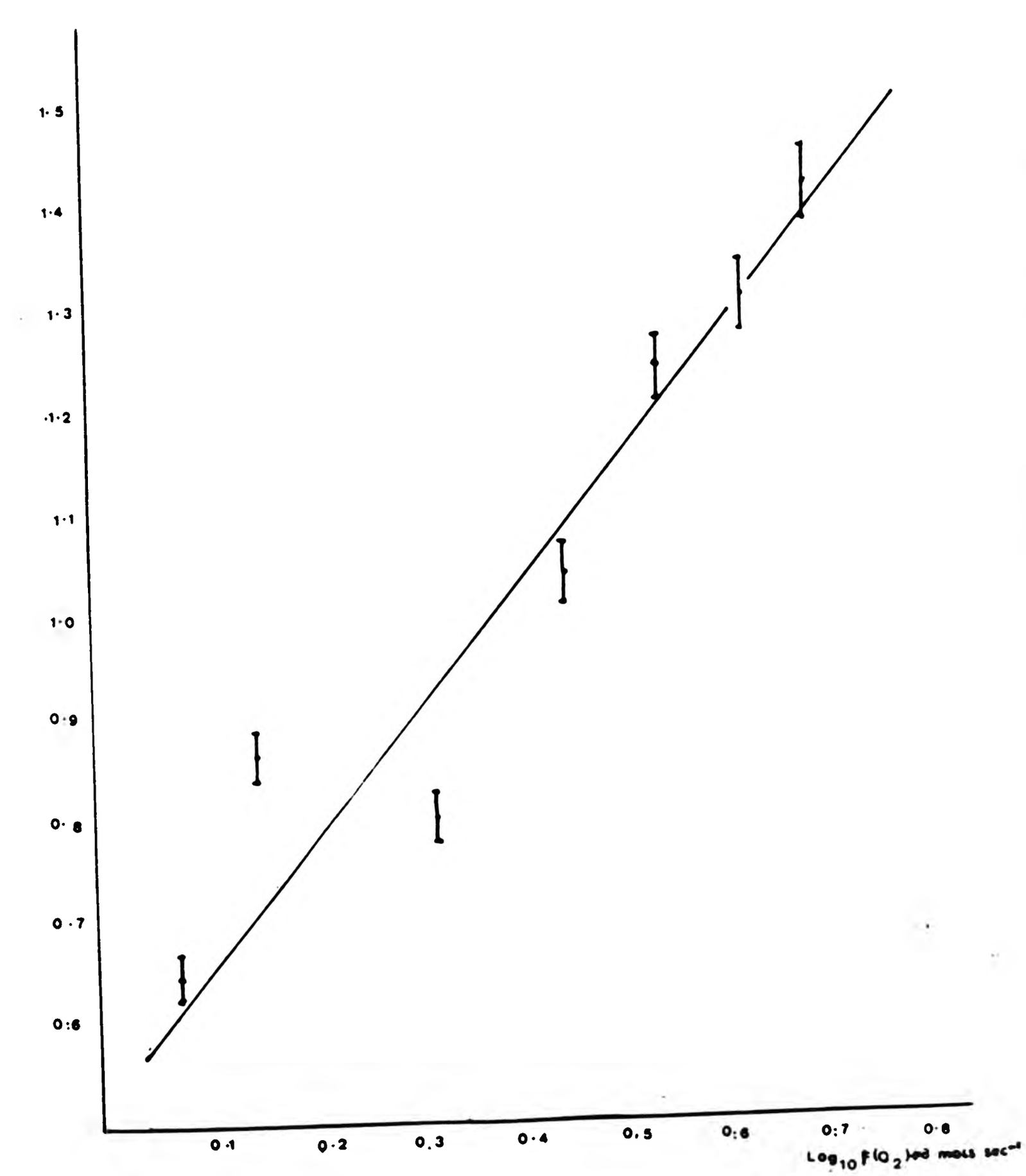

Graph 10.1. Relative ratio of formation of hydrocarbons in an aged boric acid vessel at 713K.

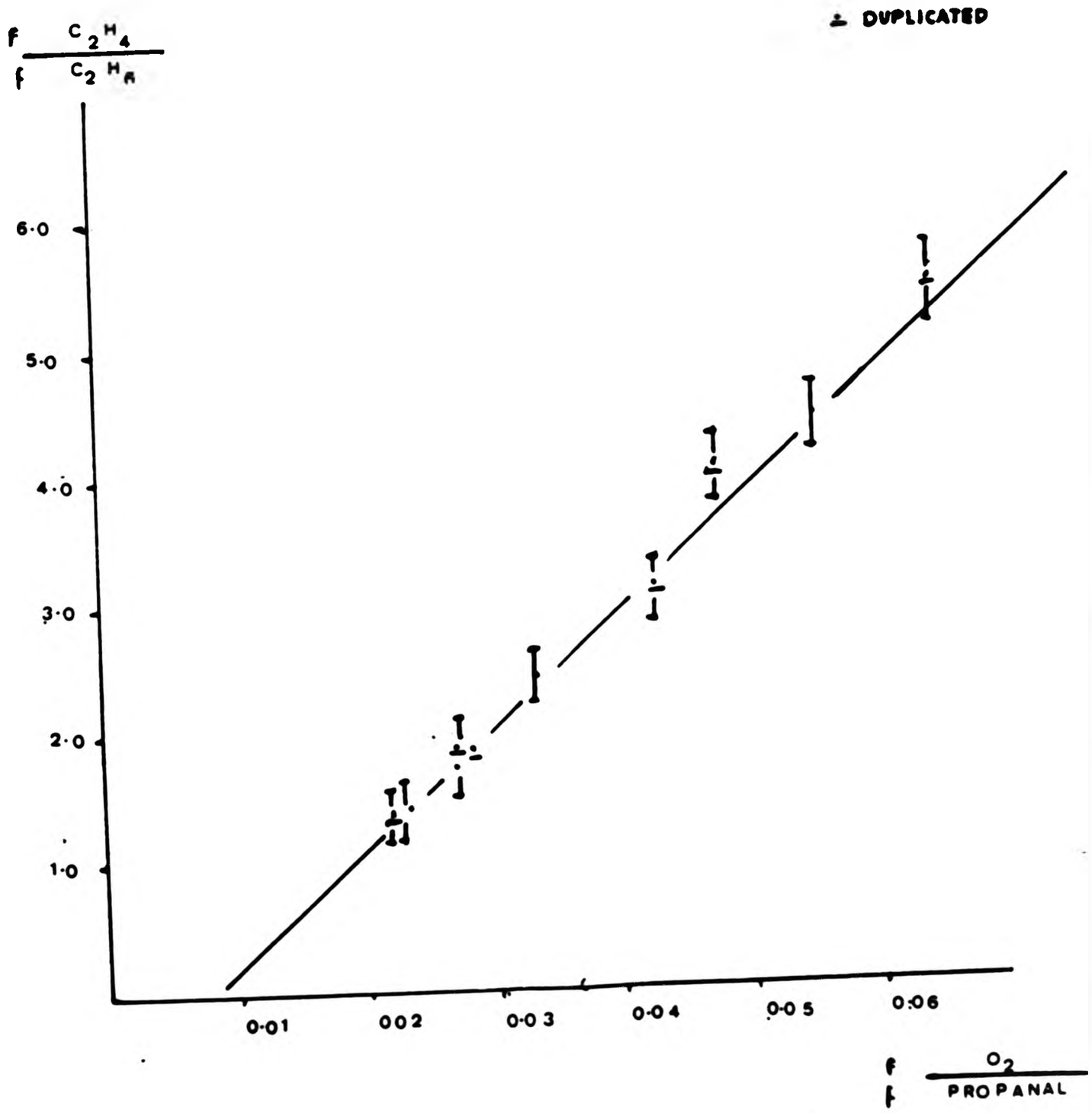

Graph 10.11. Used in the determination of the order of C_2H_4 production with respect to propanal at 713K.

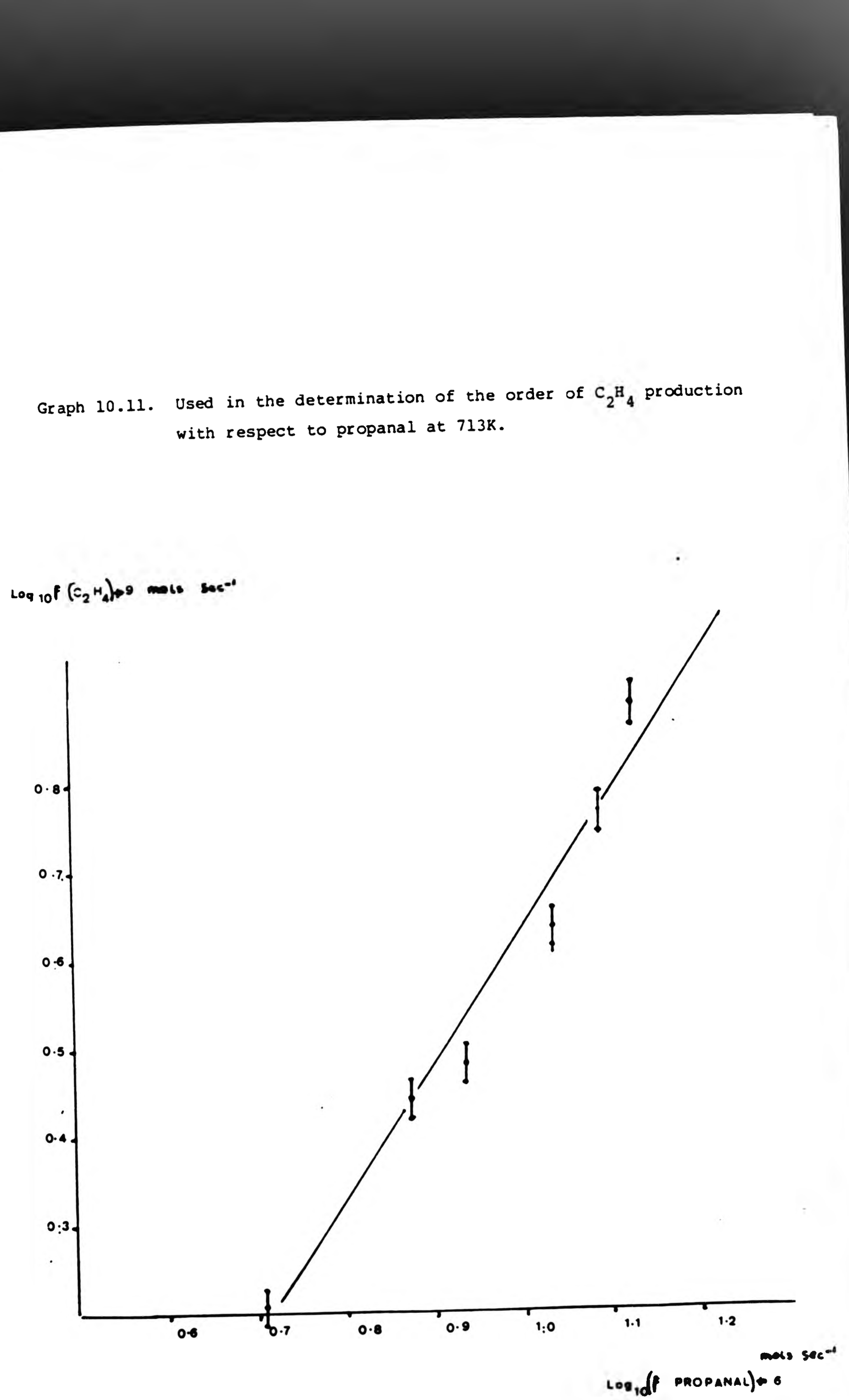

Graph 10.111. Used in determination of the order of C_2H_6 production with respect to propanal at 713K.

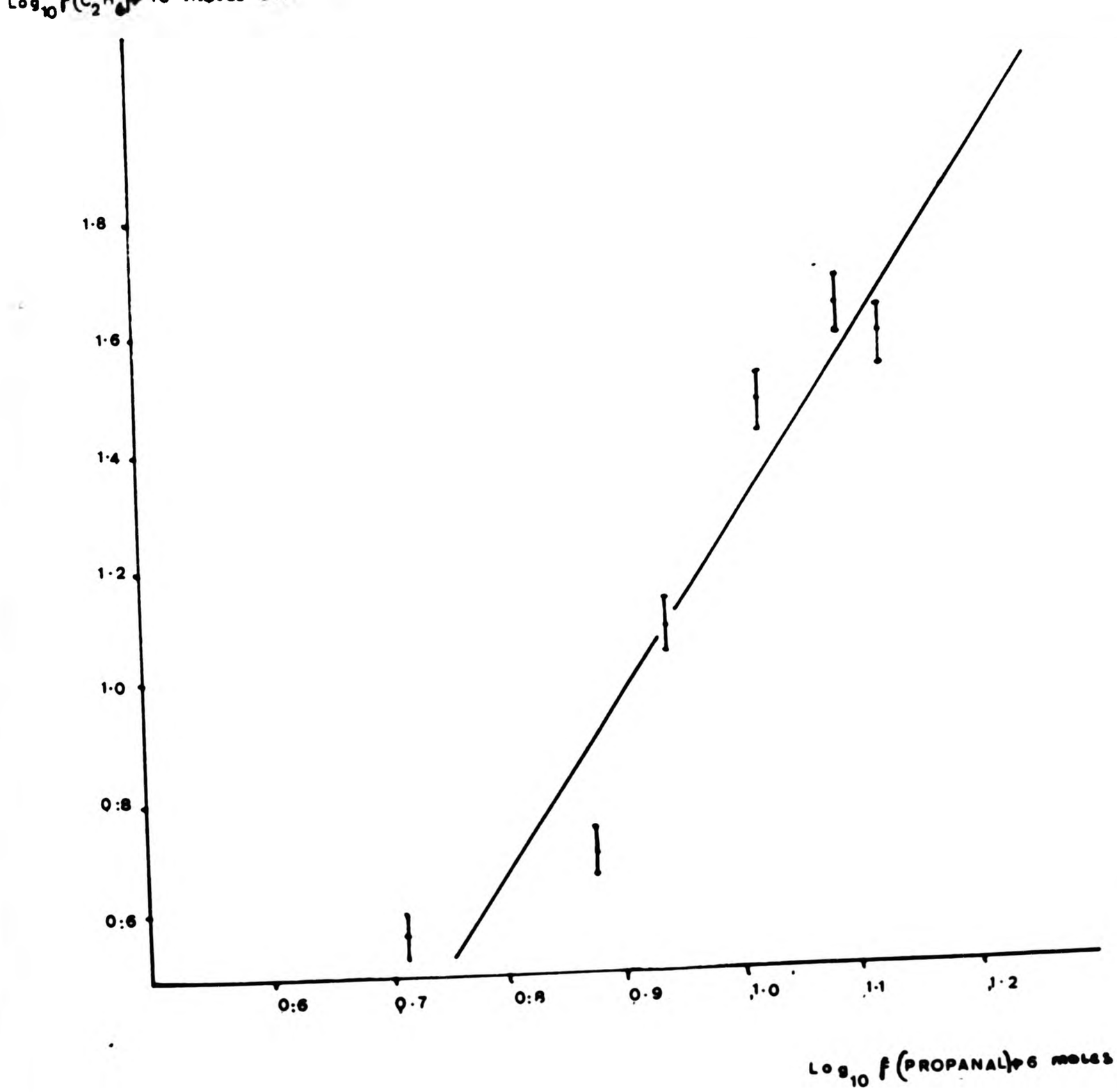

Graph 10.IV Used in determination of the order of total hydrocarbons with respect to propanal at 713K.

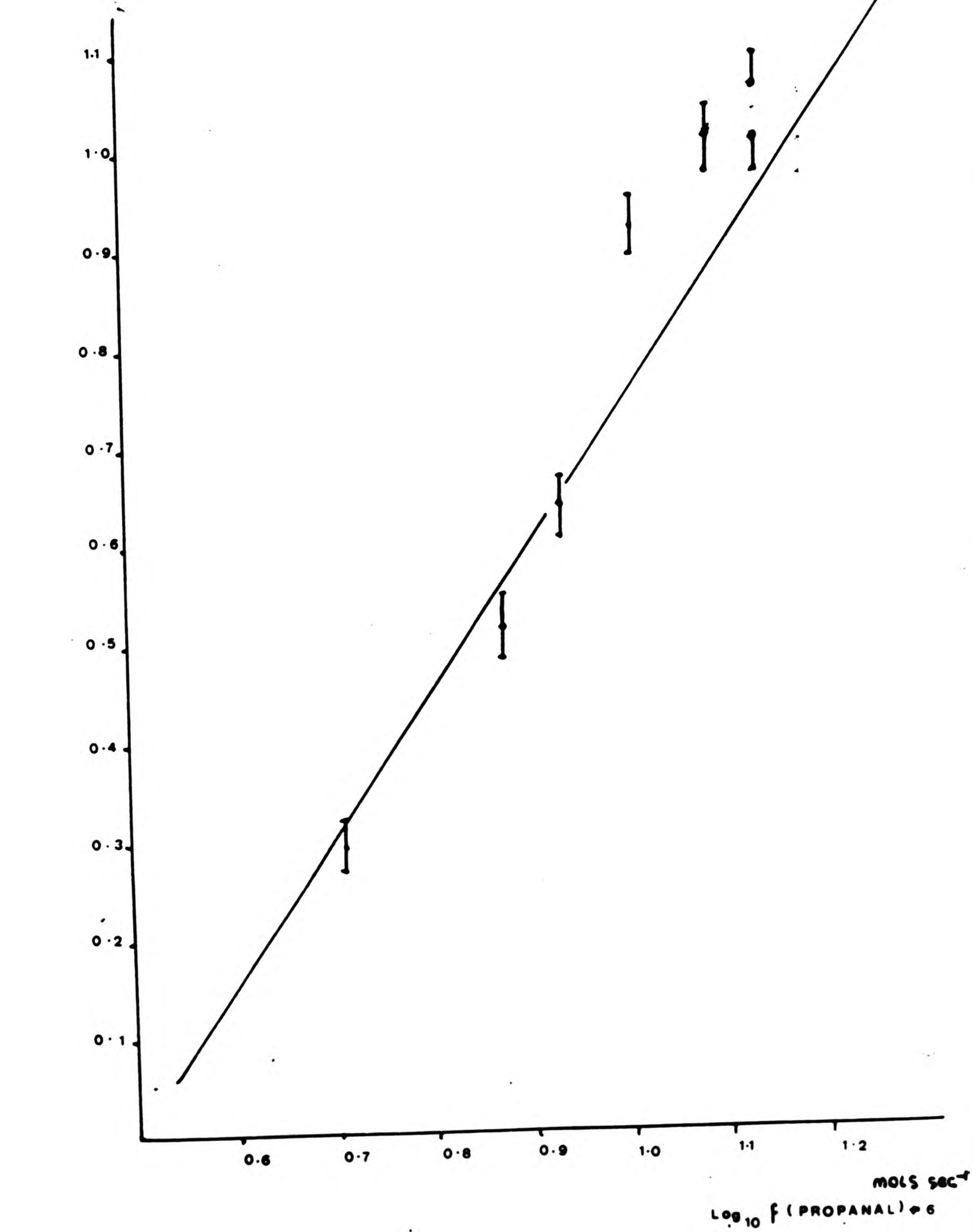

Graph 11.IV Showing total hydrocarbon formation with temperature variation.

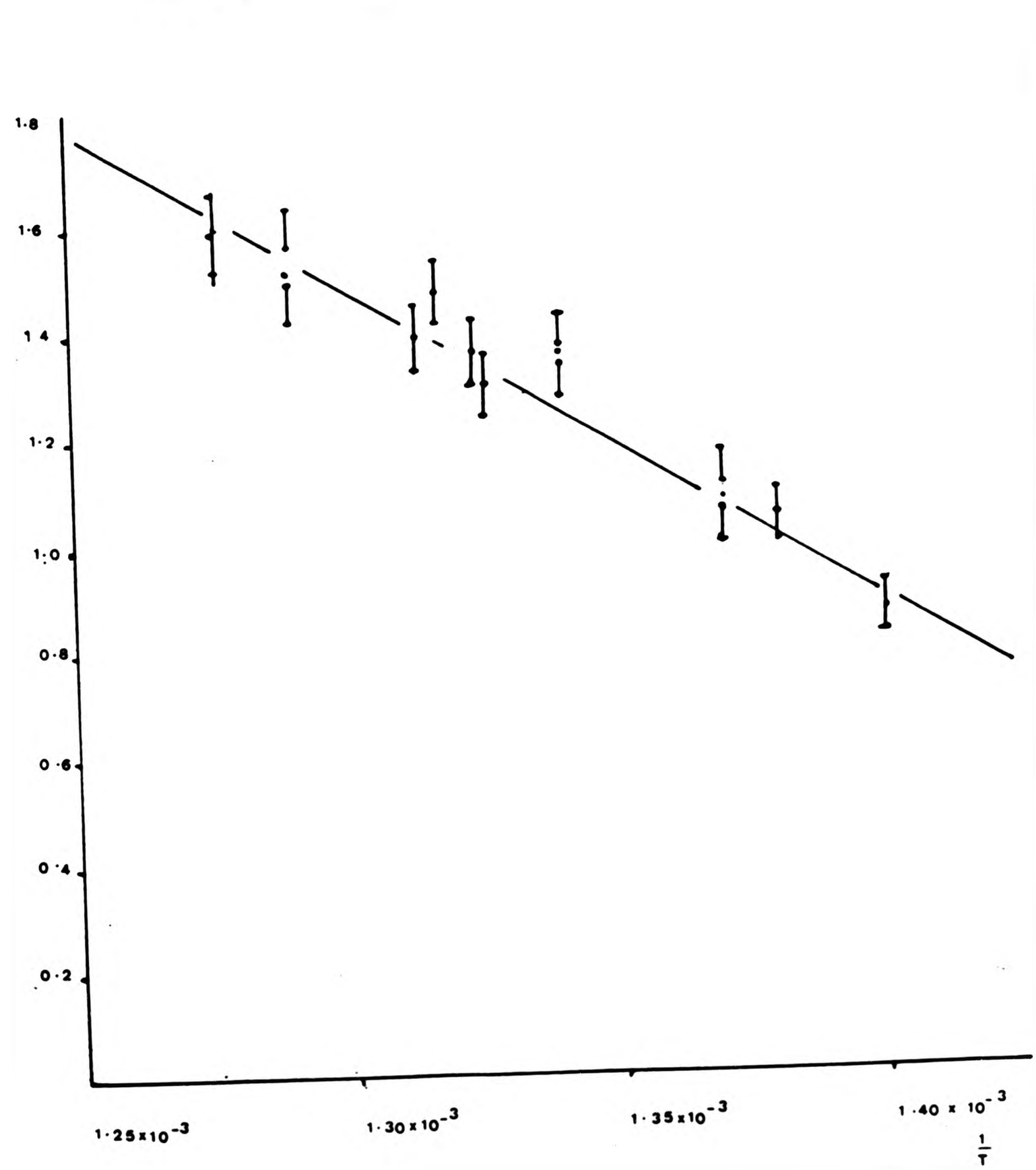

Graph 12.1. Relative ratio of hydrocarbon formation at 773K.

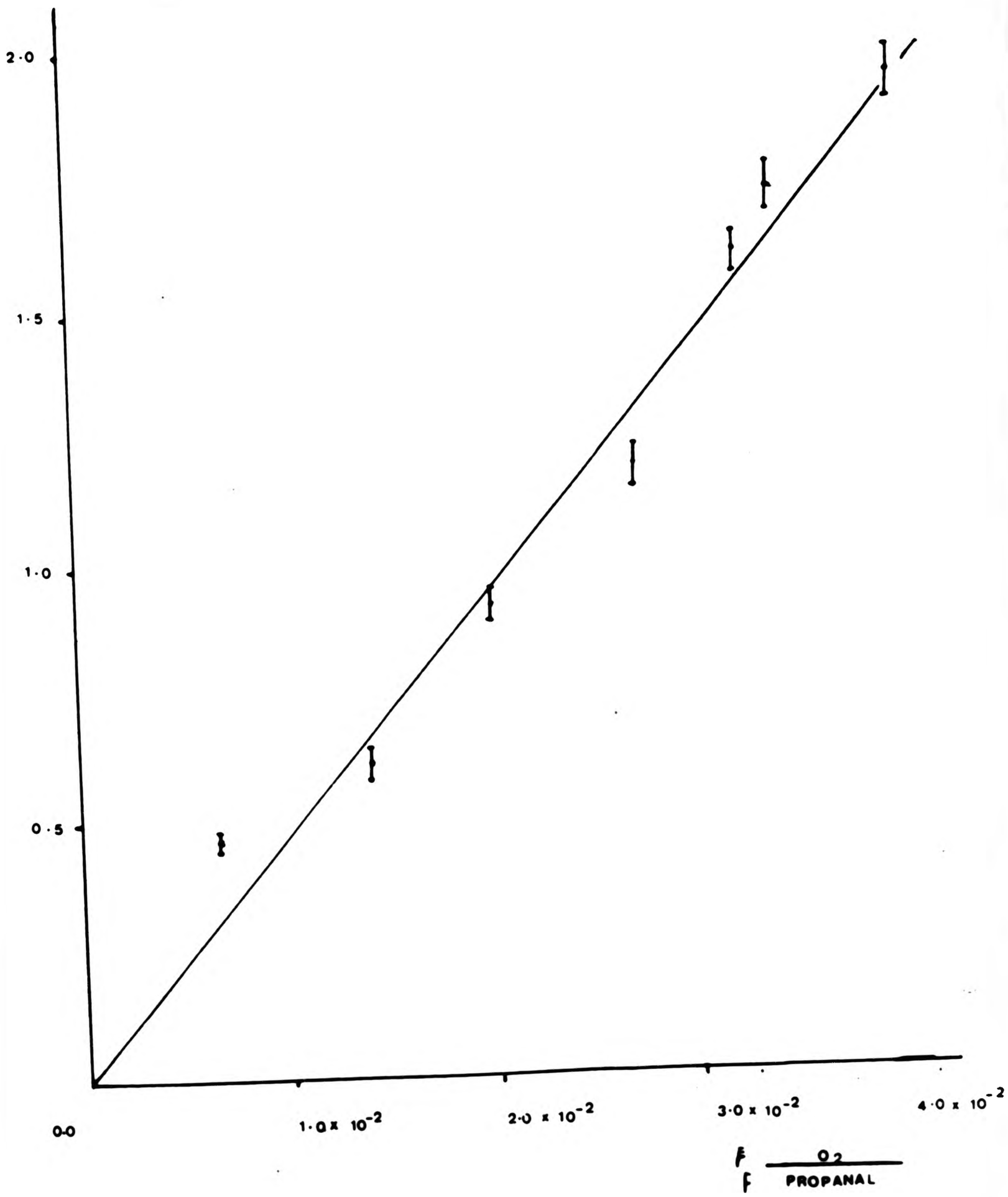

Graph 12.11. Used in determining the order of C_2H_4 production with respect to oxygen at 773K.

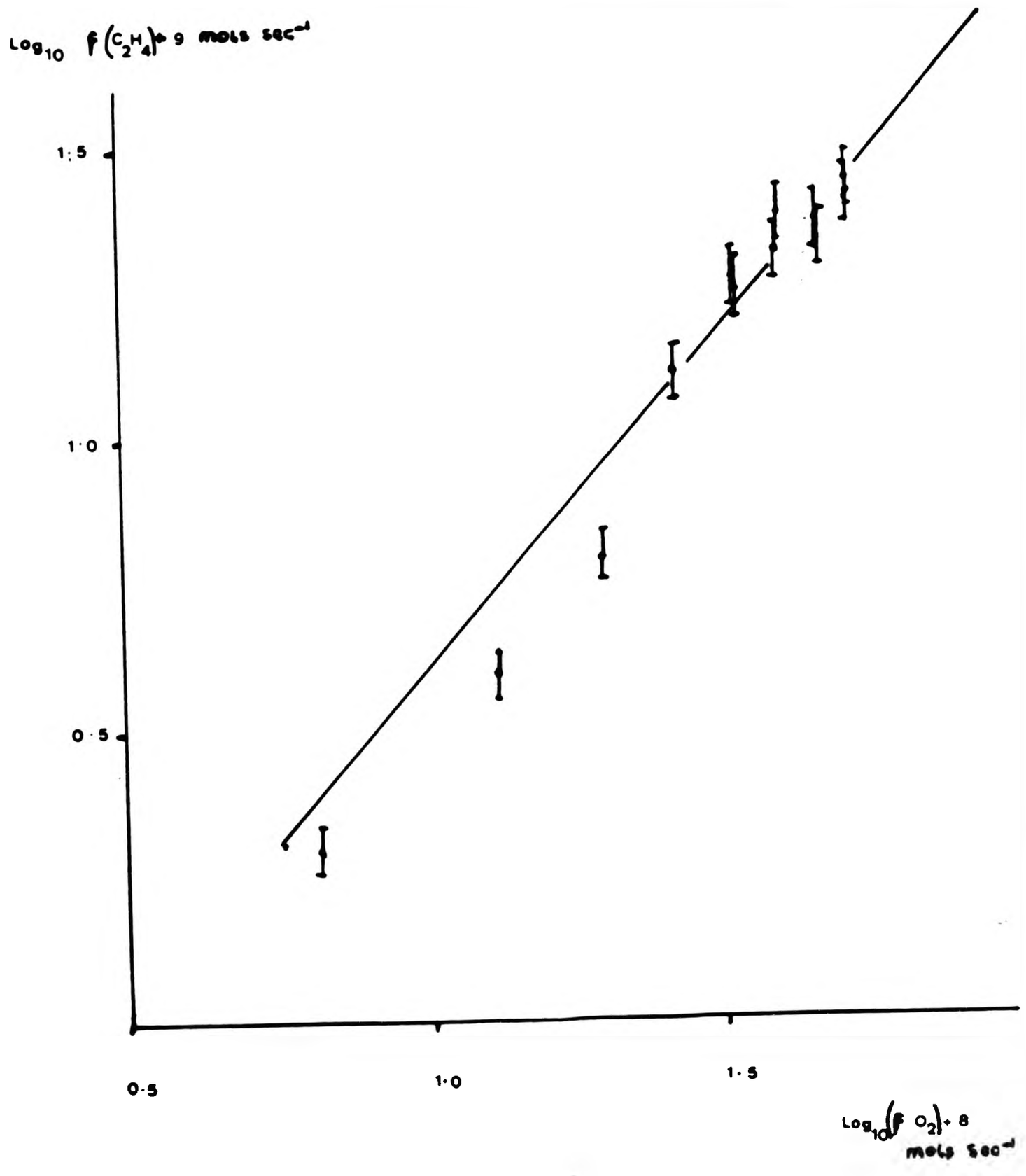

Graph 12.111. Used in determining the order of C_2H_5 with respect to oxygen at 773K.

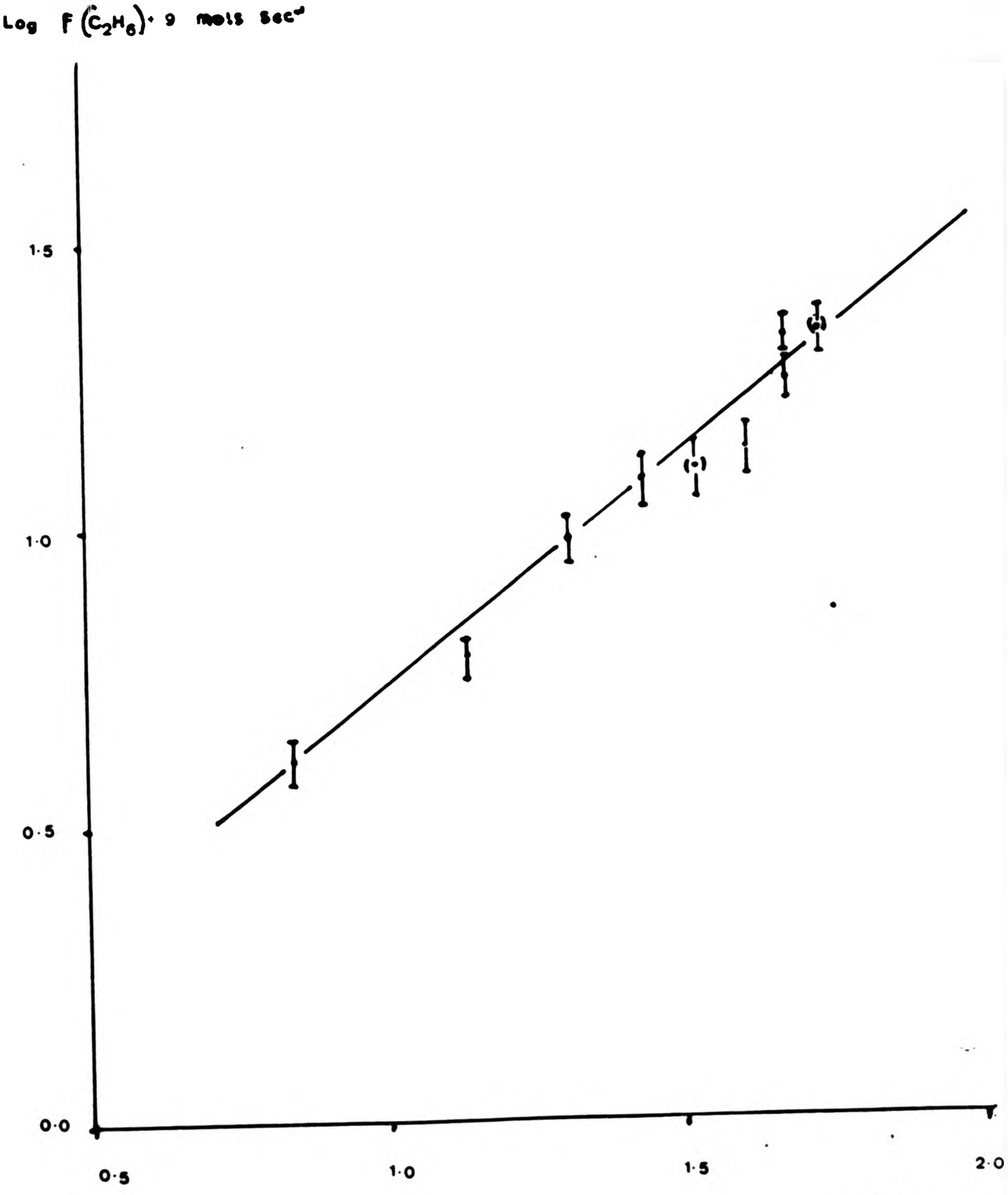

Graph 12.IV. Used in determining the order of total hydrocarbons with respect to oxygen at 773K.

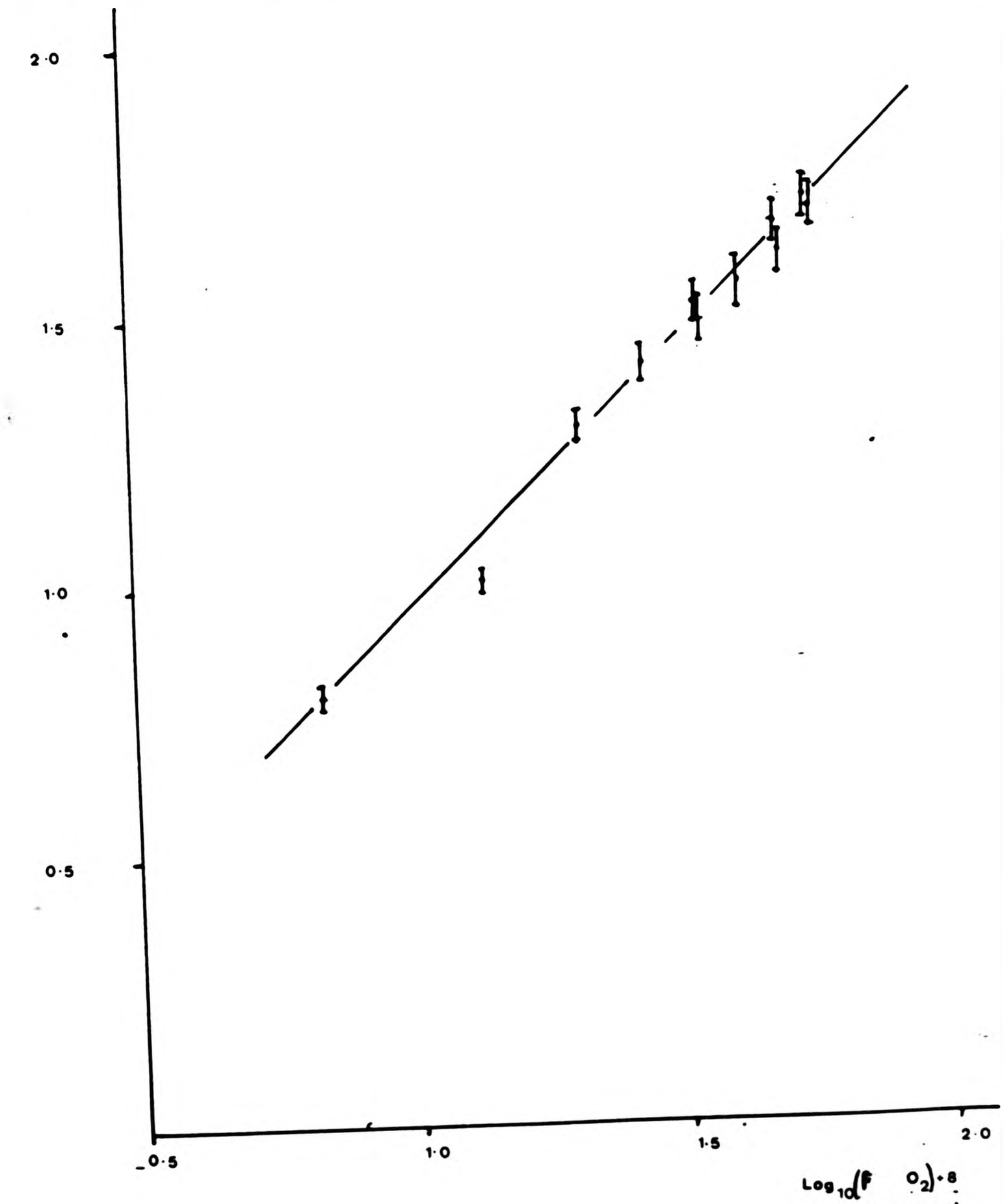

Graph 13.1. Variation in relative ratio of hydrocarbon foramtion at 773K.

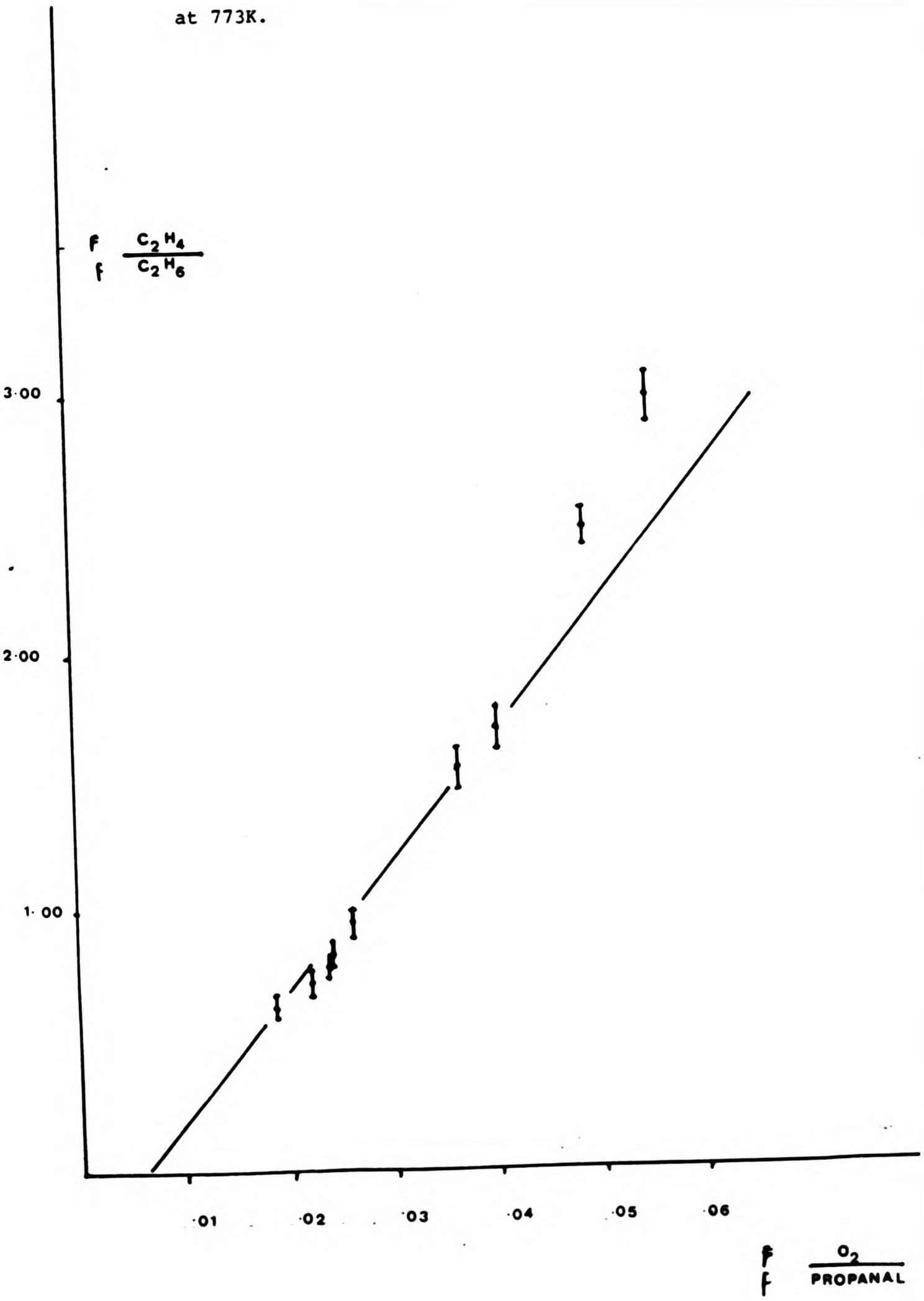

Graph 13.11. Used in determining the order of C_2H_4 production in respect to propanal at 773K.

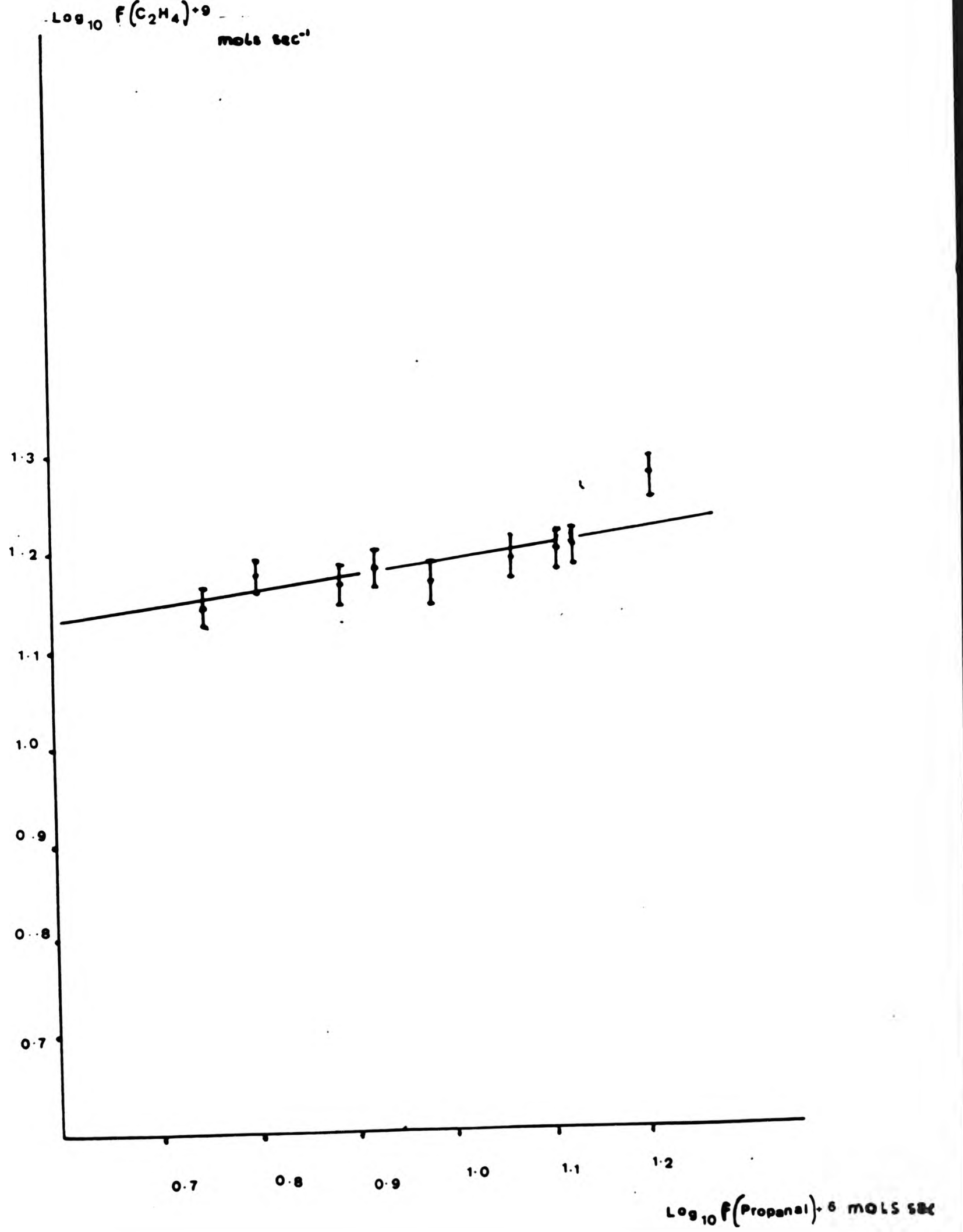

Graph 13.111. Used in determining the order of C_2H_6 production with respect to propanal at 773K.

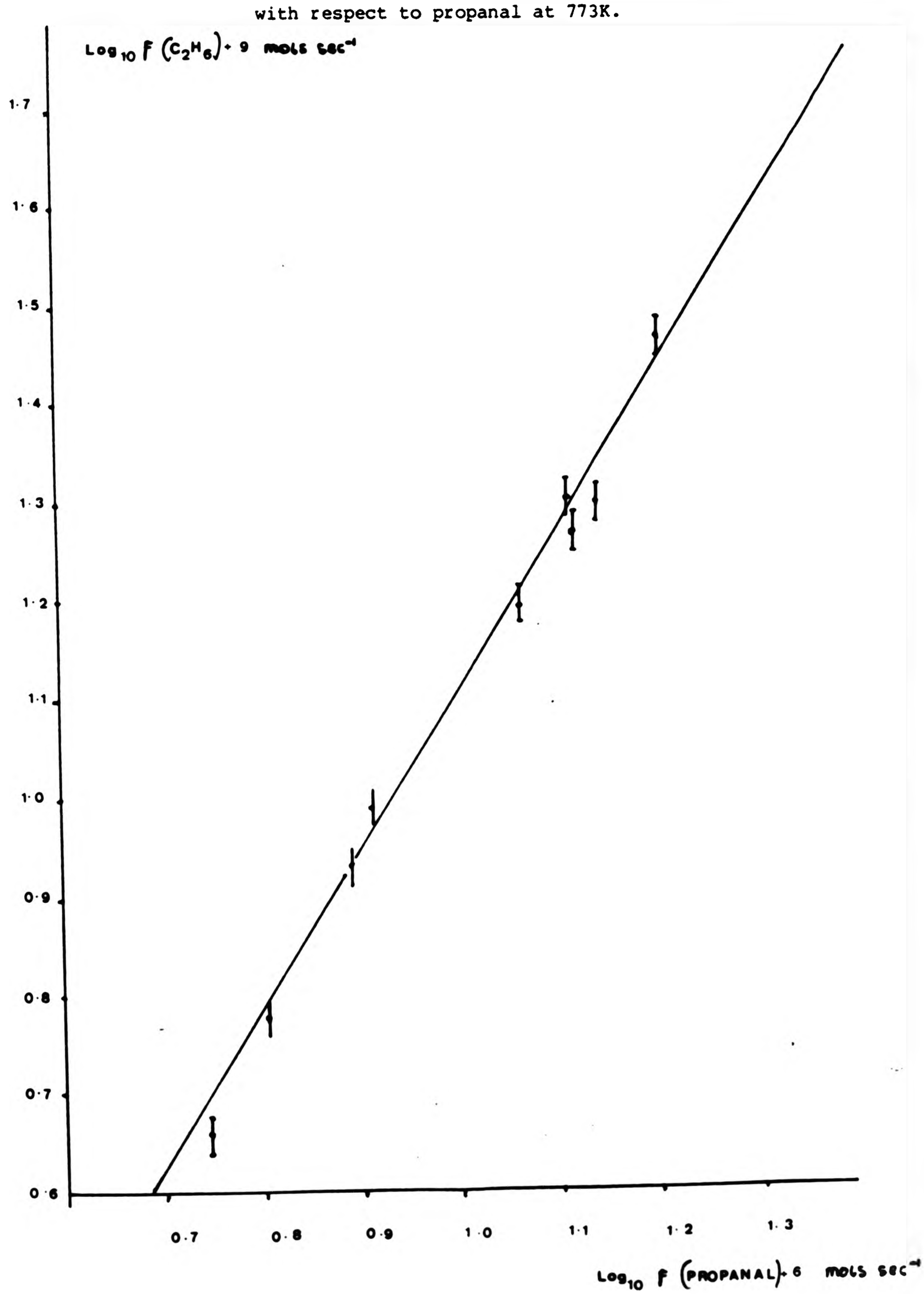

Graph 13.1V. Used in determining the order of total hydrocarbon production with respect to propanal at 773K.

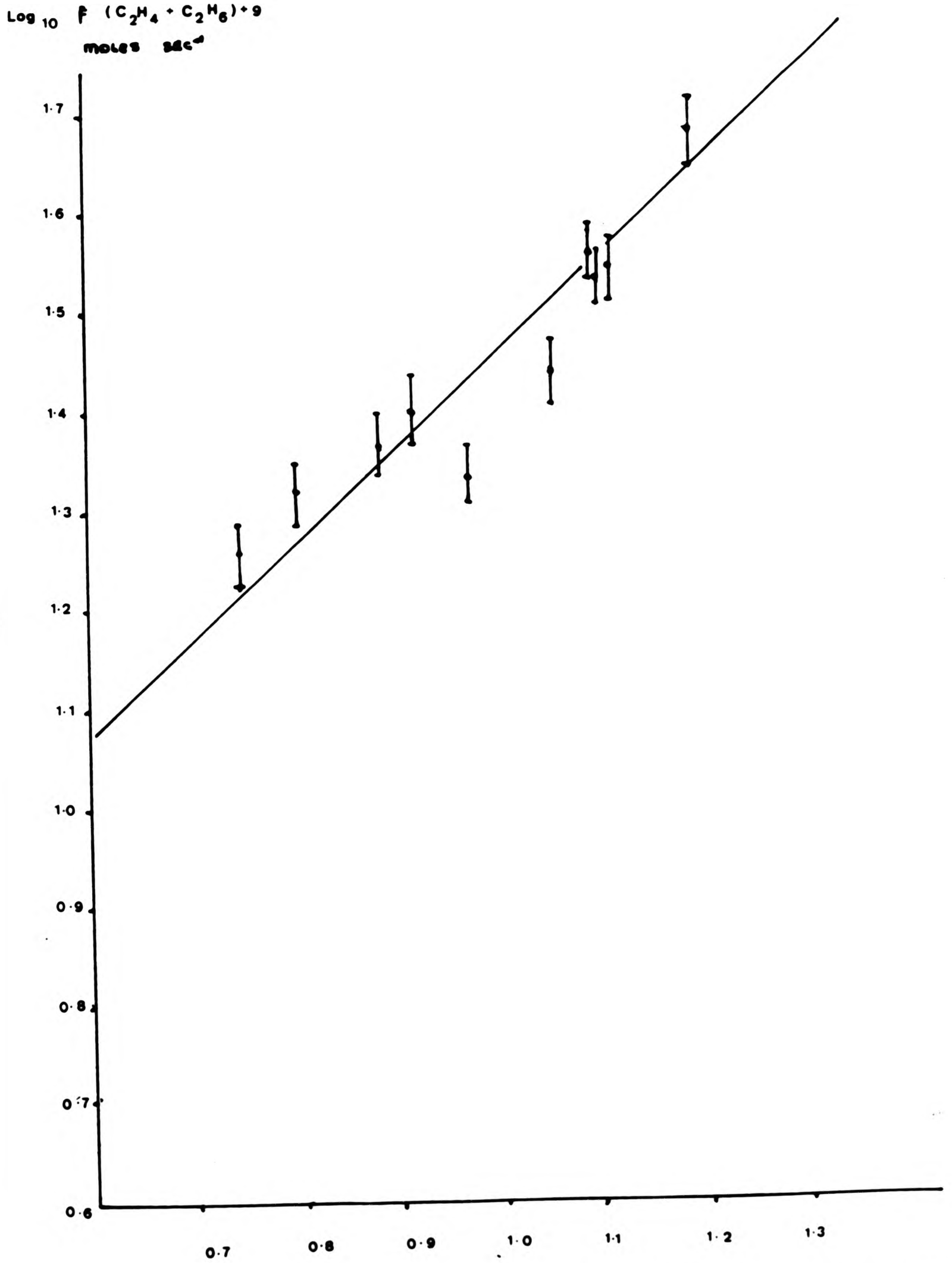

Graph 14.1. Major hydrocarbon formation with temperature variation

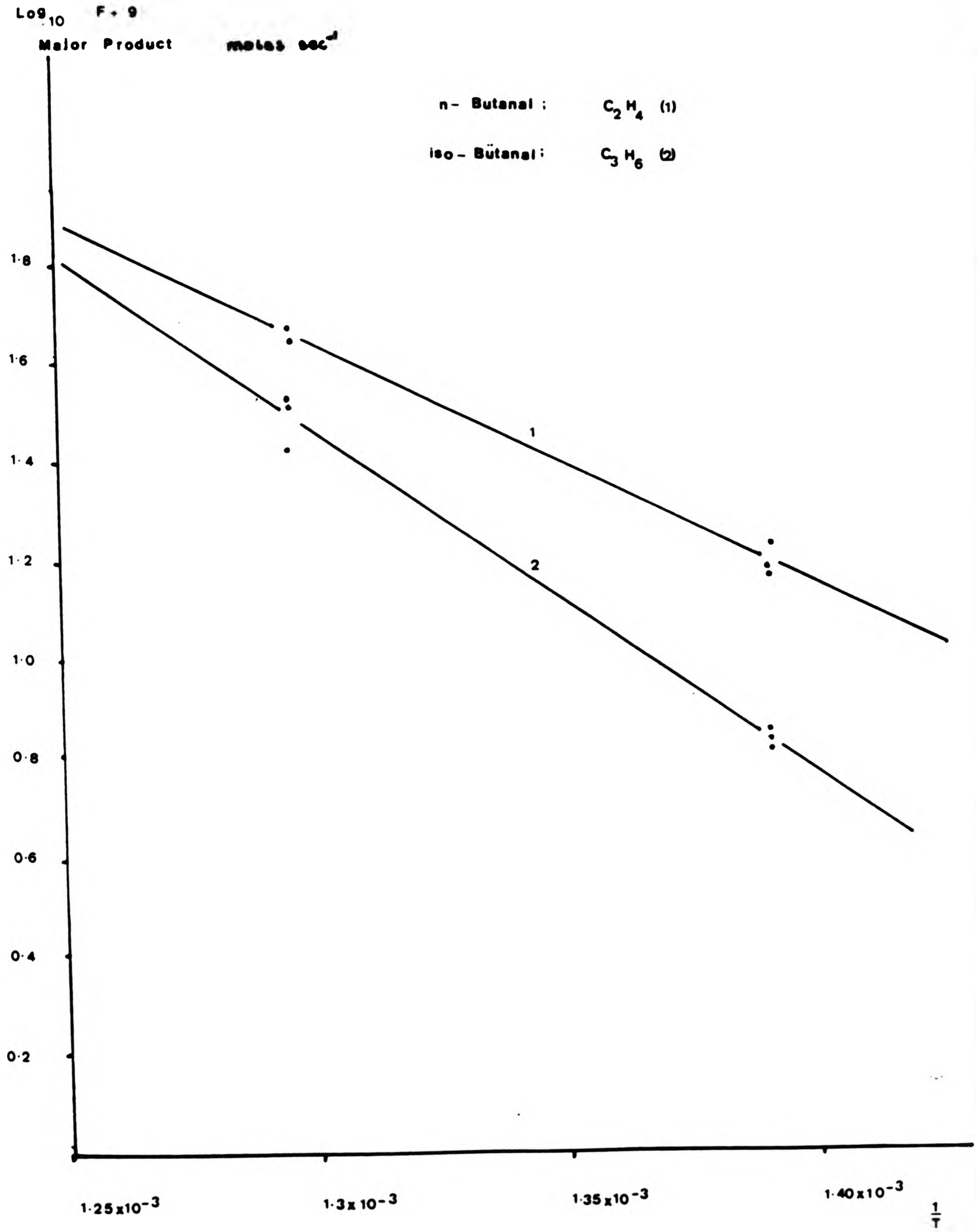

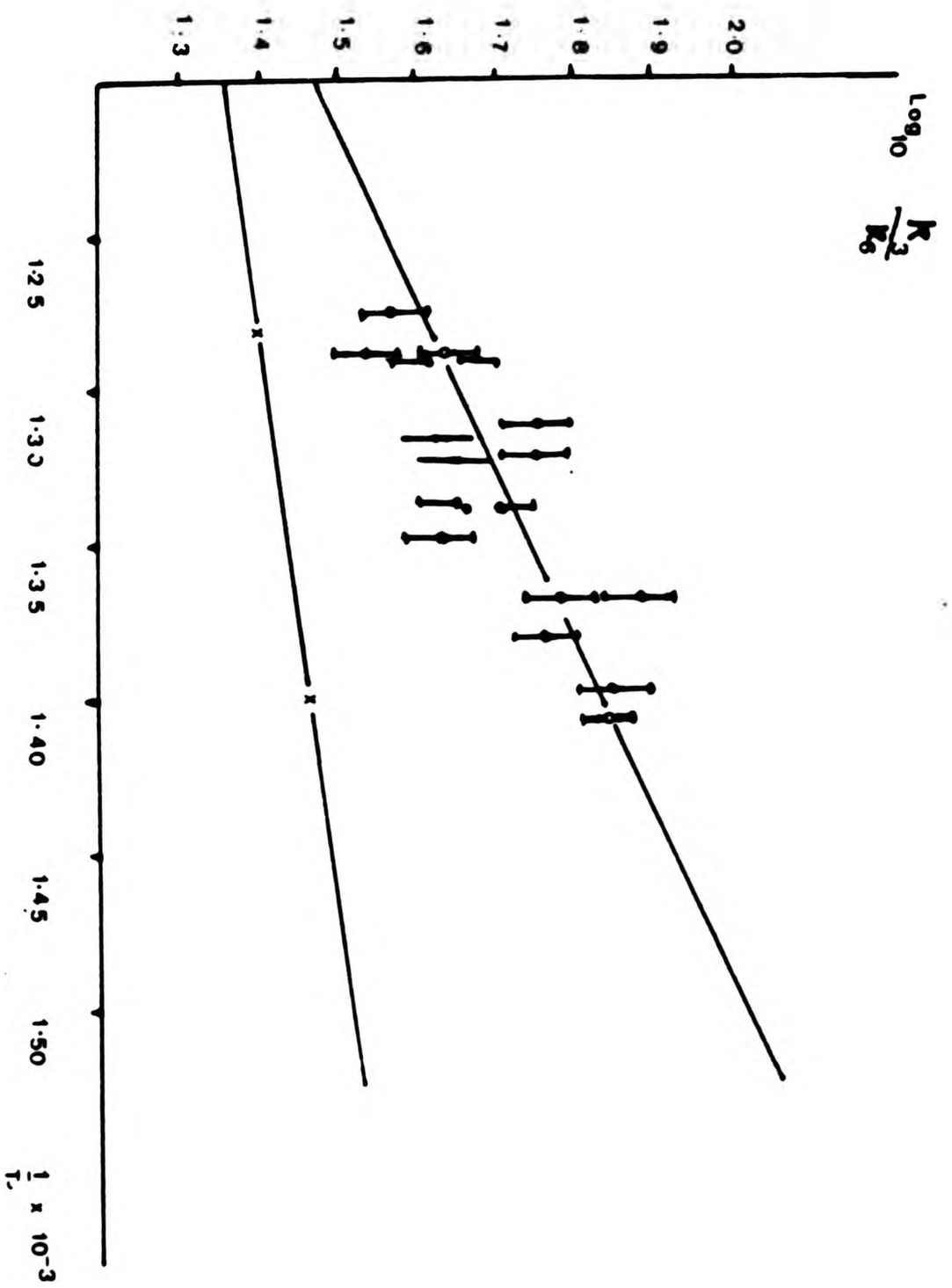

Individual results = I

Sets 7 and I 2 = I

Graph 15. Variation of rate constant with temperature

TABLE 1

Run	Temp K	f aldehyde / reactants x 10^8	f carrier / moles sec^{-1}	f oxygen	$\%C_2H_4$	$\frac{\%C_2H_4}{C_2H_6}$	f Oxygen / f Propanal	Residence time t	$\frac{k_3}{k_6}$
14	713	2300	220	0	0	-	-	1.16	-
24	713	1670	290	7.25	7.6	0.082	0.0043	1.56	19.06
17	713	2010	310	15.0	14.2	0.165	0.0074	1.32	22.29
23	713	1610	290	21.0	25.5	0.342	0.0130	1.51	26.30
21	713	2060	270	27.0	40.0	0.667	0.0130	1.29	51.30
25	713	1700	280	35.0	37.0	0.587	0.0205	1.41	28.63
18	713	1740	270	40.5	44.4	0.798	0.023	1.51	34.69
19	713	1700	290	58.0	58.3	1.398	0.034	1.53	41.11
20	713	1570	290	72.0	70.7	2.412	0.045	1.64	53.60
28	713	410	858	214	94.3	16.54	0.52	10.59	31.80
29	713	371	820	82	90.5	9.52	0.22	11.71	43.22
30	713	410	830	43	76.6	3.27	0.01	10.76	32.70
31	713	360	830	8	60.7	1.54	0.02	11.15	77.00
32	713	370	830	16	61.8	1.61	0.04	11.06	40.25
33	713	296	830	25	12.0	0.13	0.08	11.86	1.62

Data for graphs and result sets 1 and 2

TABLE 2

Run	Temp K	f aldehyde / reactants x 10^8	f carrier / moles	f oxygen / sec^{-1}	$\%C_2H_4$	$\%C_2H_4$	$\frac{\%C_2H_4}{C_2H_6}$	f oxygen / f Propanal	Residence t time	$\frac{R_3}{R_6}$
35	713	420	835	23.4	79.8	20.2	3.95	0.060	10.62	65.83
36	713	390	835	4.1	37.0	63.0	0.58	0.011	10.91	52.72
37	713	300	835	33.4	84.4	15.6	5.41	0.11	10.91	49.18
38	713	390	835	8.3	61.4	38.6	1.59	0.021	10.97	75.71
39	713	390	835	16.7	77.0	23.0	3.34	0.043	10.99	77.67
45	713	1180	835	8.35	24.45	75.65	0.323	0.007	3.02	46.14
46	713	1100	835	16.7	44.20	55.90	0.79	0.015	3.20	52.66
47	713	870	835	24.0	56.6	43.4	1.304	0.023	3.57	56.69
48	713	1100	835	33.4	61.06	38.94	1.586	0.030	3.16	51.74
49	713	1120	835	41.7	69.80	30.20	2.311	0.0372	3.10	62.12
50	713	1060	835	50.1	68.53	31.47	2.177	0.0472	3.21	46.12
51	713	1040	835	58.4	74.52	25.48	2.92	0.0417	2.71	70.02
52	713	1130	835	66.8	81.23	18.77	4.320	0.0059	2.97	73.09

Data for graphs and result sets 3 and 4

TABLE 3

Run	Temp K	f aldehyde	f carrier	f oxygen	fC_2H_4	fC_2H_6	fC_2H_4	$\frac{fC_2H_4}{fC_2H_6}$	f Oxygen	Residence	$\frac{k_3}{k_6}$	% dec
		Reactants and products x 10^8 (moles sec^{-1})							f Propanal	time t		
53	713	1068	721	56.7	6.05	1.08	7.14	7.22	0.0543	3.41	133	0.67
63	713	962	721	50.4	4.69	0.886	5.58	4.26	0.0520	3.36	81.9	0.58
55	713	1040	721	43.2	3.42	1.37	4.79	3.90	0.0415	3.45	93.9	0.46
56	713	1020	721	36.0	3.15	1.05	4.21	2.57	0.0350	3.48	73.4	0.41
57	713	902	721	28.8	3.01	0.99	4.00	1.51	0.0319	3.38	47.3	0.44
58	713	1040	721	21.6	1.24	1.13	2.37	1.16	0.0207	3.45	56.0	0.22
59	713	1050	721	14.4	1.66	1.29	2.96	0.75	0.0137	3.43	57.7	0.28
62	713	1000	721	7.21	0.434	1.15	1.58	0.36	0.0072	3.51	50.0	0.15
64	713	1020	721	108	10.8	1.40	12.2	9.37	0.105	3.48	89.2	0.19
65	713	1070	721	0	0	1.43	1.43	-	-	3.39	-	0.13
66	713	1000	721	93.7	9.28	1.02	10.2	7.48	0.090	3.52	83.1	0.10
68	713	957	721	64.8	6.03	1.01	7.04	4.18	0.067	3.56	62.4	0.73

Data for graphs and result set 5

TABLE 4

Run	Temp K	f aldehyde	f carrier	f oxygen	fC_2H_4	fC_2H_6	$fC_2H_4+C_2H_6$	$\frac{fC_2H_4}{fC_2H_6}$	f oxygen	Residence	$\frac{k_3}{k_6}$	% decomp
		Reactants and products x 10^8 (moles sec^{-1})							f propanal	time t		
97	710	1040	721	7.21	0.106	0.337	0.440	0.315	0.0069	3.47	45.45	0.042
101	710	1050	721	14.4	0.306	0.421	0.725	0.729	0.0137	3.43	53.21	0.069
102	710	1010	721	21.6	0.368	0.442	0.810	0.833	0.0214	3.52	68.92	0.063
103	710	1010	721	28.8	0.793	0.487	1.110	1.626	0.0285	3.52	57.05	0.109
104	710	1000	721	36.0	1.22	0.512	1.73	2.39	0.036	3.52	66.35	0.173
105	710	1010	721	43.2	1.53	0.537	2.07	2.84	0.0428	3.51	66.35	0.204
106	710	994	721	50.4	2.10	0.553	2.65	3.81	0.052	3.51	69.02	0.280

Data for graphs and result set 7

TABLE 5

Run	Temp K	f aldehyde	f carrier	f oxygen	fC_2H_4	fC_2H_6	$fC_2H_4 + C_2H_6$	$\frac{fC_2H_4}{fC_2H_6}$	f oxygen / f propanal	Residence time t	$\frac{k_3}{k_6}$	% decomp
		Reactants and products x 10^8 (moles sec^{-1})										
154	713	511	1140	28.6	0.161	0.036	0.197	4.47	0.055	3.67	81.27	0.038
142	713	746	915	28.6	0.277	0.052	0.327	5.50	0.038	3.66	144.7	0.043
144	713	860	772	28.6	0.303	0.124	0.427	2.44	0.033	3.72	73.9	0.049
147	713	1040	543	28.6	0.438	0.299	0.837	1.79	0.027	3.76	66.3	0.080
148	713	1210	400	28.6	0.591	0.424	1.01	1.39	0.023	3.76	59.56	0.11
152	713	1320	326	28.6	0.772	0.386	1.16	1.99	0.021	3.66	94.76	0.087
111	711	419	1580	28.6	0.351	0.064	0.415	5.58	0.068	3.57	82.08	0.099
112	711	596	1030	28.6	0.936	0.252	1.180	4.093	0.047	3.54	87.08	0.197
113	711	663	868	28.6	1.08	0.385	1.470	3.128	0.043	3.76	72.74	0.221
124	711	1010	606	28.6	0.992	0.515	1.50	1.923	0.028	3.58	68.67	0.148
115	711	1120	457	28.6	1.24	0.822	2.06	1.889	0.025	3.63	75.56	0.183
116	711	1260	372	28.6	1.32	1.170	2.49	1.414	0.022	3.44	64.27	0.197

Data for graphs and result sets 8 and 10

Overleaf data for graphs and result sets 9 and 11 .

TABLE 6

Run	Temp K	f aldehyde	f carrier	f oxygen	fC_2H_4	fC_2H_6	$fC_2H_4+C_2H_6$	$\frac{fC_2H_4}{fC_2H_6}$	f oxygen	Residence	$\frac{k_3}{k_6}$	% decomp	
		Reactants and products x 10^8 (moles sec^{-1})							f propanal	time t			
125	712	1090	650	31	0.487	0.253	0.740	1.92	0.028	3.58	68.57	0.067	
126	723	1110	650	31	0.686	0.442	1.12	1.55	0.027	3.49	57.40	0.100	
156	726	957	650	31	0.854	0.351	1.20	2.42	0.032	3.82	75.62	0.125	
161	726	1020	650	31	0.861	0.333	1.19	2.75	0.030	3.66	91.66	0.116	
164	726	1030	650	31	0.831	0.460	1.29	1.80	0.030	3.63	60.00	0.125	
128	741	1030	650	31	0.552	0.444	0.99	1.24	0.030	3.70	41.33	0.096	
166	746	962	650	31	1.36	0.940	2.30	1.44	0.032	3.68	45.00	0.239	
167	746	1040	650	31	1.32	0.998	2.31	1.44	0.029	3.52	49.65	0.222	
168	746	1010	650	31	1.29	0.947	2.23	1.36	0.030	3.56	45.33	0.220	
130	754	962	650	31	1.17	0.825	1.99	1.41	0.032	3.66	44.06	0.206	
131	755	1250	650	31	1.33	0.956	2.28	1.39	0.024	3.08	57.91	0.182	
132	759	1000	650	31	1.53	1.15	2.96	1.27	0.031	3.54	40.97	0.296	
135	761	931	650	31	1.53	1.20	2.46	1.17	0.032	3.71	36.56	0.264	
136	773	912	650	31	1.96	1.70	3.66	1.15	0.034	3.69	33.82	0.401	
173	775	1010	650	31	1.77	1.32	3.09	1.34	0.030	3.45	43.22	0.305	
174	775	1010	650	31	1.77	1.44	3.21	1.26	0.031	3.46	40.64	0.317	
140	783	1060	650	31	2.03	1.90	3.93	1.07	0.029	3.31	36.55	0.370	

TABLE 7

Run	Temp K	f aldehyde	f carrier	f oxygen	fC_2H_4	fC_2H_6	$fC_2H_4+C_2H_6$	$\frac{fC_2H_4}{fC_2H_6}$	f oxygen	Residence time t	$\frac{R_3}{R_6}$	% decomp f propanal
		Reactants and products x 10^8 (moles sec^{-1})										
179	775	1020	682	6.82	0.19	0.43	0.62	0.466	0.0067	3.42	69.76	0.060
182	775	957	682	13.64	0.39	0.63	1.02	0.611	0.0142	3.74	43.02	0.106
186	775	987	683	20.46	0.94	1.02	1.96	0.920	0.0200	3.52	46.00	0.198
187	775	989	682	27.28	1.31	1.28	2.59	1.19	0.0270	3.47	44.07	0.261
189	773	990	682	34.10	1.92	1.32	3.29	1.73	0.034	3.52	50.88	0.332
190	773	1050	682	34.10	1.82	1.32	3.14	1.60	0.032	3.35	50.00	0.299
192	773	960	682	40.92	2.17	1.45	3.62	1.87	0.042	3.62	44.52	0.377
193	773	988	682	47.74	2.22	1.90	4.12	1.46	0.047	3.41	31.86	0.417
194	773	988	683	47.74	2.40	2.24	4.64	1.34	0.048	3.46	27.90	0.469
195	773	1020	682	54.56	2.62	2.30	4.92	1.42	0.053	3.36	26.59	0.482
196	773	1020	682	54.56	2.77	2.30	5.07	1.57	0.052	3.36	30.19	0.49

Data for graphs and result set 12

TABLE 8

Run	Temp K	f aldehyde	f carrier	f oxygen	fC_2H_4	fC_2H_6	$fC_2H_4+C_2H_6$	$\frac{fC_2H_4}{fC_2H_6}$	f oxygen	Residence time t	k_3	% decomp
		Reactants and products x 10^8 (moles sec^{-1})							f propanal		k_6	
197	772	562	1170	31	1.37	0.45	1.81	3.00	0.057	3.42	54.50	0.32
198	772	636	1170	31	1.48	0.59	2.08	2.49	0.048	3.28	51.87	0.332
199	772	840	915	31	1.51	0.97	2.48	1.56	0.036	3.22	43.33	0.295
216	772	775	915	31	1.45	0.85	2.30	1.71	0.040	3.34	42.75	0.296
205	772	955	686	31	1.45	0.66	2.11	2.19	0.032	3.42	68.43	0.220
207	772	1150	515	31	1.53	1.65	3.11	0.97	0.026	3.37	37.30	0.270
210	772	1280	400	31	1.56	1.84	3.40	0.84	0.024	4.37	35.00	0.265
212	772	1270	286	31	1.59	2.00	3.60	0.79	0.024	3.60	32.91	0.283
213	772	1370	286	31	1.44	1.99	3.43	0.72	0.022	3.38	32.72	0.250
215	772	1590	194	31	1.87	2.92	4.79	0.64	0.019	3.14	33.68	0.30

Data for graphs and result set 13

TABLE 9

Run	Temp K	f Propanal	f carrier	f oxygen	f ethanal	f ethanal
		Reactants and products x 10^8 (moles sec^{-1})				C_2H_4
243	713	982	682	0	0	-
245	772	970	682	0	0	-
91	775	1000	690	6.82	0.1	-
177	775	1000	682	6.82	0.1	-
182	775	957	682	13.7	0.13	0.33
184	775	1001	682	20.4	0.22	0.23
188	775	1010	682	27.2	0.12	0.09
190	773	1050	682	34.1	0.37	0.2
196	773	1020	682	54.5	0.28	0.1
198	772	636	1170	31.0	0.21	0.14
201	772	775	915	31.0	0.37	-
211	772	1280	286	31.0	0.29	-
above results for a Boric acid coated vessel						
65	713	1000	721	0	0	-
59	713	1050	721	14.4	0.29	0.17
57	713	902	721	28.8	0.36	0.12
56	713	1020	721	36.0	0.52	0.17
54	713	902	721	50.4	0.17	-
above results for a Silica glass coated vessel						

Results showing measured flowrates of ethanal.

TABLE 9

Run	Temp K	f Propanal	f carrier	f oxygen	f ethanal	f ethanal
		Reactants and products x 10^8 (moles sec^{-1})				C_2H_4
243	713	982	682	0	0	-
245	772	970	682	0	0	-
91	775	1000	690	6.82	0.1	-
177	775	1000	682	6.82	0.1	-
182	775	957	682	13.7	0.13	0.33
184	775	1001	682	20.4	0.22	0.23
188	775	1010	682	27.2	0.12	0.09
190	773	1050	682	34.1	0.37	0.2
196	773	1020	682	54.5	0.28	0.1
198	772	636	1170	31.0	0.21	0.14
201	772	775	915	31.0	0.37	-
211	772	1280	286	31.0	0.29	-
above results for a Boric acid coated vessel						
65	713	1000	721	0	0	-
59	713	1050	721	14.4	0.29	0.17
57	713	902	721	28.8	0.36	0.12
56	713	1020	721	36.0	0.52	0.17
54	713	902	721	50.4	0.17	-
above results for a Silica glass coated vessel						

Results showing measured flowrates of ethanal.

TABLE 10

Run	Temp K	f aldehyde	f carrier	f oxygen	fC_3H_6	fC_3H_8	fC_2H_4	$\frac{fC_3H_6}{fC_3H_8}$	$\frac{\text{f oxygen}}{\text{f aldehyde}}$	Residence time t
		Reactants and products x 10^8 (moles sec^{-1})								
Isobutanal										
222	715	924	682	31	0.693	0.007	-	-	0.033	3.90
223	715	960	682	31	0.700	0.007	-	-	0.033	3.81
224	715	945	682	31	0.664	0.007	-	-	0.033	3.85
226	772	932	683	31	3.28	0.771	0.203	4.2	0.033	3.59
227	772	939	682	31	2.67	0.664	0.332	4.1	0.033	3.58
228	772	936	682	31	3.31	0.663	-	4.9	0.033	3.58
n-butanal										
229	715	1070	682	31	trace	-	1.72	-	0.029	3.30
230	715	952	682	31	trace	-	1.47	-	0.032	3.84
231	715	957	682	31	trace	-	1.51	-	0.032	3.82
232	772	895	682	31	trace	-	4.34	-	0.034	3.69
233	772	895	682	31	trace	-	4.64	-	0.034	3.68

Data for graph and result set 14.1

TABLE 11

Run	Temp K	f aldehyde	f carrier	f oxygen	FC_3H_6	FC_3H_8	FC_2H_4	FC_2H_6	Residence time t
		Reactants and products x 10^8 (moles sec^{-1})							
Isobutanal									
234	772	954	682	-	0.35	trace	-	-	3.55
235	772	960	682	-	0.43	trace	-	-	3.52
238	715	954	682	-	0.18	trace	-	-	3.80
n-butanal									
236	772	916	682	-	-	-	1.59	-	3.63
237	772	922	682	-	-	-	1.32	-	3.62
240	715	929	682	-	-	-	0.43	-	3.89
241	715	929	682	-	-	-	0.51	-	3.87
Propanal									
243	713	982	682	-	-	-	0.018	0.47	3.77
245	722	970	682	-	-	-	0.069	0.667	3.51

Data for results 14.2

REFERENCES

1. Baldwin R R and Walker R W Trans Faraday Soc 65 p792 1969.

2. Baker and Yorke J Chemical Education V 49 No.5 p351 1972.

3. Carthidge and Tipper Proc Roy Soc SA, p261, p388 1961.

4. Walker R W Reaction Kinetics VI Specialist Periodical reports, 4 p161.

5. Griffiths J R and Skirrow G Oxidation and combustion revo 3 p 47-96 1968.

6. Dixon D J Skirrow G and Tipper C F Faraday 1, 70 (6) p1078 1974.

7. Combe A Niclause M and Letort M Rev Inst. Francais petole Ann Combust liquid 10 786,929 1955.

8. Cairns and Waddington J Combustion and Flame 31 1 p972 1978.

9. Benson J American Chem Soc 87 p972 1965.

10. Baldwin R R and Walker R W Trans Faraday Soc 65 p805 1969.

11. Baldwin R R Matchan M J and Walker R W Trans Faraday Soc 67 p3521 1971.

12. Baldwin R R Langford D H Matchan M J Walker R W and Yorke D W Report on the 13th Int. Combustion Symposium p251 1970.

13. Baldwin R R Jackson D Walker R W and Webster S J Trans Faraday Soc 63 1665 1967.

14. Kerr J A Chem Revs 66,465 1966.

15. Baldwin R R Hopkins D E and Walker R W.

16. Trotman - Dickinson A F and Kerr J A J Chem Soc 1611 1960.

17. Sampson R J J Chem Soc 5059 1963.

18. Baldwin R R Cleugh C J Plaistowe J C Walker R W J S C Faraday 1 75,6 1433 1979.

19. Baldwin R R Walker R W and Yorke D A J S C Faraday II Vol 69 p826 1973.

21. Baldwin R R Matcham M J and Walker R W Combustion and Flame 15 p109 1970.

22. Kistiakowsky G B and Roberts E M J Chem Phys 21 1637 1953.

24. HO SK Proc Royal Soc A276 (1365) P278 1963.

25. Laidler K J and Lieu Proc Royal Soc A297 p365 1967.

26. Laidler K J and Eusuf Canadian J Chem 43,1 p268 1965.

27. Baldwin R R Pickering I A and Walker R W J S C Faraday 76 p2374 1980.

28. W C Herndon J of Chemical Education Vol 41 8 1964 p425

29. M F R Mulcahy and D J Williams Australian J of Chemistry 14,535 1961.

30. J P Longwell and Weiss M A Ind, Eng Chem 47 1634 1955.

31. M F R Mulcahy J of Physical Chem vol 73 1969.

32. Szwarc J Cemical physics 17,431,1949.

33. C W P Crowne V J Grigulis and J J Throssell Trans Faraday Soc 556 V 65 p 4 page 1051.

34. J M Sullican A E Axeworthy and T J Houser J of Phys Chem V 74 13 1970 p2611.

35. B F Gray and P G Felton Combustion and flame 23 1974, p295.

36. A C Baldwin I M T Davidson and A V Howerd J C S faraday 1 1975 p972.

37. W E Falconer T F Hunter and A F Trotman-Dickenson J Chem Soc 1961 p609.

38. S W Benson and M Weissman Int J of Chemical kinetics vol 13 1297 1981.

39. J M Sullivan and T J Houser Chemistry and Industry June 1965 p1057.

40. M F R Mulcahy Gas Kinetics, studies in modern chemistry Nelson 1973.

41. F P Greenspan and D J Mackellar Anal Chem 20 1061 1948.

42. D Swern Organic reactions 7 378 1953.

43. Bryukhoevetsku V A Levush S S Mouri F B Scherchuk V U Ukr Khim Zh (Russ Ed) 1976 42(6) 623-7.

44. Bryukhoevetsku et al Kheim prom-st 1975 (II) 819-21.

45. Benson S W Thermochemical kinetics 2nd Edition 1976.

46. Baldwin R R Walker R W Cleugh C J J C S Faradayl, V72 p1715, 1976.

47. Laidler K J and Lin M C Can J Chem 44 2927 1966.

ACKNOWLEDGEMENTS

I dedicate this thesis to my parents in appreciation of their support and encouragement throughout the course of this work.

I am especially indepted to Dr C W P Crowne for suggesting the topic and for his continued help, discussion and motivation during the past five years and wish to express my sincere thanks. In general I would like to thank the staff of the Chemistry department of the City of London Polytechnic for their hospitality.

I am particularly grateful to Mr G Curtis and Mr S Blackmore for their glass blowing services, to Dr J D Barnes for useful discussion and Mr R S Cowley for technical advice and finally my typist and friend Miss Susan Thomas for the preparation of the typescript of this thesis.

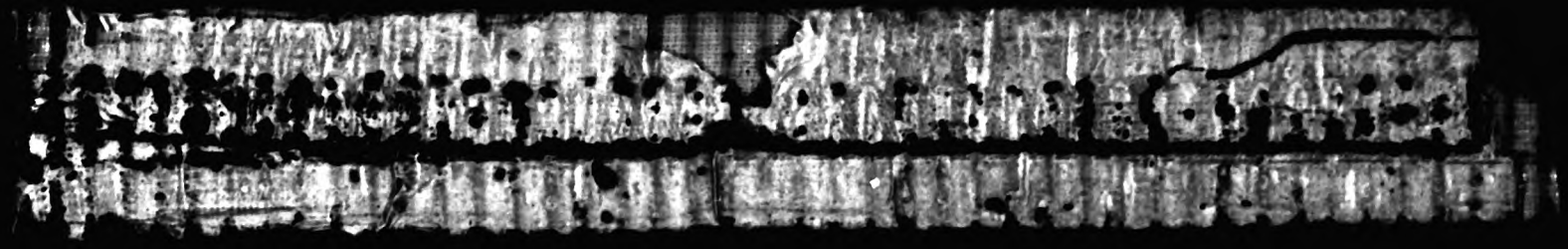

D44596 '83

END